86-9B3-THERM-R1

Advanced Diesel Oil Fuel Processor Development - Final Report

A. P. Murray
Chemical and Process Engineering

June 1986

Contract Number: DAAK-70-85-C-0003

Belvoir Research and Development Center
Power Generation Division
Fort Belvoir, Virginia 22060-5606
Project Monitor: Amos J. Coleman
STRBE-GGC

Westinghouse R&D Center
1310 Beulah Road
Pittsburgh, Pennsylvania 15235

12

86-9B3-THERM-R1

Advanced Diesel Oil Fuel Processor Development - Final Report

A. P. Murray
Chemical and Process Engineering

June 1986

Contract Number: DAAK-70-85-C-0003

Belvoir Research and Development Center
Power Generation Division
Fort Belvoir, Virginia 22060-5606
Project Monitor: Amos J. Coleman
STRBE-GGC

Westinghouse R&D Center
1310 Beulah Road
Pittsburgh, Pennsylvania 15235

NOTICE

DISCLAIMERS

DISPOSITION

SECURITY CLASSIFICATION OF THIS PAGE (When Data Entered)

REPORT DOCUMENTATION PAGE

READ INSTRUCTIONS BEFORE COMPLETING FORM

1. REPORT NUMBER: DAAK-70-85-C-0003	2. GOVT ACCESSION NO.: AD-A172 750
3. RECIPIENT'S CATALOG NUMBER:	
4. TITLE (and Subtitle): Advanced Diesel Oil Fuel Processor Development - Final Report	5. TYPE OF REPORT & PERIOD COVERED: Final Report 10/16/84-5/21/86
	6. PERFORMING ORG. REPORT NUMBER:
7. AUTHOR(s): A. P. Murray	8. CONTRACT OR GRANT NUMBER(s): DAAK-70-85-C-0003
9. PERFORMING ORGANIZATION NAME AND ADDRESS: Westinghouse Electric Corporation, Research and Development Center, 1310 Beulah Road, Pittsburgh, PA 15235-5098	10. PROGRAM ELEMENT, PROJECT, TASK AREA & WORK UNIT NUMBERS: 62733A, 1L162733AH20, EK, 003
11. CONTROLLING OFFICE NAME AND ADDRESS: Belvoir R, D and E Center, STRBE-FGC, Fort Belvoir, VA 22060-5606	12. REPORT DATE: June 1986
	13. NUMBER OF PAGES: 208
14. MONITORING AGENCY NAME & ADDRESS(if different from Controlling Office): DCASMA, Pittsburgh, 1626-S Federal Buiilding, 100 Liberty Avenue, Pittsburgh, PA 15222	15. SECURITY CLASS. (of this report): Unclassified
	15a. DECLASSIFICATION/DOWNGRADING SCHEDULE:

16. DISTRIBUTION STATEMENT (of this Report)

Approved for public release; distribution unlimited

17. DISTRIBUTION STATEMENT (of the abstract entered in Block 20, if different from Report)

Approved for public release; distribution unlimited.

18. SUPPLEMENTARY NOTES

A. P. Murray, "Waterless Diesel Fuel Processor for Fuel Cell Systems" 32nd Power Sources Symposium, Cherry Hill, NJ; June 1986.

19. KEY WORDS (Continue on reverse side if necessary and identify by block number)

fuel, cell, systems, processors, diesel, oil, logistics, reformer, catalysts, experiments

20. ABSTRACT (Continue on reverse side if necessary and identify by block number)

This report presents the analysis and test results for a diesel oil, fuel cell system. It shows such a fuel cell system to be technically practical, although with significant size and weight penalties as compared to existing, diesel-electric generator sets.

DD FORM 1 JAN 73 1473 EDITION OF 1 NOV 65 IS OBSOLETE

SECURITY CLASSIFICATION OF THIS PAGE (When Data Entered)

Contents

List of Figures

List of Tables

Advanced Diesel Oil Fuel Processor Development

A. P. Murray
Chemical and Process Engineering

Abstract

The Westinghouse ~~Research and Development~~ Center has been conducting a fuel processing program for Army phosphoric acid fuel cell (PAFC) systems, with the objective of an advanced system that ~~utilizes~~ uses diesel fuels and does not require an external water source. An autothermal reforming approach is followed, and six design variations proposed. Analyses and experimental tests have been performed, and indicate this is a viable technical approach. However, the diesel fuel cell system is estimated to be considerably heavier than its methanol fuel counterpart, which will limit its use for mobile and portable power applications.

1. Summary

The Westinghouse Research and Development Center has been conducting a 19-month program on fuel processing for Army phosphoric acid fuel cell (PAFC) systems. The objective is to develop an advanced fuel processor that does not require an external water source and utilizes diesel fuels as feedstocks. Such a system has the advantages of lower fuel flow rates, fewer logistical requirements, fuel compatibility with Army vehicles, lower toxicity, and implied multi-fuel capability. Autothermal reforming has been investigated as the principal technical approach, and the studies include oxygen enrichment, hydrogen recovery, cathode water recycle and power recovery as system variations.

The program has accomplished the objective by equilibrium, kinetic, and system analyses, and by fabrication, assembly, and testing of an experimental system. The analyses indicate that the equilibrium concentrations change little over the 1340-2130°F temperature range, and significant quantities of carbon monoxide will be encountered (15-25%). Thus, shift conversion is mandatory. Carbon deposition is not thermodynamically favored in this regime, although small quantities could form during heatup at around 800°F. The kinetic calculations indicate that reformer fuel conversion is strongly influenced by the inlet temperature: 2100-2600°F is required for 85-90% conversion, with a lower steam/carbon ratio (S/C ~ 2). This is attainable with catalyst volumes comparable to present, methanol systems (.2-.3 ft^3), although the high temperatures require significant fuel combustion and an enriched oxygen/air supply.

System analyses have been performed on six variations of the autothermal approach, and include PSA[a] /oxygen enrichment, membrane recovery of hydrogen, turboexpansion/power recovery, and cathode water recovery/recycle. The latter recovers 60-80% of the required water at an S/C ratio of 2, and, hence, it is inadequate by itself. Only the autothermal/cathode water recovery and autothermal/cathode water/PSA oxygen/turboexpansion combinations offer realistic operating conditions, good overall system efficiencies (24-28%), and low feed fuel flow rates (.45-.5 gph). These compare favorably with present, methanol system values. However, because of the extra, diesel fuel processing operations (heat exchanger, desulfurizer, and shift reactor), the diesel system is larger and some three times heavier than the methanol counterpart and existing, diesel-electric generators.

A 5 KW hydrogen equivalent experimental system was fabricated to investigate the fuel processor. The system is comprised of three test rigs, and includes the burner/mixer, reformer, let-down heat exchanger, desulfurizer, and shift reactor. The envelope dimensions are 10'W x 4'D x 7'H. Ten tests were initiated, and five successful hot tests accomplished. No successful reforming or hydrogen production was observed because of equipment problems or limitations, although stable temperatures of 1832-2102°F were obtained operating on air or up to 45% oxygen. However, the tests indicate several subtle characteristics of diesel fuel reforming: inadequate nozzle atomization, water condensation in the downstream packed beds, pressure drop fluctuations (up to 12 psig), high metal wall temperatures (1600°F), insulation requirements, and long system heat-up times (estimated at ~ 10 hours). These characteristics require resolution in a prototype system design, and have the ramifications of increased size, weight, and cost.

Summarizing, the "waterless," autothermal diesel fuel reforming approach is a practical alternative, provided the system includes cathode water recovery and recycle. Use of oxygen enriched air (e.g.:

a. PSA - Pressurized Swing Adsorption

from a PSA molecular sieve system) is beneficial, and can be accomplished with no efficiency penalties. The other design aspects are:

- the system is more complex, larger, heavier, and more expensive than present methanol fuel cell systems and diesel-electric generators.
- a let-down heat exchanger, desulfurizer, and shift reactor are necessary components, in addition to the reformer and burner.
- a relatively large shift reactor is required ($> 1\ ft^3$), and some inlet methane formation can be expected.
- a relatively long start-up time will be required, with high initial fuel flow rates.
- effective fuel atomization is required.
- the design must accomodate high process and metal wall temperatures.
- the impurities (sulfur, ammonia, and metals/ash) require treatment and removal.
- water condensation in the system during start-up.

Further tests should be performed in the present experimental system to demonstrate reforming and hydrogen production. Based upon successful results and Army requirements, a more involved program should be undertaken to incorporate PSA/oxygen enrichment and turboexpansion into the present test system, and conduct a more comprehensive test plan. Finally, the merits of a diesel fuel, solid oxide fuel cell system should be investigated, because it eliminates the shift reactor, which represents 20-30% of the system's weight.

2. Introduction

The Westinghouse Research and Development Center has been conducting a 19-month program on fuel processing for Army phosphoric acid fuel cell (PAFC) systems. The program's objective is to develop an advanced, methanol fuel processor for Army PAFC systems that does not require an external water source nor involve cathode gas water recovery as the principal route. The program intends to accomplish this using an autothermal reforming approach, including computer model analyses and "proof of principle" experimental demonstration in the 3-5 kWe hydrogen equivalent, fuel processor size range.

Five months into the program, a modification notice deleted methanol as the fuel, and substituted diesel fuel in its place. Analyses indicated the autothermal approach is still valid, albeit requiring a more complex system with more experimental uncertainties and difficulties. Consequently, program effort concentrated on fabricating, assembling, and testing the experimental, diesel fuel processing system.

The program's ultimate objective is a "waterless" PAFC system: i.e., one that requires no external water source nor a fuel/water premix supply. Figure 2.1 illustrates a simplified, PAFC system schematic. The fuel cell system consists of three major subsystems:

- The fuel processor: This converts the fuel into hydrogen and carbon dioxide via endothermic (energy consuming) steam-reforming reactions.
- The fuel cell stack: This electrochemically produces electricity from hydrogen oxidation, and generates water vapor in the cathode exit gases. Carbon monoxide concentrations must be below ~3% for satisfactory operation.

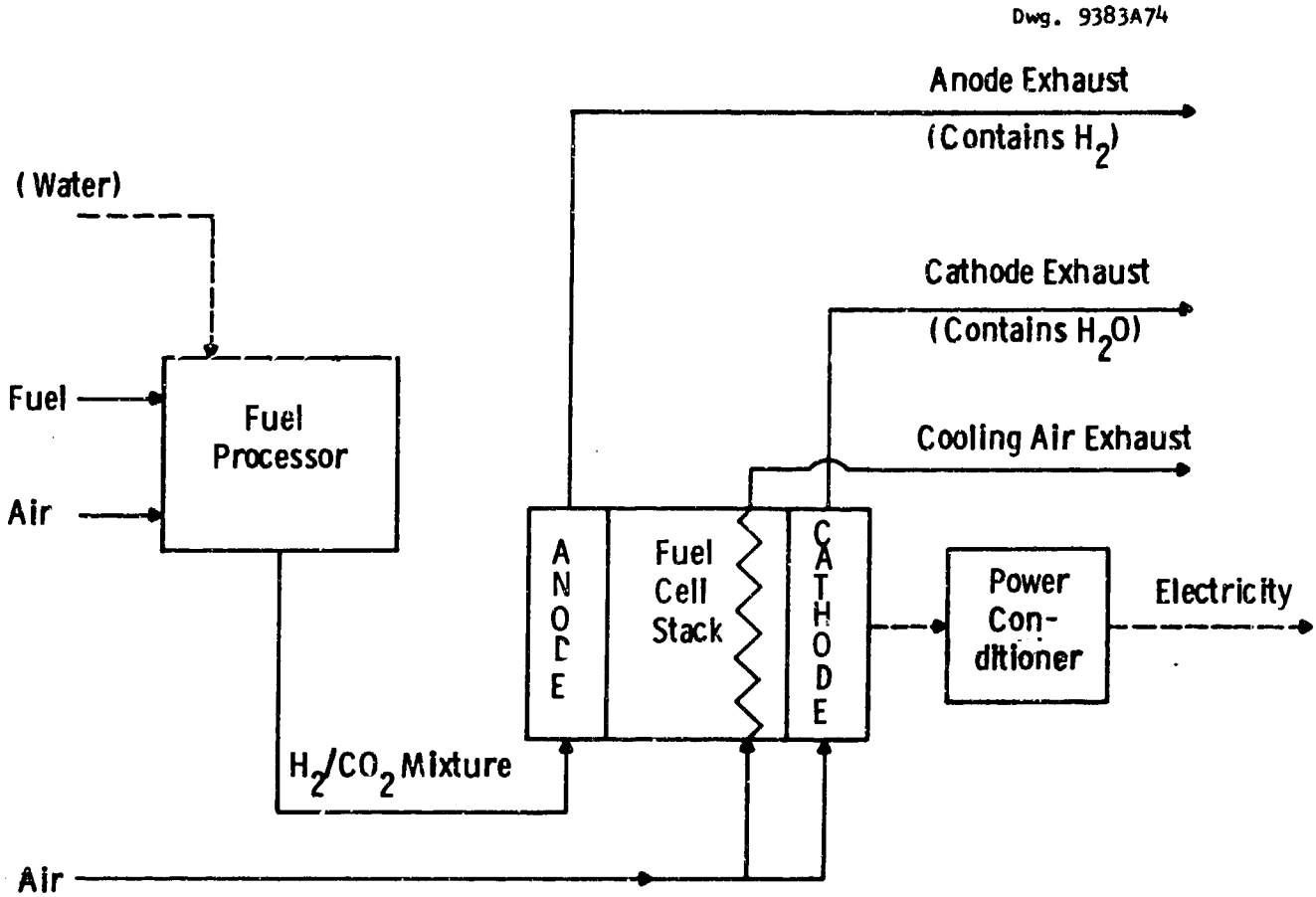

Figure 2.1 — Simplified Schematic of a PAFC System

- The power conditioner: This uses solid state devices to modify the stack's direct current output to suitable alternating current voltages and frequencies.

The fuel processor is the only subsystem that requires water (or steam). The fuel cell stack itself generates water, which leaves as vapor in the cathode exhaust, and contains traces of the phosphoric acid electrolyte. This water can be condensed, purified, and returned to the fuel processor. Another potential water source is the spent anode gas stream. This contains hydrogen (typical PAFC hydrogen utilization is in the 70-80% range). The hydrogen can be recovered and recycled directly. Alternatively, it can be combusted, and used to generate water and heat for the fuel processor. Finally, the fuel itself contains hydrogen, which can be burnt to generate water (steam) and heat for the fuel processor directly. This involves partial combustion of the fuel, and is an extension of autothermal (adiabatic) reforming.

All three approaches increase the PAFC system's size, complexity, and load follow times. Cathode gas water recovery and recycle requires a condensor, water purification, and a surge/storage tank. Anode gas hydrogen recovery requires a membrane or molecular sieve system, with the associated compressors and tanks. Anode water recovery necessitates a burner, and a condenser or ammonia scrubber. The autothermal approach generates high fuel processor temperatures, may require oxygen enriched air, and puts a maximum limit on overall fuel cell system efficiency. However, the autothermal approach has several key advantages not possible with the other routes:

- Maintain rapid response/load following.
- High temperatures generated where needed in the fuel processor, and provide high kinetic rates.
- Greater potential for multi-fuel capability.
- Reduced fuel flow rates compared to present, fuel/water premix systems.

Consequently, the autothermal approach was selected as the basis for this program. This report provides analyses of several, autothermal reforming approaches, and discusses the fabrication, assembly, and testing of a complete experimental, fuel processor system.

3. Conclusions

The following aspects are concluded from this effort:

1. "Waterless," diesel oil reforming is a practical alternative, provided the system includes cathode water recovery and recycle. The projected, 5 KW system efficiency is ~ 23%, with a fuel feed rate of .5 gph, and with prototype weight and cost estimates of 1388 lbs and $82,800 respectively.

2. Cathode water recovery and recycle is inadequate by itself, and recovers 60-80% of the required water (S/C ratio of 2) at cathode air utilizations of 33-50%.

3. Use of oxygen-enriched air is beneficial: it increases burner temperature while decreasing gas flow rates, and suppresses ammonia formation. A PSA/oxygen system is easily integrated into the autothermal/cathode water recycle combination, and allows the benefits with no energy penalties. The calculated, 5 KW system efficiency is 28%, with a fuel feed rate of .45 gph, and with prototype weight and cost estimates of 1718 lbs and $113,200 respectively.

4. A let-down heat exchanger, desulfurizer, and shift reactor are necessary components, in addition to the reformer and burner. Thus, the diesel oil fuel processor is more complex, larger, heavier, and more expensive than the present methanol systems and existing, diesel-electric generator sets.

5. A relatively large shift reactor is required (> 1 ft^3) because of the low steam/carbon (S/C) ratio. This will result in some methane formation at the reactor inlet.

6. A relatively long start-up time is anticipated, with a high, initial fuel flow. For the experimental system, the estimated operational time is 8-10 hours for thermal steady state. Heat capacity calculations indicate this should only be ~ 1 hour at full flow; the reason for the disparity is unclear.

7. The long heat-up time will result in partial oxidation (hence, inactivation) of the shift reactor catalyst, which will only be reduced and activated after the reformer starts producing hydrogen. This increases system start-up time further. For complete hydrogen reactivation of the catalyst, the manufacturer recommends a 4-8 hour time period. This implies an alternate method of shift reactor heat-up, other than direct, process gas flow, is desirable.

8. Rapid system start-up requires higher system flow rates (at least four times the steady state values) and higher system pressure drops. Of course, this contradicts the steady-state design philosophy of low flow rates to minimize pressure drops and parisitic power requirements.

9. Combustion water vapor condenses during system start-up. This delays system heating, and results in pressure drops as high as 12 psig.

10. Inadequate fuel atomization and nozzle purging/cleanout will result in system inoperability. Pressure atomization nozzles are inadequate for this task. Air atomizing nozzles are acceptable, but failed (plugged) in the experimental system after four tests. Ultrasonic nozzles may be the best atomization approach, although no satisfactory means for system sealing and high temperature protection was found to allow their use.

11. High gas (1832-2102°F) and metal wall (up to 1600°F) temperatures will occur. With the insulation present, the metal wall temperature is only 200°F lower than the process gas temperature.

12. Fuel impurities require treatment and removal. Sulfur compounds from the fuel should hydrocrack to hydrogen sulfide, which is removed by the desulfurizer. (Approximately .5 ft^3 of zinc oxide provides for ~ 119 hours of operation.) The calculated ammonia concentrations are ~ 30-50 ppm, and may be acceptable for PAFC use. Fuel metal and ash components will also require treatment.

13. The portable, diesel-fuel, PAFC system designs presented herein have slight, projected performance advantages as compared to diesel-electric generator systems. However, the full cell system designs have disadvantages in the size and weight comparisons.

4. Recommendations

The recommendations fall into five areas:

1. additional system experiments to verify hydrogen production and size capabilities.
2. definition of system mission requirements.
3. design implications (size, weight, and performance) of spent anode water recovery/recycle.
4. comprehensive test program and demonstration, including a 5 KW nominal size, fuel cell stack.
5. investigation and analysis of a solid oxide fuel cell system integrated with a diesel fuel processor.

The reported experimental tests have provided valuable information about diesel fuel processing and its requirements; namely effective atomization, dependable ignition, catalyst bed water condensation, pressure surges, temperature ranges and system heat-up. However, the experimental ramifications of these parameters also prevented successful hydrogen production by the test unit. Consequently, a short (4-5 month) test program should be pursued to demonstrate hydrogen production and flow rate/reaction sizing effects. This would also allow a better definition of the system's size and weight for a given power level.

There has been no clear communication of the fuel cell system's mission, the associated requirements, and alternate/competing technologies. These should be defined, particularly power levels, mobile versus base applications, and allowable weight/size/efficiency/time ranges. Thus, coupled with the sizing/test information, this will allow an analysis and determination of viable fuel cell applications and the target specifications. This analysis should be performed.

This program has shown that effective water/hydrogen management is crucial to the successful operation of "waterless" fuel cell systems, and the low hydrogen content of diesel fuels makes this a critical issue. Cathode water recovery and recycle is ineffective by itself, even at a low steam/carbon ratio of two. Consequently, alternate water/steam recovery and management techniques should be pursued, specifically anode recovery. Such anode techniques, if successful, would allow for internal water recycle at higher steam/carbon ratios (3-3.5), where successful reforming is easier, and less carbon monoxide is produced (i.e., reduce the shift reactor volume and weight).

If satisfactory results are obtained on the first three areas, then a comprehensive test and demonstration program should be conducted. This would be of 12-15 month duration, and should include:

- PSA/oxygen enrichment system
- turboexpander and generator
- 5 KWe PAFC stack
- parametric/part load tests
- 1000 hour demonstration/life test
- system cycling
- refined, prototype system design

This approach will provide the Army with a demonstrated, diesel oil, fuel cell system prototype design, backed by experimental hardware and test results.

Finally, a diesel fuel, PAFC system is projected to be two to three times as large (size and weight) as the present, methanol pre-mix, PAFC prototypes and established, diesel-electric generator units. A considerable fraction (20-30%) of the diesel/PAFC system's weight accrues from the shift reactor. Consequently, its elimination is

desirable. Solid oxide fuel cells (SOFC's) utilize carbon monoxide directly as a fuel, and, therefore, do not need a shift conversion. Present day, SOFC stacks are fabricated and tested in the 5 kw size range. Consequently, the merits of a diesel fuel/SOFC system should be investigated and analyzed for performance improvements and weight reduction, as compared to the PAFC and diesel-electric generator systems.

5. Liquid Fuel Processor System Analyses

5.1 METHANOL FEEDSTOCK

Methanol represents an ideal fuel for PAFC systems. It volatilizes readily, reforms easily, and usually does not form carbon deposits. It has three drawbacks: it is a special fuel and as such, is not "logistically available;" it has a relatively high toxicity (TLV=200 ppm for 8 hours); and it has a relatively low energy per weight value (LHV=8592 BTU/lb, or 56613 BTU/gal). Even with these drawbacks, small, methanol/water premix-fueled PAFC systems have been developed and successfully tested.

Methanol readily reforms with steam at moderate temperatures to produce hydrogen and carbon oxides, using either a nickel or a copper/zinc, low temperature shift catalyst. The overall reaction sequence is:

$$CH_3OH + H_2O \rightarrow CO_2 + 3H_2 \quad (5.1)$$

$$CO + H_2O \rightleftarrows CO_2 + H_2 \quad (5.2)$$

Equation 5.1 is the reforming reaction, and Equation 5.2 represents the water gas shift reaction equilibrium. Equation 5.1 indicates that methanol and water react on a 1:1 molar basis, and, conceptually, a maximum, anode feed, hydrogen content of 75 mole % can be achieved. Experimentally, a 58% methanol-water premix fuel (i.e., no excess water by Equation 5.1) has been reformed at ~500°F with >99% conversion of the methanol,[1] with acceptably low carbon monoxide concentrations, and, therefore, a separate, shift conversion reactor is unnecessary. An analysis of the data indicates that Equation 5.1 dominates and is kinetically (i.e., a selective catalyst), rather than equilibrium, controlled.

The autothermal reformer approach uses partial combustion to provide the water for Equation 5.1, i.e.

$$CH_3OH + \frac{3}{2} O_2 \rightarrow CO_2 + 2H_2O + \text{heat} \quad (5.3)$$

Therefore, the fuel processor, reformer reaction rearranges to:

$$2CH_3OH + O_2 \rightarrow 2CO_2 + 4H_2 \quad (5.4)$$

This scheme has several immediate consequences:

1. At least one-third of the fuel is burnt to provide the steam (and heat) for the reformer reactions.

2. The reaction is steam rather than heat limited, and, consequently, high temperatures are to be expected (>2000°F).

3. The high temperatures will produce unacceptably high carbon monoxide concentrations, which mandate cool down and a shift reactor prior to the fuel cell. Shift conversion is difficult to accomplish without a steam excess.[2]

4. Equation 5.4 indicates a maximum anode stream, hydrogen concentration of ~67%, but only when pure oxygen is used. For air combustion, the maximum hydrogen concentration drops to ~40%.

However, the autothermal approach also offers reduced fuel consumption and higher efficiencies as compared to the present, fuel premix system. Figure 5.1 outlines the most basic form of the autothermal fuel processor.

The hydrogen rich stream produced by the fuel processor flows to the anode side of the fuel cell stack, as Figure 5.2 illustrates. The porous anode contains a platinum catalyst that dissociates molecular hydrogen at its surface. The PAFC uses a matrix impregnated with hot, concentrated phosphoric acid as the electrolyte, which allows the

Dwg. 9383A76

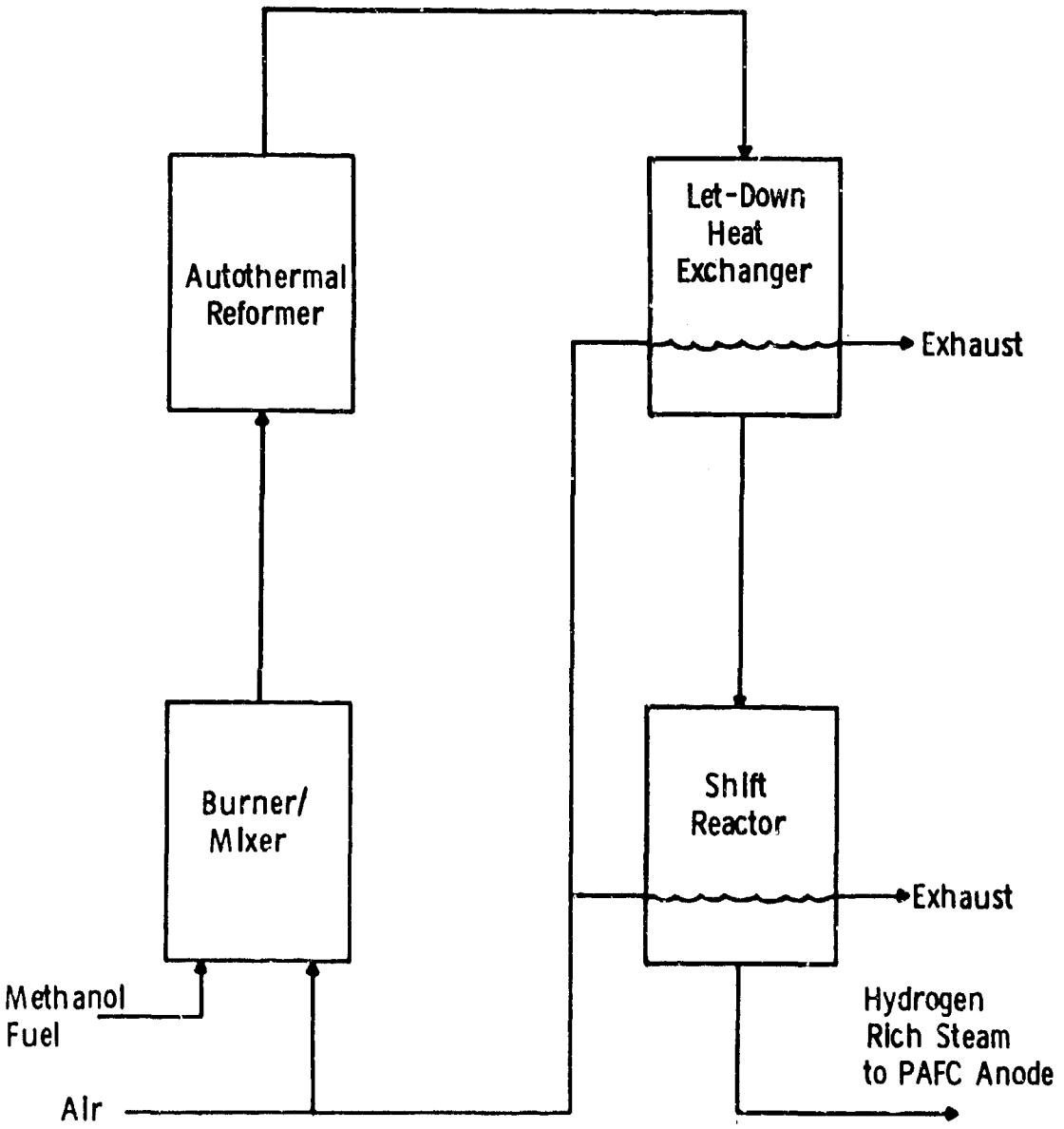

Figure 5.1 -- Simplified, Autothermal Fuel Processor

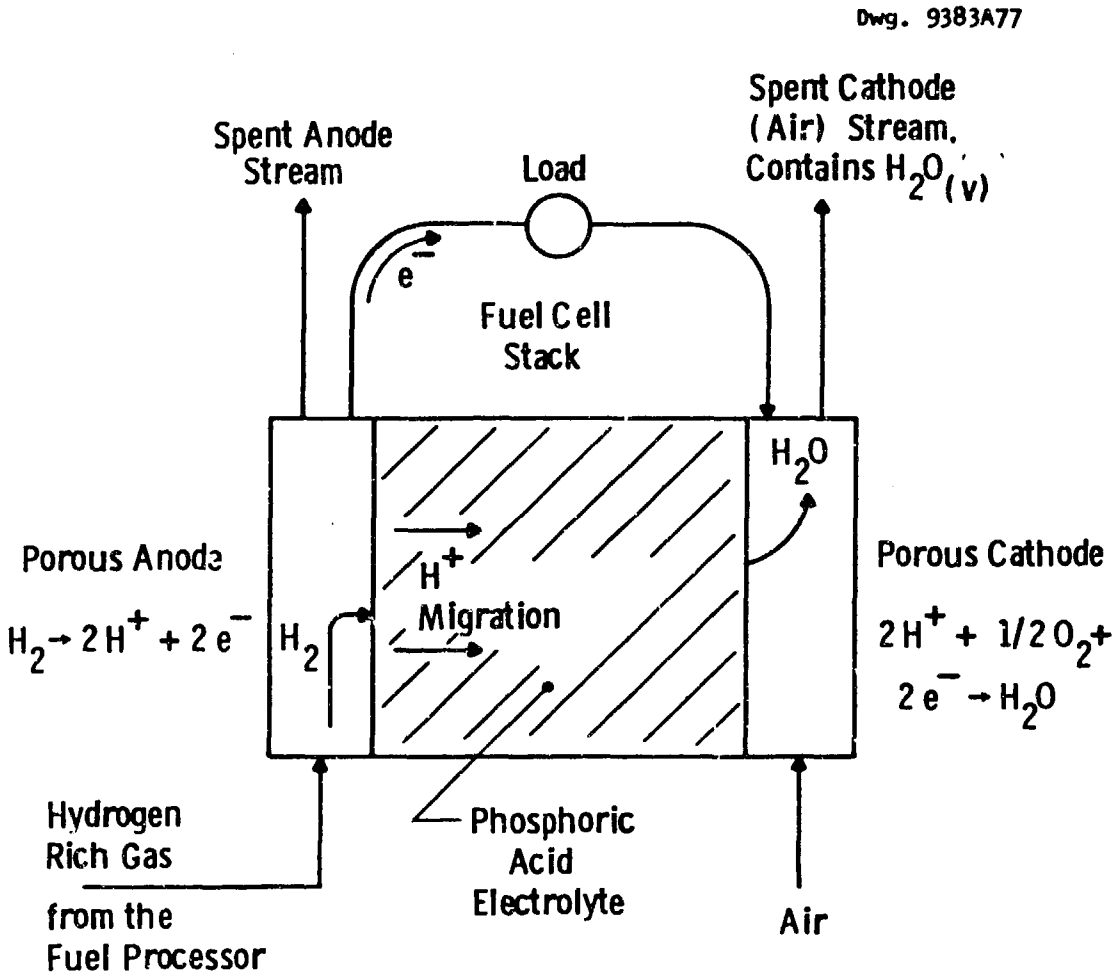

Figure 5.2 -- Simplified Fuel Cell Schematic

migration of the hydrogen ions to the cathode. At the cathode, the hydrogen combines with atmospheric oxygen to form water vapor, which leaves via the cathode exhaust (with traces of phosphoric acid). Hence,, the fuel cell reaction is:

$$H_{2(g)} + \frac{1}{2} O_{2(g)} \rightarrow H_2O_{(g)} \qquad (5.5a)$$

or, balanced for the methanol reforming reaction, Equation 5.1:

$$3H_{2(g)} + \frac{3}{2} O_{2(g)} \rightarrow 3H_2O_{(g)} \qquad (5.5b)$$

Therefore, the cathode exhaust gas contains approximately three times the water required by the fuel processor.

Consequently, cathode gas water recovery and recycle represents an alternative approach to autothermal reforming, although water condensation, purification, and surge storage are necessary.

Equilibrium calculations have been performed for the autothermal fuel processor using a chemical equilibrium program at the R&D Center. Figure 5.3 illustrates the results. For air combustion, the compositions remain unchanged above ~1140°K (1592°F): ~27% hydrogen, ~15% carbon monoxide, ~5% carbon dioxide, ~15% steam, and ~38% nitrogen. The high carbon monoxide concentration mandates an effective shift reactor prior to the fuel cell. Methane formation is a potential problem below ~900°K (1160°F). Figure 5.4 illustrates the equilibrium ammonia concentrations, as a function of reformer temperature. PAFC systems have ammonia tolerances in the 30-50 ppm range, and, consequently, it may not be an operational problem, although it could become a detection concern (the olfactory limit for ammonia is ~5 ppm). Figures 5.5 and

Curve 751924-A

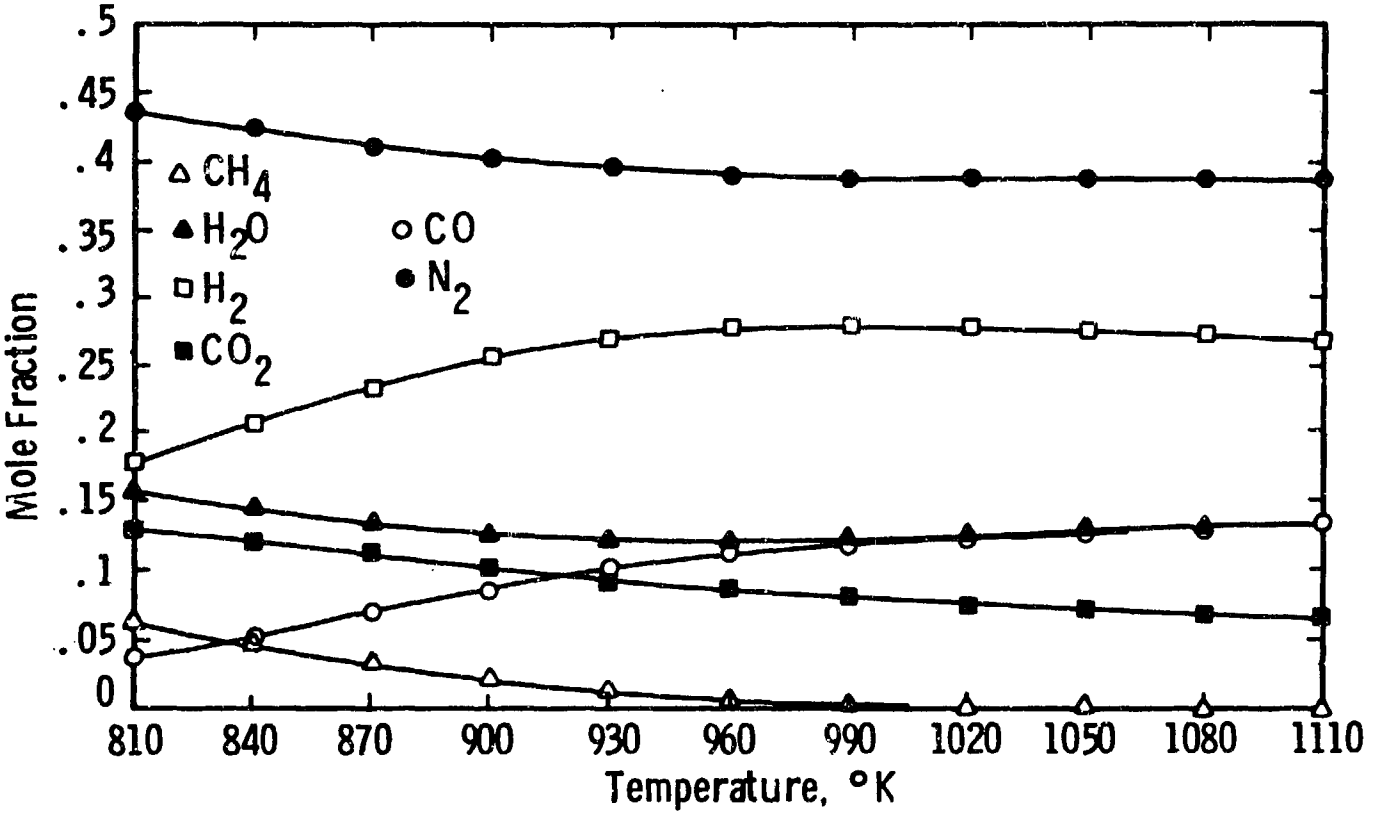

Figure 5.3A — Methanol Reformer-Equilibrium Results, 810-1100°K (1.5 atm)

Curve 751919-A

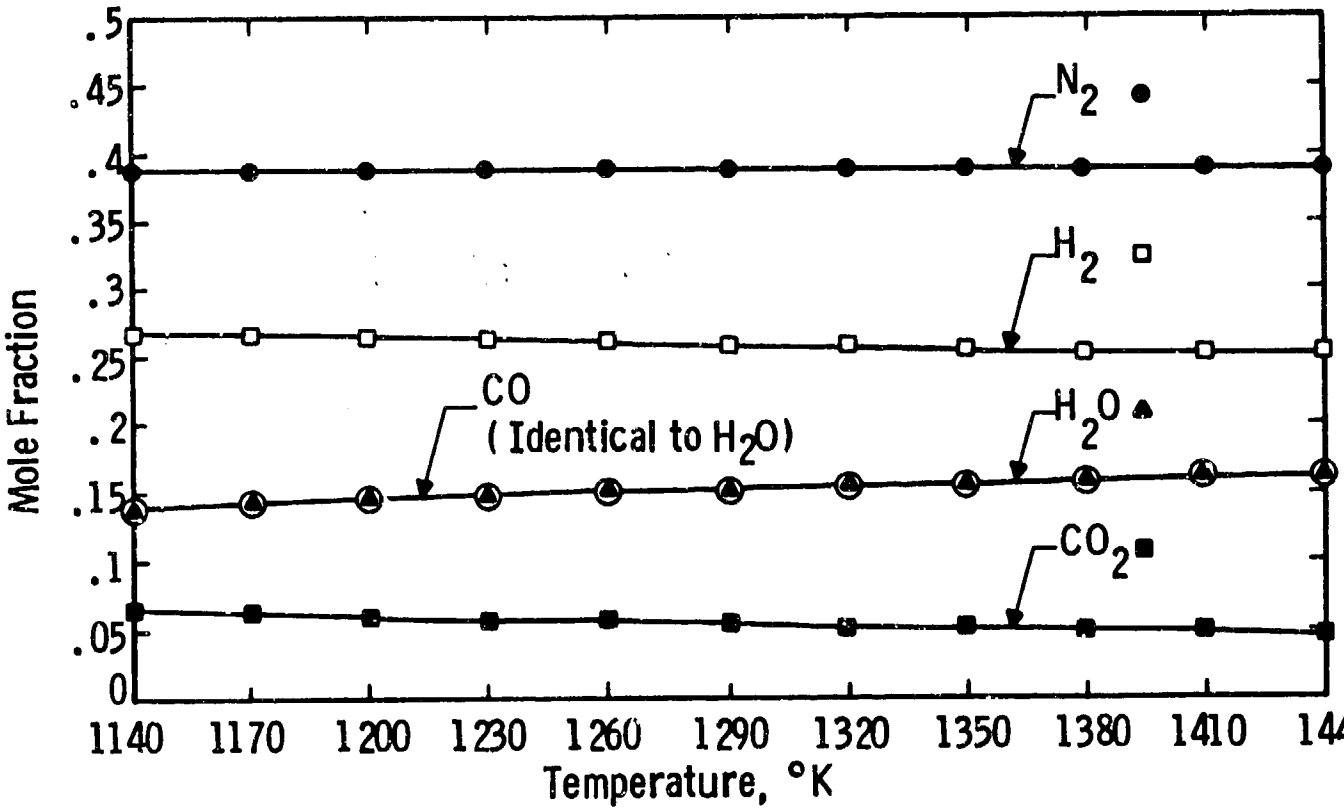

Figure 5.3B — Methanol Reformer-Equilibrium Results, 1140-1440°K (1.5 atm)

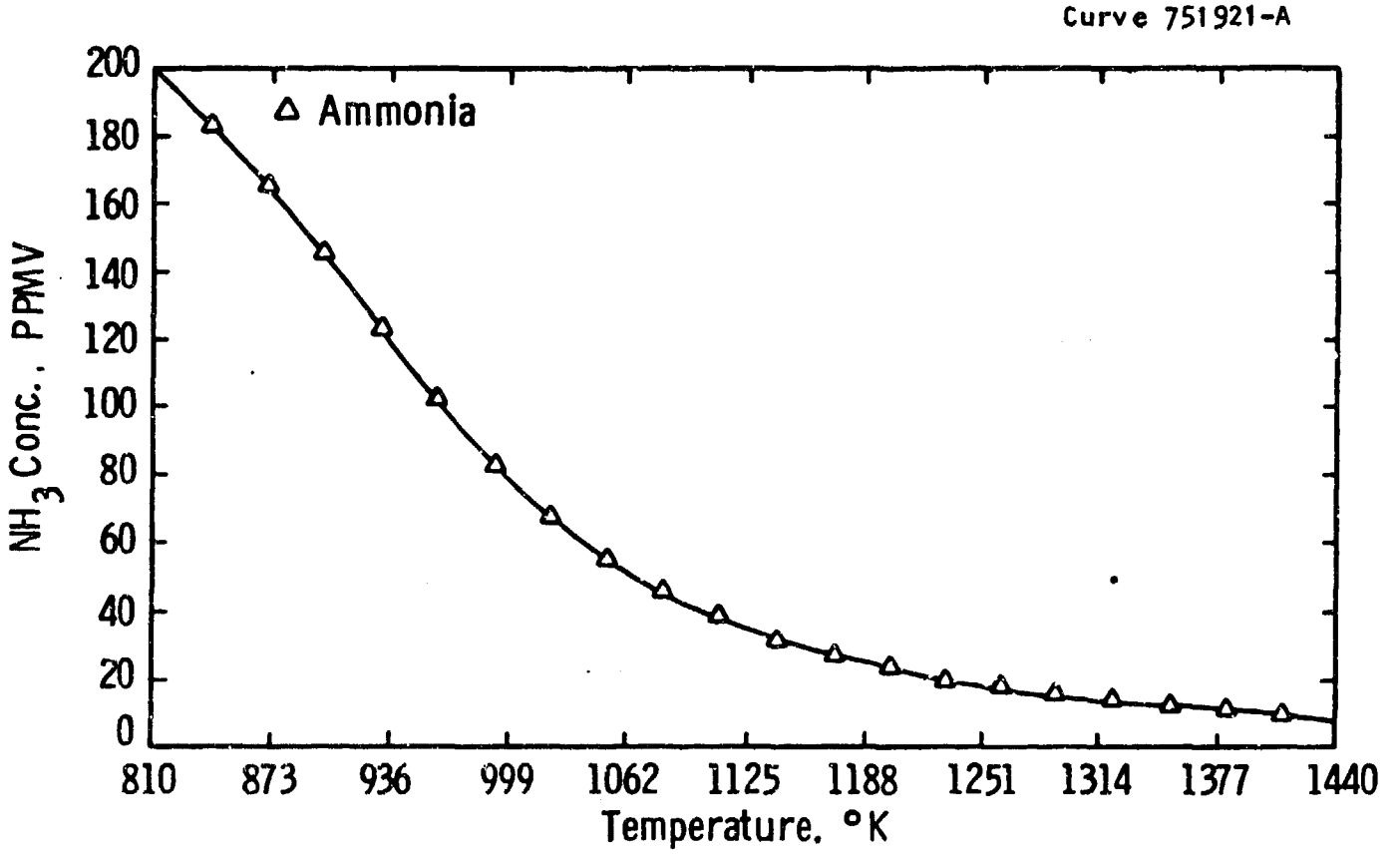

Figure 5.4 — Equilibrium Ammonia Concentrations for Autothermal/Air Case

Curve 751923-A

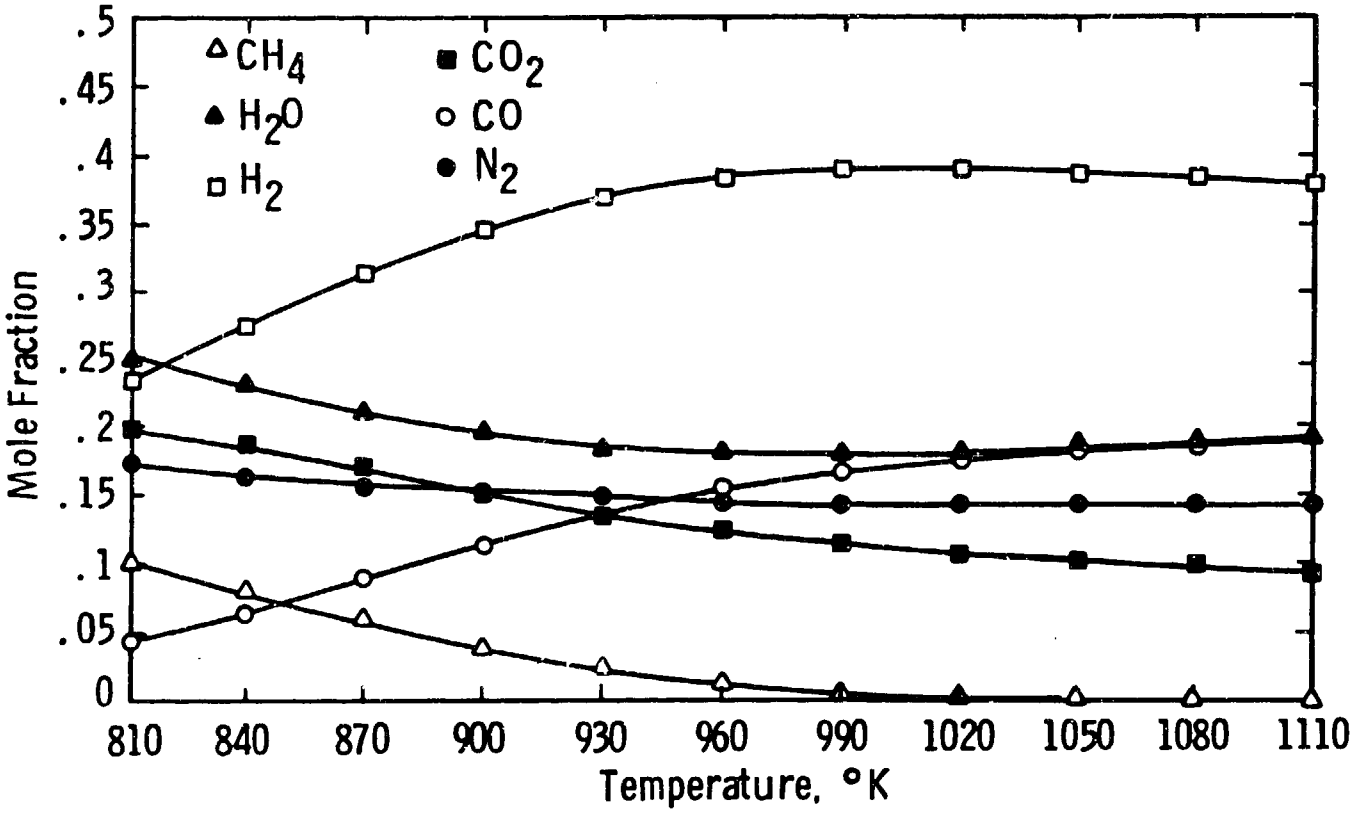

Figure 5.5 — Methanol Reformer-Equilibrium Results
Using 50% Oxygen for Combustion

5.6 display the same calculations for 50% oxygen in the combustion air, and the same trends are observed.

Figure 5.7 shows the enthalpy balance and expected temperatures for the methanol system air and 50% oxygen conditions. As expected, the burner/reformer temperatures are high: the burner exit temperatures are ~2100°F and ~2600°F for the two systems, while the reformer effluent temperatures are ~1330°F and 1640°F for the air and 50% oxygen conditions, respectively. These temperatures are neither prohibitively high nor beyond the current technology (e.g., steel manufacturing, aircraft/rocket engines, and MHD experiences). However, they necessitate careful design and fabrication to ensure adequate component life without premature failure.

5.2 DIESEL FUEL UTILIZATION

Diesel fuels are a mixture of components, and, unlike methanol, numerous reactions occur. Diesel oils are readily available, and, for Army purposes, represent the principal logistic fuels of interest. Table 5.1 lists the specifications for diesel fuels. There are three classifications for military applications.:

Military Symbol DF-A. Arctic-grade diesel fuel oil, for diesel/gas turbine engines and heaters, where ambient temperatures lower than -32°C generally occur (not for slow-speed engine use).

Military Symbol DF-1. Winter-grade diesel fuel oil for engine use, where ambient temperatures as low as -32°C may occur.

Military Symbol DF-2. Regular-grade diesel fuel oil, for engine use in temperate climates (used where the cloud point is at or below the location's tenth percentile minimum temperature, which normally corresponds to around -10°C).

Diesel fuel has a considerably larger specific combustion enthalpy than methanol, typically in the 19000-20000 BTU/lb range (LHV

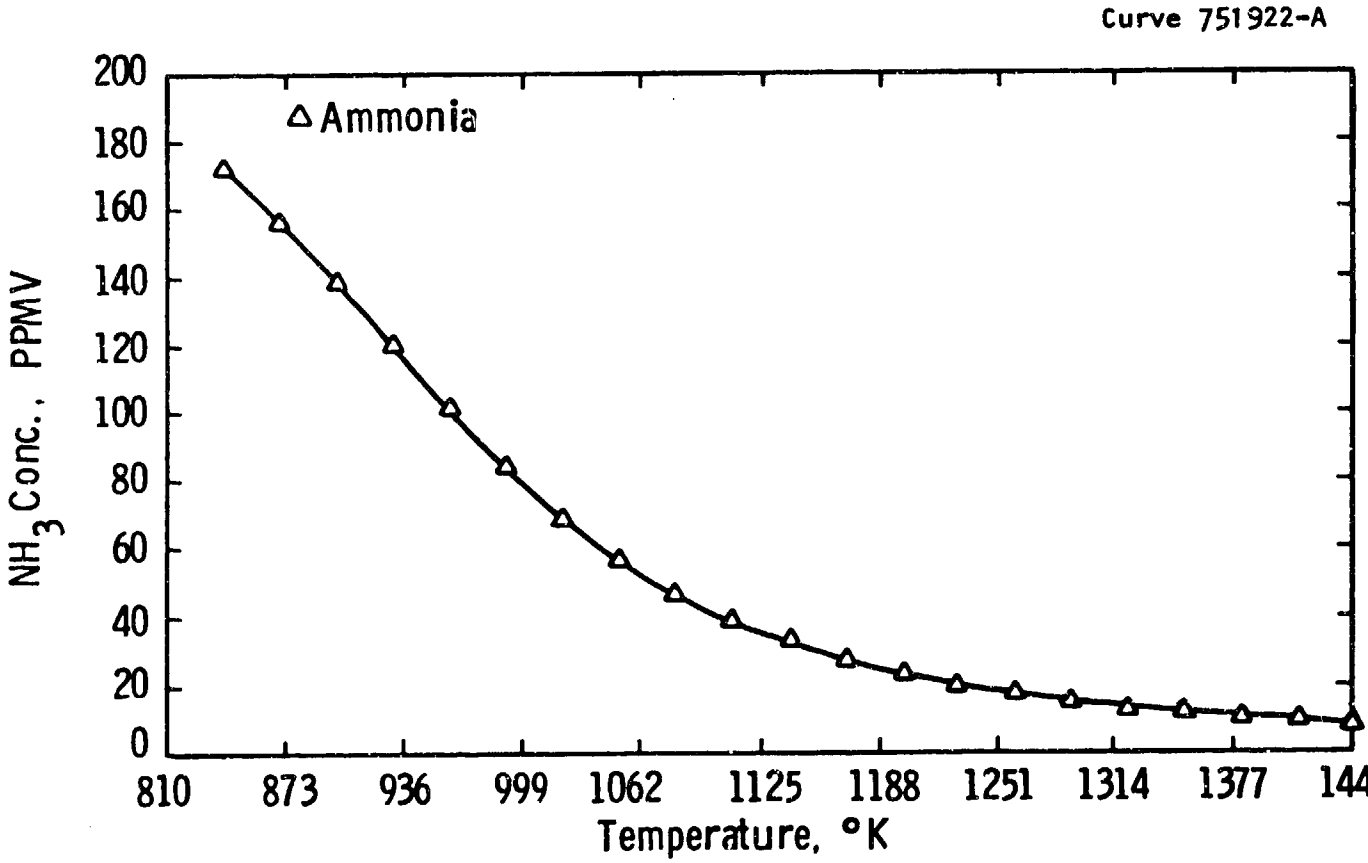

Figure 5.6 — Equilibrium Ammonia Calculations for Autothermal/50% Oxygen Condition

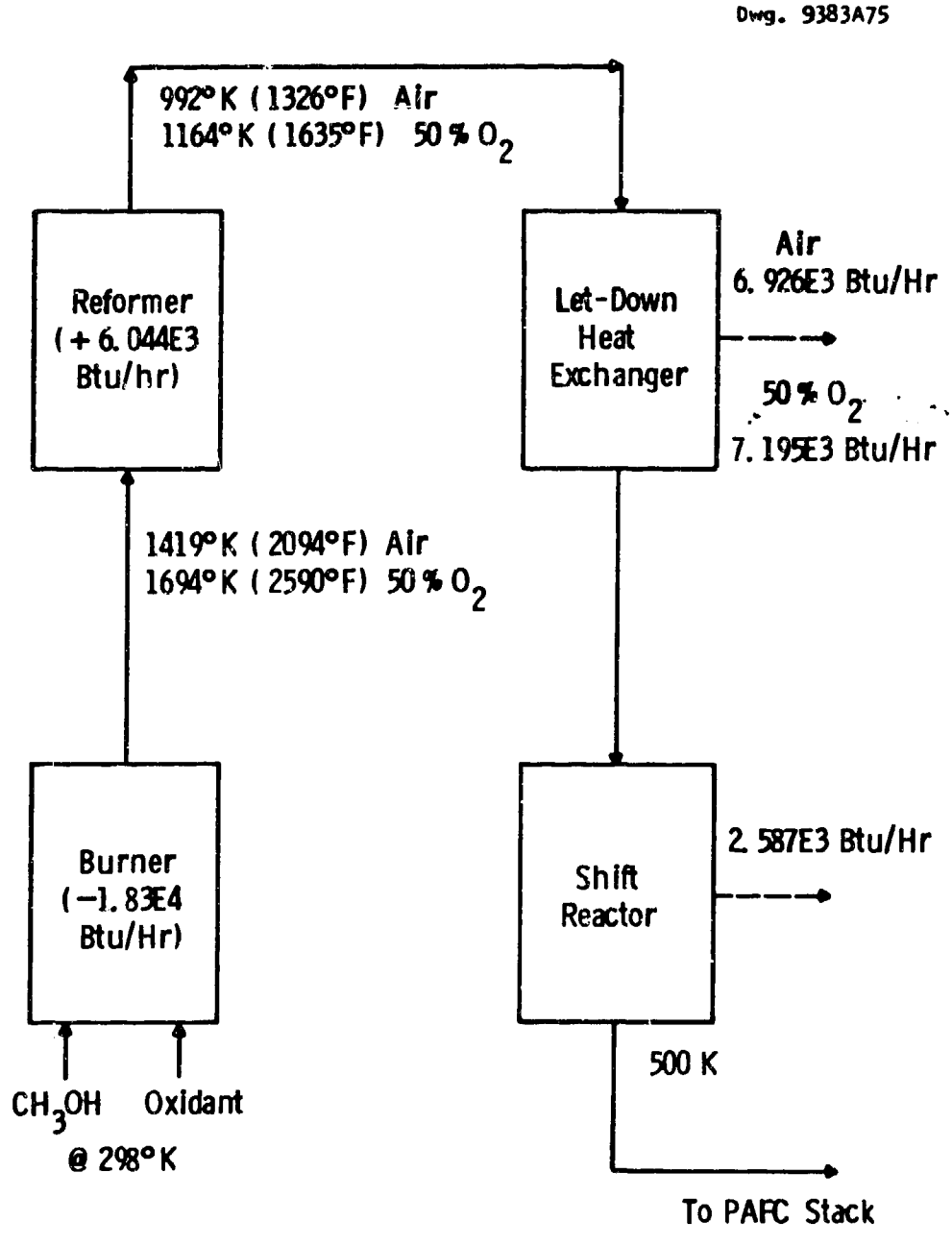

Figure 5.7 -- Methanol Autothermal Processor - Enthalpies and Temperatures

Table 5.1 -- Army Diesel Fuel Physical and Chemical Property Specifications*

	Values			
			Grade DF-2:	
	Grade DF-A	Grade DF-1	CONUS+	OCONUS+
Density, kg/L @ 15°C	Report	Report	Report	0.815 to 0.860
Flash point, °C min.	38	38	52	56(1)
Cloud point, °C max.	-51	(2)	(2)	(2)
Pour point, °C max.	Report	Report	Report	(3)
Kinematic viscosity @ 40°C (20°C), cSt	1.1 to 2.4	1.3 to 2.9	1.9 to 4.1	(1.8 to 9.5)
Distillation, °C:				
50% evaporated	Report	Report	Report	Report
90% evaporated, max.	288	288	388	357
End point, max.	300	330	370	370
Residue, vol. %, max.	3	3	3	3
Carbon residue on 10% bottoms, mass %, max.(4)	0.10	0.15	.35	.20
Sulfur, mass %, max.(7)	0.25	0.50	0.50	0.70
Copper Strip corrosion, 3 hrs. @ 50°C max. rating	3	3	3	1
Ash, mass %, max.	0.01	0.01	0.01	0.02
Accelerated stability, total insolubles mg/100 mL, max.(5)	1.5	1.5	1.5	1.5
Neutralization number, TAN, max.	0.05	--	--	0.10
Particulate contamination, mg/liter, max.	10	10	10	10
Cetane number, min.(6)	40	40	40	40

*MILSPEC VV-F-800C
+CONUS = Continental United States
OCONUS = Outside the Continental United States

Table 5.1 (continued)

(1) DF-2 intended for entry into the Central European Pipeline System shall have a minimum value of 58°C.

(2) As specified by the procuring activity based on guidance in the MILSPEC, Appendix A. DF-2 for Europe and S. Korea shall have a maximum limit of minus 13°C.

(3) As specified by the procuring activity. DF-2 for Europe and S. Korea shall have a maximum limit of minus 18°C.

(4) See MILSPEC, Appendix B. If the fuel contains cetane improvers, the test must be performed on the base fuel blend only.

(5) This requirement is applicable only for military bulk deliveries intended for tactical, OCONUS, or long term storage (greater than six months) applications (i.e., Army depots, etc.).

(6) If cetane quality is determined as calculated cetane index, the minimum cetane index shall be 43 for Grades DF-A, DF-1, and CONUS DF-2.

(7) Diesel fuel intended for consumption in Southern California shall meet the requirements of the Southern California Air Quality Management District and Air Resource Board, which currently limits sulfur in diesel fuel to .05 mass percent maximum.

of 134,500-141,600 BTU/gal). Consequently, for the same input energy requirements, the diesel fuel supply would be 55% less than the corresponding neat methanol feed stream. Therefore, there is great interest in running fuel cell systems on diesel fuels.

Diesel fuels do not reform easily. Effective reforming only occurs at high temperatures (~1500-1800°F) and high steam/carbon ratios (usually 3:1 to 4:1).[3-7] Higher temperatures reduce the steam requirements. Careful design and operation are necessary to avoid carbon deposition, particularly around the fuel atomization/mixing area. Sulfur-tolerant catalysts have to be used. Considering diesel fuel as $C_{10}H_{18}$, the overall reactions are:

$$C_{10}H_{18} + 20\ H_2O = 29H_2 + 10CO_2 \qquad (5.5)$$

$$CO + H_2O = CO_2 + H_2 \qquad (5.2)$$

Equation 5.5 represents a 2:1 steam/carbon ratio. Many intermediates exist during reforming, such as ethylene. These are affected by the catalyst type, and are briefly discussed in Section 5.3. The diesel fuel combustion reaction is:

$$C_{10}H_{18} + \left(\frac{29}{2}\right) O_2 = 10CO_2 + 9H_2O + \text{heat} \qquad (5.6)$$

For waterless, autothermal reforming, Equations 5.5 and 5.6 combine to yield:

$$C_{10}H_{18} + 10\ O_2 = 10\ CO_2 + 9H_2 \qquad (5.7)$$

The consequences of Equation 5.7 become:

1. Over 50% of the fuel has to be burnt to provide the steam and heat for the reformer reactions.

2. The reactions are extremely steam limited, primarily due to the low hydrogen content of diesel fuels.

3. Higher temperatures than the methanol case can be expected.

4. As with the methanol case, relatively high carbon monoxide concentrations can be expected, and a shift reactor will be necessary.

5. Equation 5.7 implies a maximum anode stream, hydrogen concentration of ~47% when pure oxygen is used. For air combustion, this value drops to ~16%, which is too low for fuel cell utilization. Consequently, methods for oxygen enrichment and/or hydrogen beneficiation have to be used.

Unlike the methanol example, cathode water recovery and recycle becomes a viable, almost mandatory approach. As presented in Section 6, the fuel cell utilizes ~80% of the input, anode hydrogen, which appears as water in the cathode exhaust gases. An ambient air condensor can recover ~69% of this water, or approximately 55% of the input hydrogen. Consequently, Equation 5.7 modifies to:

$$\frac{13}{9} C_{10}H_{18} + \frac{58}{9} O_2 + 16H_2O = 29 H_2 + \left[\frac{130}{9}\right] CO_2 \qquad (5.8)$$

Thus, cathode water recycle provides 80% of the water requirements at a steam/carbon ratio of 2. The remaining water comes from combustion of ~31% of the fuel feed. Therefore, an autothermal/cathode water recycle combination is a viable approach.

Figure 5.8 presents equilibrium results for the diesel fuel/air basic autothermal reformer conditions. The principal concentrations are essentially constant. Approximately 400 ppmv of hydrogen sulfide is present. The ammonia concentration decreases from ~50 ppmv to under 10 ppmv as the temperature increases. The CO/CO_2 ratio is approximately four. Figure 5.9 shows the equilibrium concentrations when 50% oxygen is used for combustion. The concentrations are constant above about

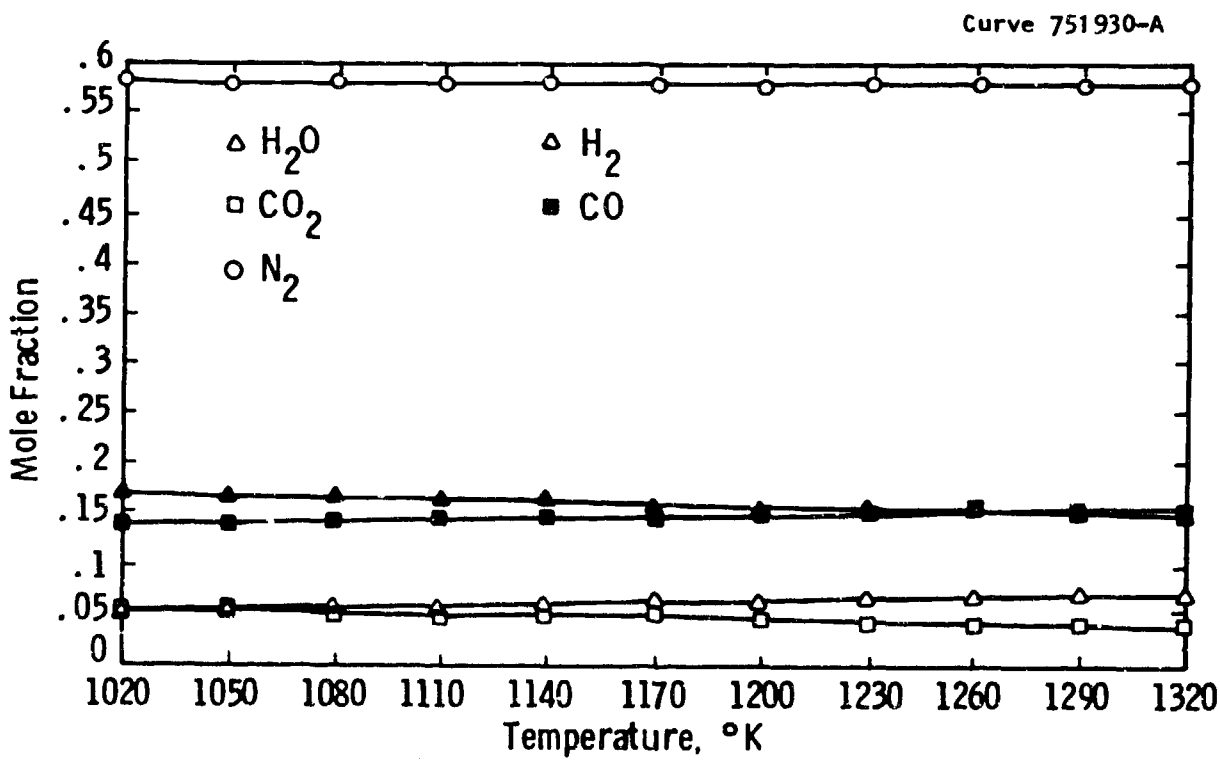

Figure 5.8A — Diesel Fuel/Air Autothermal Reformer Equilibrium

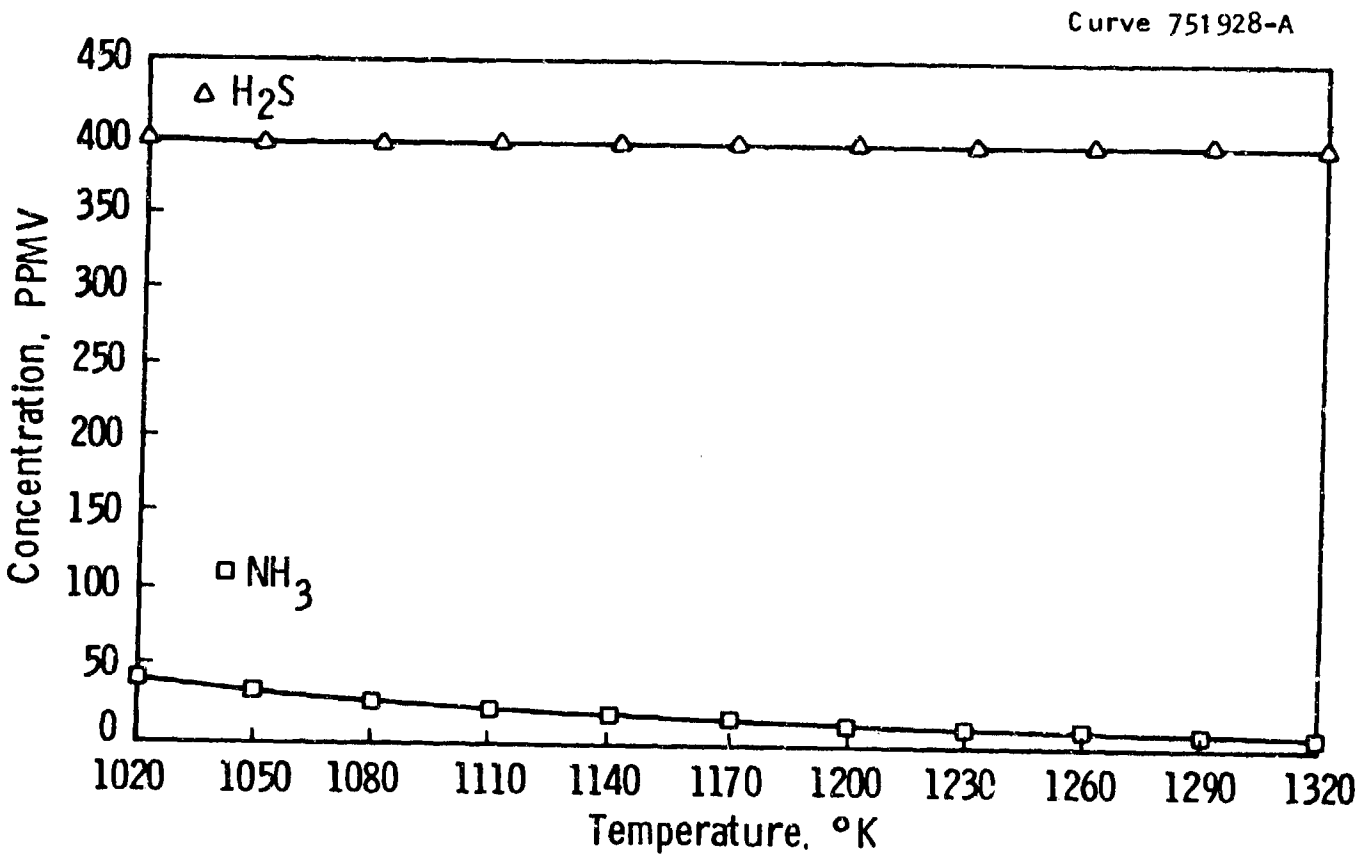

Figure 5.8B — Diesel Fuel/Air Autothermal Reformer Equilibria - Contaminant Values

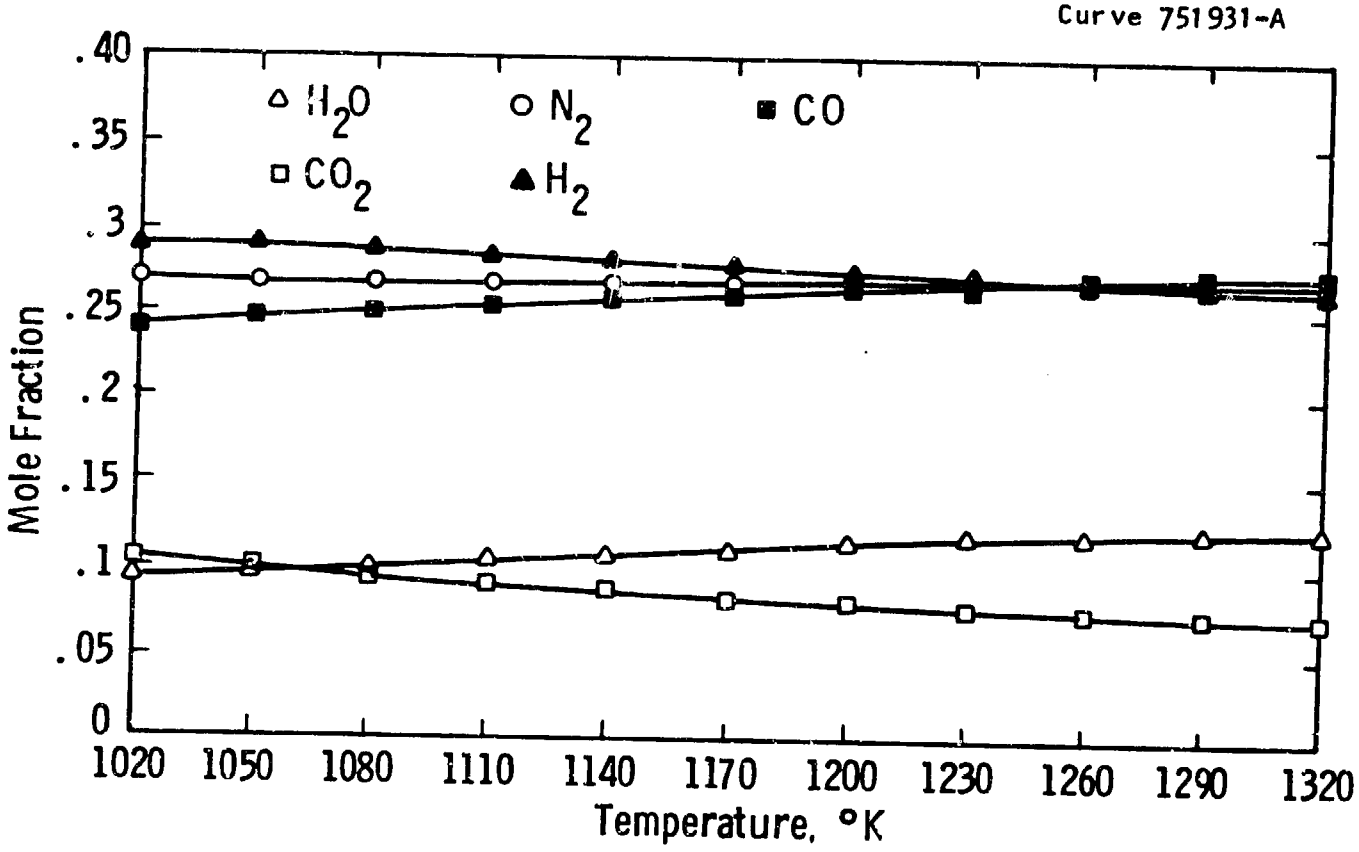

Figure 5.9A — Diesel Fuel/50% Oxygen Autothermal Reformer Equilibria

Curve 751929-A

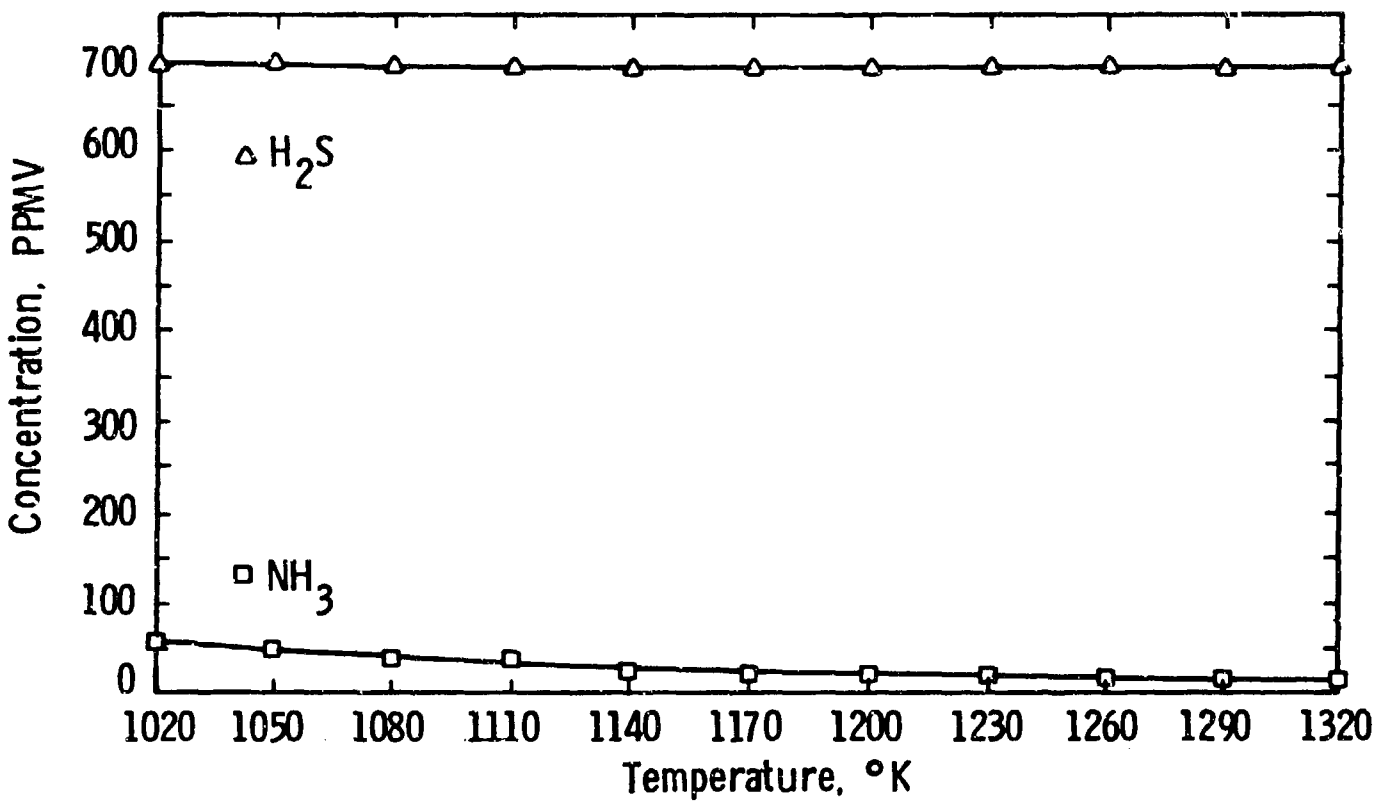

Figure 5.9B — Diesel Fuel/50% Oxygen Autothermal Reformer Equilibria - Contaminant Values

1260°K (1808°F). The CO/CO_2 ratio remains around four. The hydrogen sulfide concentration is higher (~700 ppmv) because of less nitrogen dilution. The ammonia concentration and dependency remains about the same: the reduced dilution and lower nitrogen concentration effects offset each other. In both examples, carbon formation is not thermodynamically favored above 1050°K, and additional oxygen is needed to complete the reactions.

The basic, autothermal diesel fuel processors generate ~86350 BTU/hr (21760 Kcal/hr) as waste heat, and achieve adiabatic, reformer exit temperatures of 3561°F and 5871°F for the standard air and 50% oxygen conditions, respectively. These values are unrealistic, but indicate prohibitively high temperatures are involved, and that too high a percentage of the fuel is being combusted. Application of the cathode water recycle method greatly ameliorates the situation. The exit reformer temperatures reduce to 1394°F and 1776°F for the air and 50% oxygen conditions, respectively. The latter temperature is probably the best for eliminating methane slip in the reformer effluent. The heat exhaust also decreases to ~25496 BTU/hr (~6425 Kcal/hr). Consequently, the combined autothermal/50% oxygen/cathode water recovery system becomes a practical approach.

5.3 FUEL PROCESSING APPROACHES AND CATALYTIC METHODS

Several different catalytic methods and approaches are possible with phosphoric acid fuel cell (PAFC) systems. Table 5.2 lists typical system characteristics. A reforming operation performs the initial lysis of the fuel molecules, and produces a hydrogen/carbon-oxides/steam mixture. If no adverse catalyst-sulfur reaction occurs, the bound sulfur in the fuel is converted into hydrogen sulfide (H_2S), which is subsequently removed by desulfurization treatment. Shift conversion reduces the carbon monoxide concentration to <1% via the water gas shift reaction. A final, small, adsorbent guard bed protects the fuel cell from residual levels of sulfur and halogens.

Table 5.2 -- Typical Fuel Processing Characteristics for PAFC Systems

PAFC System Characteristics

- Operating temperature: 350 to 400°F
- Pressure: 1 atm (1 to 5 atm for fuel processor)
- Feed steam/carbon ratio: ~3
- Tolerances: sulfur <5 ppm as H_2S, carbon monoxide <1% preferred, <3% acceptable
- Efficiency: ~40% (~8900 BTU/kWh) maximum

Fuel Processor Operations

- Reforming
- Heat exchanging (high temperature)
- Desulfurization
- Shift conversion
- Sulfur/halogen guard

Different catalysts and systems have been proposed for treating the feedstocks. Table 5.3 lists typical fuel processor catalytic operations, and Table 5.4 provides some specific catalyst examples. Gasoline reforming is similar to light naphtha reforming.[8,9] A steam/gasoline mixture is reacted over a nickel/alumina catalyst at 600 to 700°C, and, after a cooldown to 150 to 300°C, the carbon monoxide level is reduced in a shift reactor consisting of a copper/zinc oxide based catalyst. The fuel oils are more difficult to treat, and both autothermal (ATR) and high temperature steam reforming (HTSR) have been proposed and tested on a small scale.[3-5] With autothermal reforming (also called adiabatic reforming), air is introduced into the fuel/steam mixture, and a fraction of the fuel (typically 11 to 13%) is combusted. This causes a rapid temperature rise (to 1900 to 2000°F), and the gas mixture is passed through a noble (platinum) or nickel based catalyst bed. The sensible heat of the gas mixture provides the endothermic enthalpy of the reforming reactions. Hence, no external heat transfer is required, and the ATR reactor becomes simply an open pipe with a high temperature resistant lining (e.g., ceramic or Inconel). The ATR reactor effluent is subsequently cooled, desulfurized in a zinc or regenerable metal oxide desulfurizer, and shift converted as before. The ATR approach has the advantage of rapid transient response, but it also includes several distinct disadvantages which can limit its effectiveness. These are:

- It introduces a relatively large amount of nitrogen, which forms ammonia under the reducing conditions. This ammonia has to be removed before the PAFC stack.

- The ATR reactor temperature profile is similar to the hot stream in a co-current flow heat exchanger. Consequently, the last part of the catalytic reactor is poorly utilized, and unreacted hydrocarbons are present in the exit stream (i.e., a "methane slip"), resulting in less than one hundred percent conversion. High exit temperatures are required to alleviate this problem.

Table 5.3 -- Typical Fuel Oil, Fuel Processor Operations

Operation	Fuel	Catalyst	Conditions
Reforming**	Gasoline	Ni/alumina, Fe, Ru/SiO_2	600 to 705°C; no S or Pb; S/C* ~2.5 to 3.5
	JP-4	Ni/alumina, Fe, Ru/SiO_2	650 to 800°C; little S, no Pb; S/C ~3 to 3.5
	DF-2, DF-A	CaO/alumina	800 to 1050°C; tolerates S; S/C ~3.5 to 4+
Autothermal Reforming	Gasoline, JP-4, DF-2, DF-A	$Pt/Ni/Al_2O_3$ or Ni/Al_2O_3	up to 1100°F prefers low S; S/C ~3 to 4
Shift Conversion	Reformer effluent	Fe/Cr oxides (high) CuO/ZnO (low)	300 to 500°C, 150 to 300°C; no S or Pb; excess steam
Desulfurization	Reformer effluent	ZnO, Fe/Ni oxides	600 to 900°F max

* S/C is defined as steam/carbon molar ratio.

\+ Decreases to S/C ~2-2.5 above 2000°F.

** Methanol reforming can be accomplished over a low temperature shift catalyst (CuO/ZnO) at 400-500°F.

Table 5.4 -- Specific Catalyst Examples

- Reforming and Autothermal Reforming
  - Halder Topsoe RKN/RKNR (Ni/Al_2O_3)
  - United Catalyst C14-2-01 (Ni/Al_2O_3)
  - United Catalyst C15-1-04 (Cr_2O_3/Al_2O_3)
  - Toyo (T.E.C.) T12/T48 catalysts (calcia aluminates)
  - Ruthenium/silica catalyst (for gasoline)
  - Iron, Fisher-Tropsch catalyst (for gasoline)
  - United Catalyst G43-0379 ($Pt/Ni/Al_2O_3$)
- Shift Conversion
  - Halder Topsoe 201 ($CuO/ZnO/Cr_2O_3$)
  - United Catalyst C18 HC ($CuO/ZnO/Al_2O_3$)
  - Englehard "New Shift Catalyst" ($CuO/ZnO/ZnFe_2O_4$)

• The nickel based catalysts are inactivated by sulfur in the fuel (e.g., catalyst sulfidation) below ~1600°F, although the platinum-based catalysts are relatively unaffected. However, at temperatures above ~1650°F, platinum has a measurable vapor pressure,[2] and the catalyst will lose its activity over time.

• Fuel oils carbon deposit on both the nickel and platinum based catalysts, necessitating relatively high steam and air to carbon ratios, with projected frequent catalyst replacement.

• Electric Power Research Institute (EPRI) data and calculations indicate low overall PAFC system efficiencies of 10,500 to 11,000 BTU/kWh heat rate (i.e., efficiencies of 31 to 33%).

In contrast, the high temperature steam reforming (HTSR) route[3-7,10] is capable of overcoming many of these problems for fuel oil processing. The HTSR route uses a two catalyst system to steam reform fuel oils into hydrogen, carbon monoxide, and carbon dioxide at high temperatures (1500 to 2000°F). The "front-end" catalyst, designated T12, is a silica and nickel-free calcium aluminate containing a high loading of calcium (e.g., CaO/Al_2O_3). Table 5.5 presents the actual catalyst composition. The T12 catalyst serves three functions: it allows the fuel oil/steam mixture to be heated, it minimizes and/or prevents carbon deposition, and it performs the initial lyses of the fuel oils into simpler hydrocarbon molecules. This catalyst has a relatively low activity, typically 30 to 50% of commercial nickel reforming catalysts.

The "back-end" or polishing catalyst, designated T48, consists of nickel, calcium oxide, and alumina, and is similar to other commercial nickel reforming catalysts. The T48 catalyst reforms the mixture further, so that the effluent is essentially hydrogen, steam, and carbon oxides. Table 5.6 presents typical effluent compositions generated by EPRI.[1] It should be noted that a small amount of methane slip (up to

Table 5.5 -- Toyo Catalyst T12 Properties*

Form:	Ball (O.D.=5 mm)
Crush Strength:	200-400 kg/cm^2
Surface Area:	1.3 m^2/g, by BET
Apparent Specific Gravity:	4
Bulk Density:	1.3 g/cm^3
Chemical Composition (%):	
CaO	51.46
Al_2O_3	47.73
SiO_2	.06
Fe_2O_3	.18
MgO	.25
Na_2O+K_2O	.3
Chemical/Crystalline Form:	$Ca_{12}Al_{14}O_{33}$, $Ca_3Al_2O_6$

*from reference 6.

Table 5.6 -- Typical Toyo Effluent Compositions*

Species	T12 Only	(2/1) Volume Ratio, T48/T12
H_2	36	66.3
CO	8	14.2
CO_2	20	14.6
CH_4	34	5
C_2H_4	4	(-)
Total	100	100.1

*Space velocities of 0.825 - 1.81 kg(feed+steam)/(liter catalyst)(hr) at temperatures of 950° to 1000°C.
(From Reference 1)

~5) may be present in the T12/T48 combination effluent. Hence, a secondary, conventional nickel catalyst reformer is often necessary to complete the reformer reactions. The T12/T48 system also functions like a hydro-desulfurization catalyst, and consequently, the effluent sulfur is present as hydrogen sulfide. Therefore, the effluent gases should be cooled and desulfurized if secondary reformer treatment is necessary. This will avoid potential nickel catalyst sulfidation and inactivation, which occurs rapidly below 1500 to 1600°F.

Two other points deserve mention. First, the T12/T48 transition zone should be above ~1800°F to avoid carbon deposition. Second, it is unclear whether a different, higher activity catalyst (such as chromia/alumina) could be substituted for the T48 catalyst.

The T12/T48 HTSR system appears to be well suited to handle sulfur-containing fuel oils such as DF-2 and DF-A. The system would also be able to handle JP-4 and gasoline. The advantages of the T12/T48 system are:

1. Experimentally proven, stable, carbon-free operation on fuel oils, albeit in electrically heated reactors (EPRI tests).
2. Highly tolerant of sulfur.
3. No observed catalyst degradation.
4. Provides multi-fuel capability to the fuel cell system.

The disadvantages of this system are:

1. High temperatures required.
2. Elimination of methane slip requires a secondary reformer or high exit temperatures.
3. Limited, fundamental understanding of the kinetics/parameters, which makes design and scale-up difficult.

Small, experimental tests at Toyo, Kinetics Technology International (KTI), and United Technologies Corporation (UTC)[3-6] have demonstrated the ability of the T12/T48 catalyst system to steam reform fuel oils containing up to .5% sulfur, without catalyst deactivation or carbon formation problems. The following empirical rate equation was derived by UTC for the T12 catalyst:

$$\frac{-dP}{dt} = K \exp\left(\frac{-EA}{RT}\right) P_{Fuel} \qquad (5.9)$$

K is the frequency factor, lb mol/lb cat-hr psia
EA is the activation energy, cal/g-mole
R is the ideal gas constant, 1.99 cal/g mol °K
T is the absolute temperature, °K
P_{Fuel} represents the fuel partial pressure, psia
t is time, hours

UTC reports values of 8640 for K and 25000 for the activation energy. KTI developed a related expression:[4]

$$\frac{dC}{d\theta} = - K \exp\left(\frac{-EA}{RT}\right) \left(\frac{S_o}{C_o}\right)^2 C \qquad (5.10)$$

(S_o/C_o is the inlet steam to carbon molar ratio
C represents the fraction unconverted carbon
θ is the reactor space time, liters catalyst - hr/kg (feed+steam)

KTI assigned the values of ~30,000 kg(feed+steam)/(liters of catalyst) hr to K and ~30,400 for the activation energy EA. Hence, while the expressions are slightly different and do not illustrate the reaction mechanisms and intermediate products, both UTC and KTI analyses imply a

first order reaction with a high activation energy. These equations indicate a reactor volume of 5-7 liters is required for a 5 kW equivalent, diesel fuel reformer at 1900-2000°F.

Other, high temperature steam reforming catalysts are available, although even less experimental data is available. Therefore, it seems practical to pursue the autothermal approach to the waterless fuel processor utilizing HTSR catalysts, such as the T12/T48 combination, keeping in mind that the maximum system efficiency will be limited to ~33%. Consequently, four catalysts and one packing have been procured for the experimental section of the program. Table 5.7 lists the catalysts, manufacturers, and their properties. Figures 5.10-5.14 display catalyst samples in their as-received forms.

Numerous reactions occur during steam/diesel oil reforming, in both series and parallel combinations. Simplification is required for design and analysis. Figure 5.15 displays sample HTSR composition profiles for carbon-containing species generated from EPRI experimental data. These profiles imply the following:

- The fuel oil rapidly decomposes into fragments containing fewer than 4 carbon atoms.

- Methane, ethylene, carbon dioxide, and propylene appear to be primary reaction products.

- The slow carbon monoxide concentration rise suggests that it is formed from carbon dioxide via the water gas shift reaction.

- The low ethane (C_2H_6) concentration indicates that is is not a primary reaction product, and it is probably formed by the hydrogenation of ethylene:

Table 5.7 -- Catalyst and Packing Materials for the Experimental System

Catalyst Manufacturer/ Designation	Use	Form	Approximate Chemical Size	Bed Density (lb/ft^3)	Color/ Appearance	Lot #	Date Received
United Catalyst C15-1-04	Reformer	Cr_2O_3 on Alumina	1" OD x .7" H x .44" ID rings	75	Green rings	(-)	8/28/85
Toyo (Japan), T12S	Reformer	CaO on Alumina, with potassium	5 mm dia.	93.8	White spheres	600705	9/17/85
Toyo (Japan), T48S	Reformer	Ni on Alumina (perhaps Cr_2O_3 well)	5 mm dia.	112.5	Green spheres	600709	9/17/85
United Catalyst C7-2-01	Desulfurizer	ZnO	Pellets, ~1/8" dia. x 3/8" H	66	White pellets	(-)	3/31/85
United Catalyst C18HC-RS	Shift	Zn/CuO	Tablets, 1/4" dia. x 1/8" H	80	Black tablets, with some fine powder	85-01	5/1/85

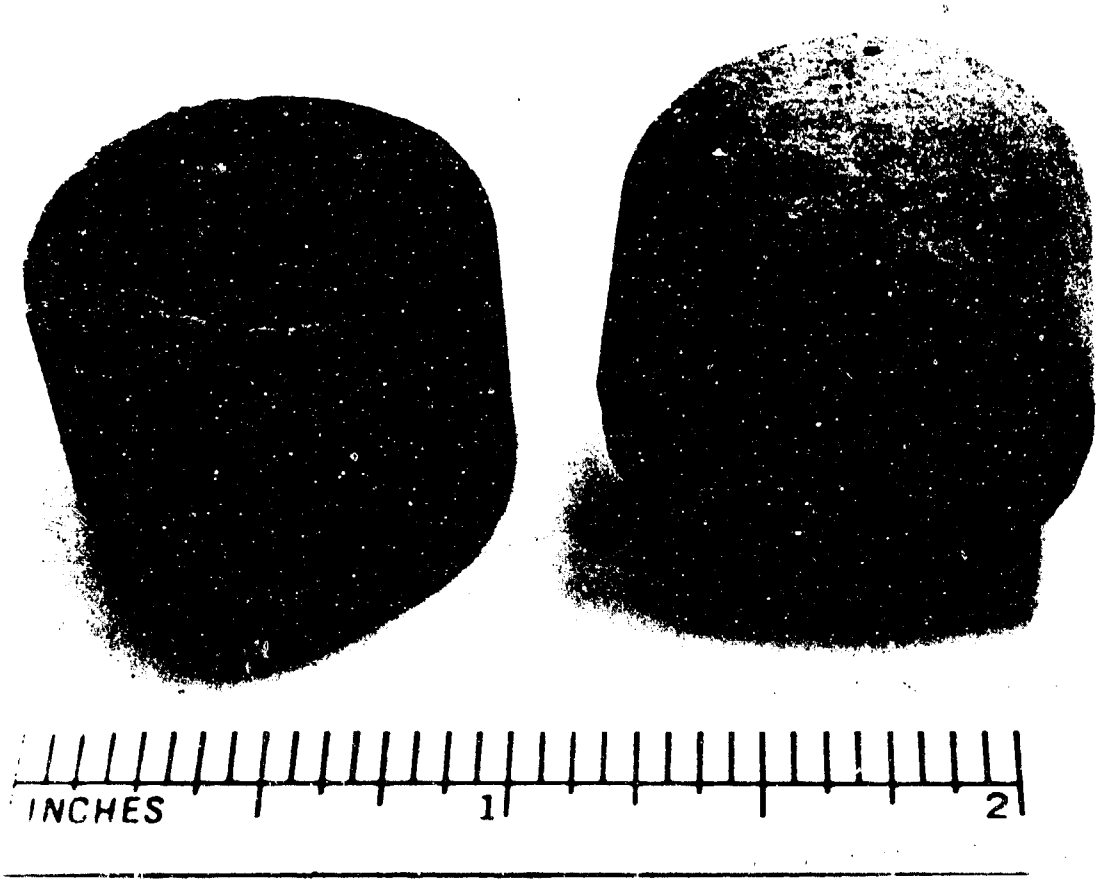

Figure 5.10 -- Chromia Reformer Catalyst C15-1-04

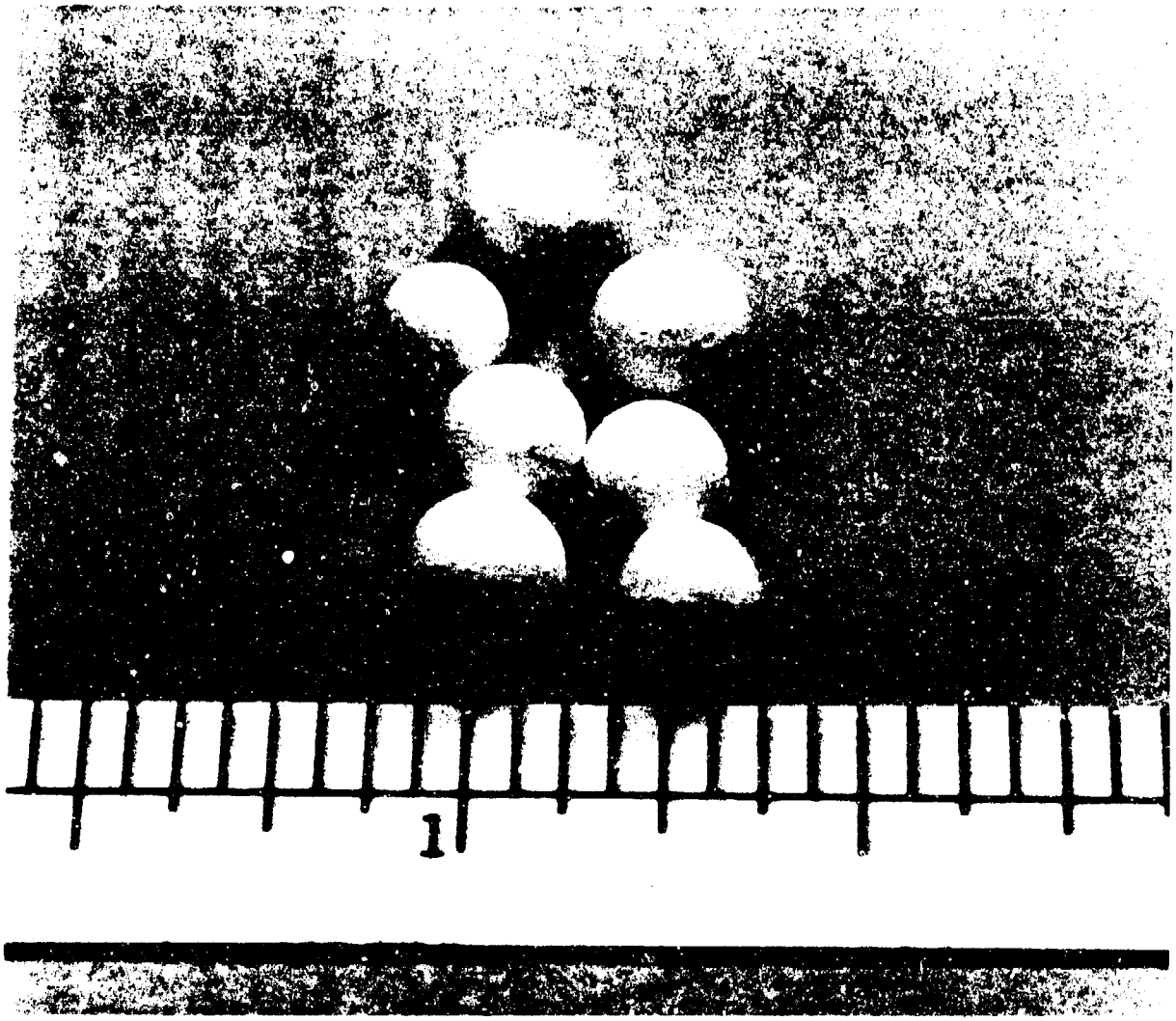

Figure 5.11 -- Toyo T12S Reformer Catalyst

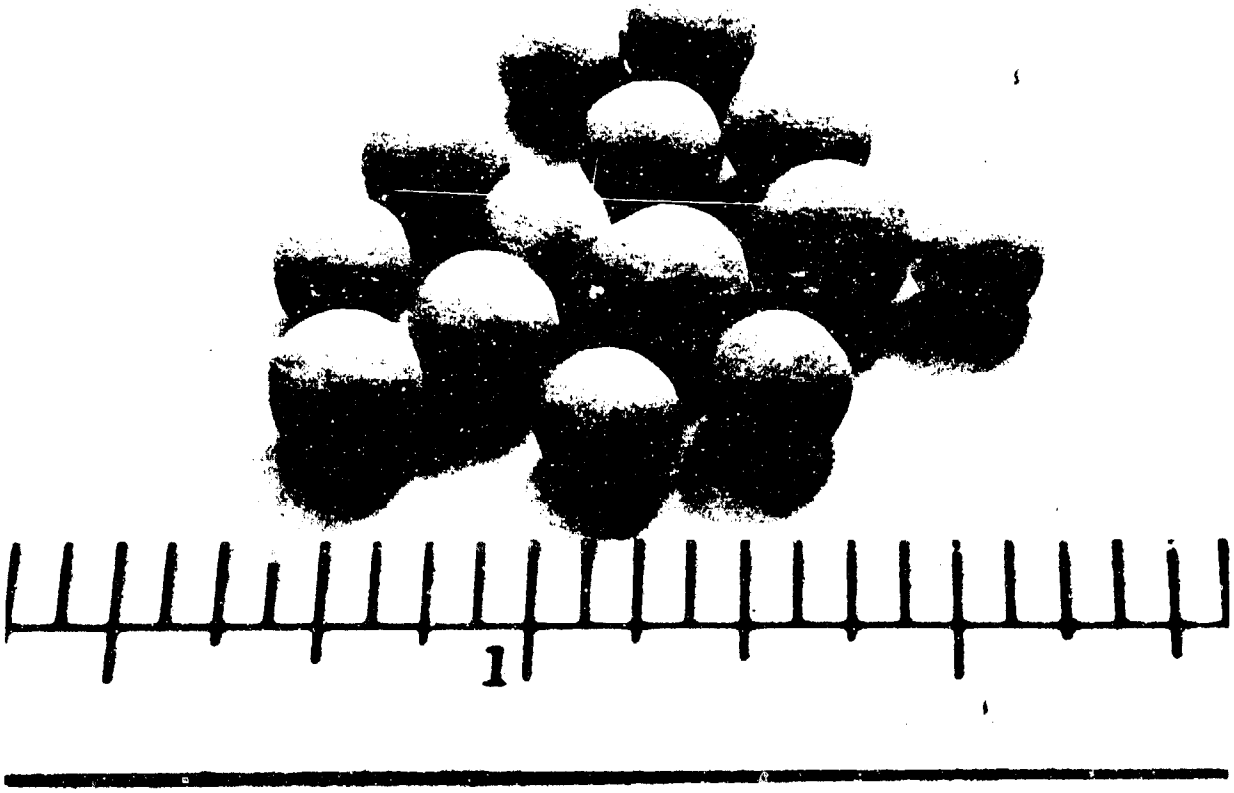

Figure 5.12 -- Toyo T48S Reformer Catalyst

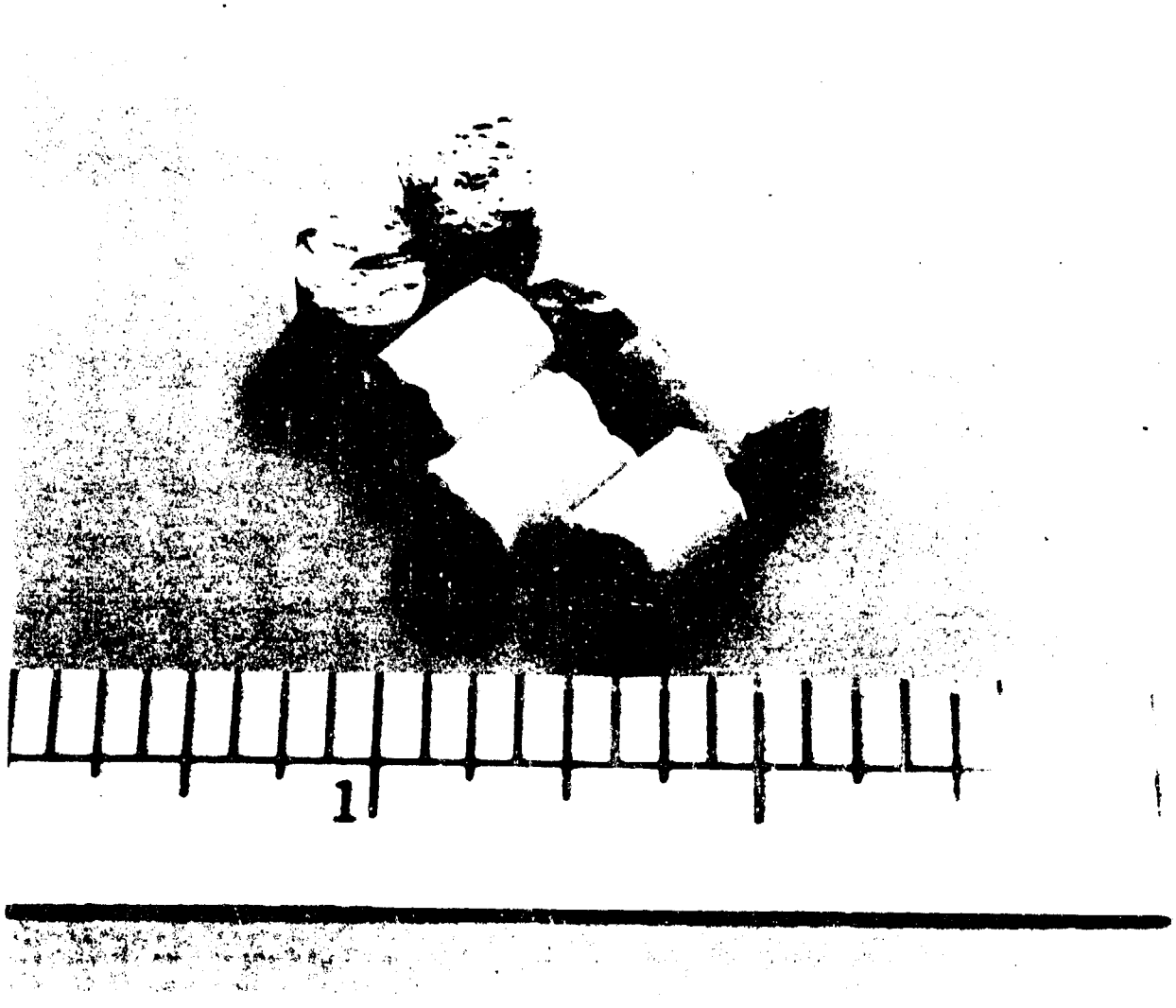

Figure 5.13 -- Zinc Oxide Desulfurizing Pellets (C7-2-01)

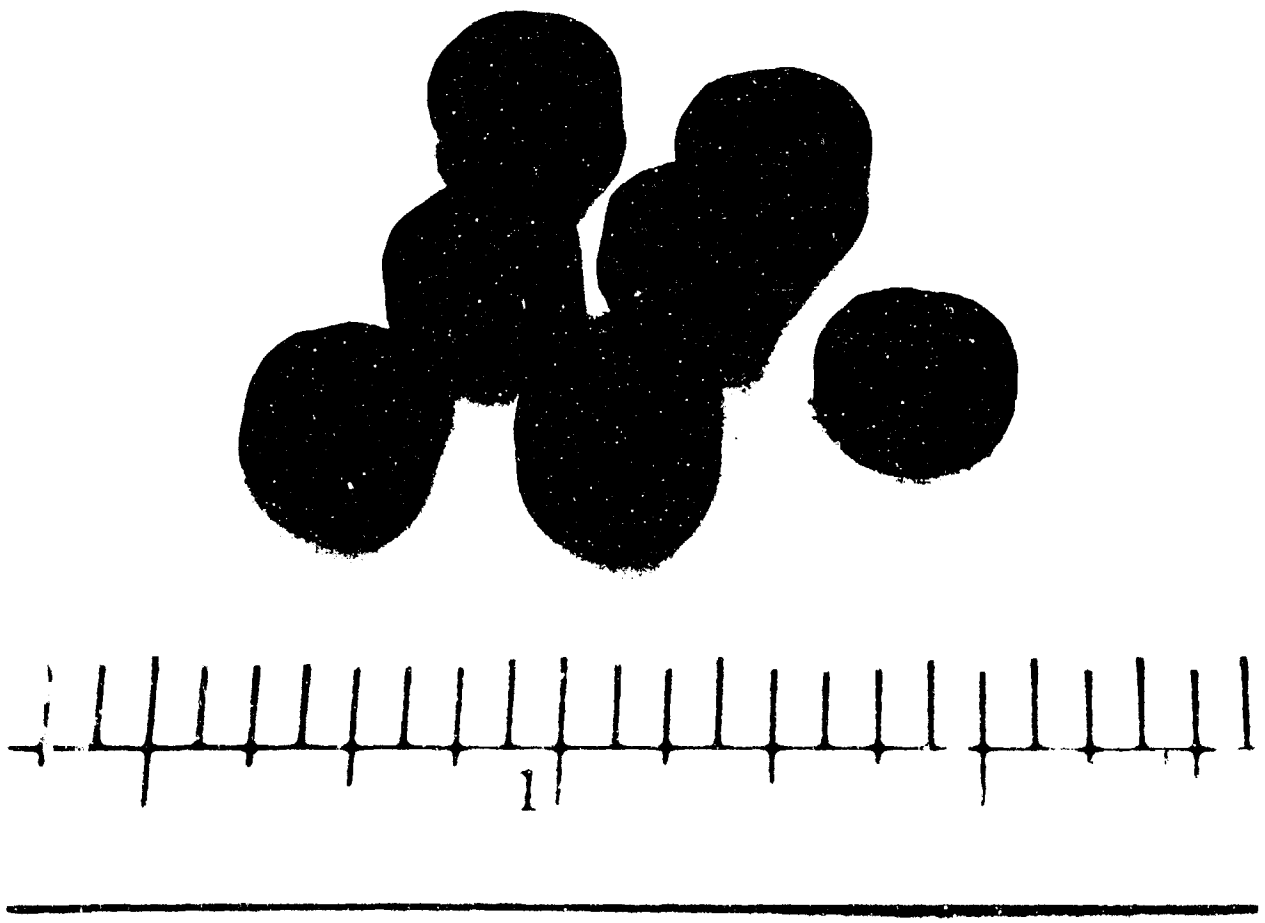

Figure 5.14 -- Shift Reactor Catalyst (C18HC-RS)

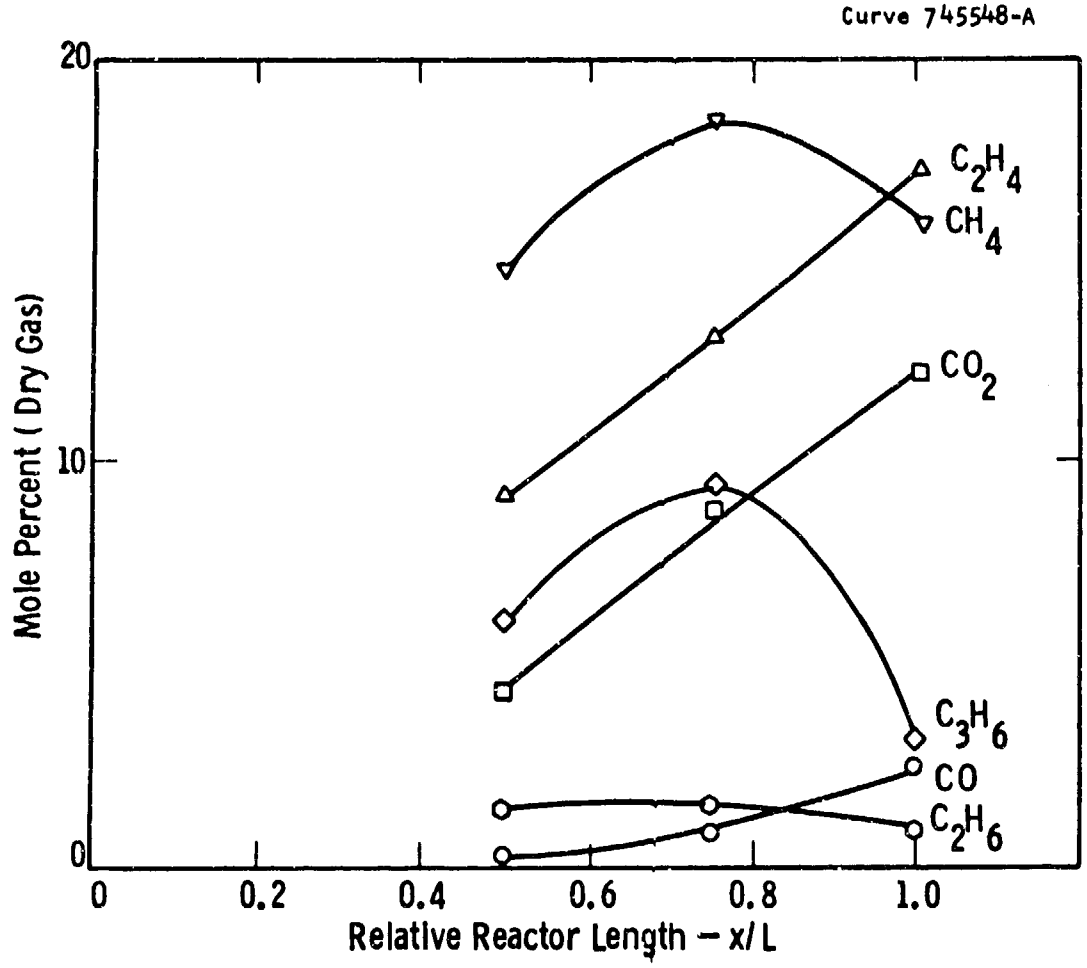

Figure 5.15 -- Sample HTSR Composition Profiles Using Fuel Oil Feedstock; (T12 Catalyst Only; Less Than 1 Mole % (dry); C_4 Detected at all Times).

$$C_2H_4 + H_2 \rightarrow C_2H_6 \quad (5.11)$$

• Both ethylene and propylene may evolve directly from the fuel oil fragmentation, although the rapid decrease in propylene near the reactor exit coupled with the continued increase in ethylene concentration suggests that propylene may be the principal fuel oil fragment, and it subsequently reacts to form ethylene.

• In the hydrogen-rich environment of the HTSR, ethylene should hydrocrack to methane.

• Bound sulfur (e.g., in mercaptans) should be converted into hydrogen sulfide.

Therefore the following reaction scheme can be postulated such that it does not contradict the experimental data presented in Figure 5.15:

Fuel Oil	→ propylene	(5.12)
Propylene	→ ethylene	(5.13)
Ethylene	→ methane	(5.14)
Methane	→ carbon dioxide	(5.15)
$CO + H_2O$	→ $CO_2 + H_2$	(5.16)

The reaction scheme of Equations 5.12 through 5.16 represents a simplified but plausible model for the HTSR, allows intermediate prediction, and should not be calculationally intractable.

Fuel oil is a mixture of many different hydrocarbons. Typically, fuel oil only contains the elements of carbon, hydrogen, and sulfur with a hydrogen/carbon molar ratio of ~1.8. There are usually between nine and sixteen carbon atoms per fuel oil "molecule." The principal hydrocarbon constituents are saturated paraffins, naphthenes (alicyclical ring compounds, such as cyclohexane), and aromatic

compounds (e.g., benzene, toluene, etc.). For the sake of mass and reaction balancing, fuel oil can be characterized by the following, semi-empirical formula:

$$\text{Fuel Oil} = [C\ H_{CX}\ S_{CY}]_{CZ} \tag{5.17}$$

where CX and CY represent the molar ratios of hydrogen and sulfur to carbon, respectively, and CZ represents the average number of carbon atoms per molecule as determined by a molecular weight analysis. All three "characteristics" (CX, CY, CZ) are easily determined by standard analytical techniques. Consequently, one can insert the simplified formula Equation 5.17 into the proposed reactions, Equations 5.12 through 5.16, to obtain balanced equations. These equations are presented in Table 5.8. Overall system balances can be estimated from these reactions. For example, for a C_{12} diesel oil, the overall reforming reaction can be represented by Equation 5.18:

$$(CH_{1.8}S_{.01})_{12} + 24\ H_2O = 34.68\ H_2 + 12\ CO_2 + 0.12\ H_2S \tag{5.18}$$

The R&D Center has developed a kinetic based computer model for the design and analysis of fuel processors in diesel oil fed, PAFC systems.[10] This model is termed PLUTO. The model assumptions are listed in Table 5.9 using the reaction basis of Table 5.8. Figure 5.16 displays the general model geometry. Eleven components are followed, and the program can model two catalyst systems. The model considers a reformer tube heated by a separate combustion gas stream. Consequently, as an approximation for autothermal reforming, the heat transfer variables are equated to zero. The analysis of the 5 kW reformer (1.3' high x 5" I.D.) considers a low activity catalyst only (e.g., the T12), with 5 kW equivalent diesel fuel and air flow rates. Figure 5.17 shows the expected conversion to carbon oxides (complete conversion). For conversions of ~90%, inlet temperatures of ~2600°F are necessary.

Table 5.8 -- Fuel Oil HTSR Reaction Basis

Reaction 1: if CX ≤ 2:

$$[CH_{CX}\ S_{CY}]_{CZ} + CZ\ (2\text{-}CX)\ H_2O = \frac{(CZ)\ (CX)}{6}\ C_3H_6 + \frac{CZ}{2}\ (2\text{-}CX)\ CO_2 + CZ(2 - CX - CY)\ H_2 + (CZ)(CY)\ H_2S \quad (5.19a)$$

Reaction 1: if CX >2:

$$[CH_{CX}\ S_{CY}]_{CZ} \xrightarrow[\text{heat, catalyst}]{} \left[\frac{CZ}{3}\right]\ C_3H_6 + (CZ)\ (CY)\ H_2S + CZ\ (CX - 2 - CY)\ H_2 \quad (5.19b)$$

Reaction 2:

$$2\ C_3H_6 \rightarrow 3\ C_2H_4 \quad (5.20)$$

Reaction 3: ethylene hydrogenation

$$C_2\ H_4 + 2\ H_2 \rightarrow 2\ CH_4 \quad (5.21)$$

Reaction 4: steam/methane reforming

$$CH_4 + 2\ H_2O \rightarrow CO_2 + 4\ H_2 \quad (5.22)$$

Reaction 5: water gas shift reaction

$$CO + H_2O \leftrightarrow CO_2 + H_2 \quad (5.23)$$

Table 5.9 -- PLUTO Reformer Model Assumptions

1. Unidimensional (i.e., plug) flow.
2. Uniform catalyst particle temperature, which is the same as the local gas temperature.
3. Negligible intra-particle diffusion.
4. Pseudo first-order kinetics, that represent a global (overall) rate for the catalyst.
5. A five reaction basis (Table 5.8) that includes eleven components.
6. No carbon deposition.
7. Ideal gas behavior.
8. Negligible manifold and entrance effects.
9. Negligible heat losses to the environment (<10% of the total heat duty).
10. The Ergun equation models bed pressure drops adequately.
11. Forced-convection heat transfer only.
12. A single reformer tube is analyzed. Thus, all tubes behave independently of each other.
13. Olefinic-type (fuel oil) or methane feedstocks are used. (The model can be used as an approximation for naphtha [paraffinic] feedstocks, but the physical properties and reaction routes may not be estimated correctly.)

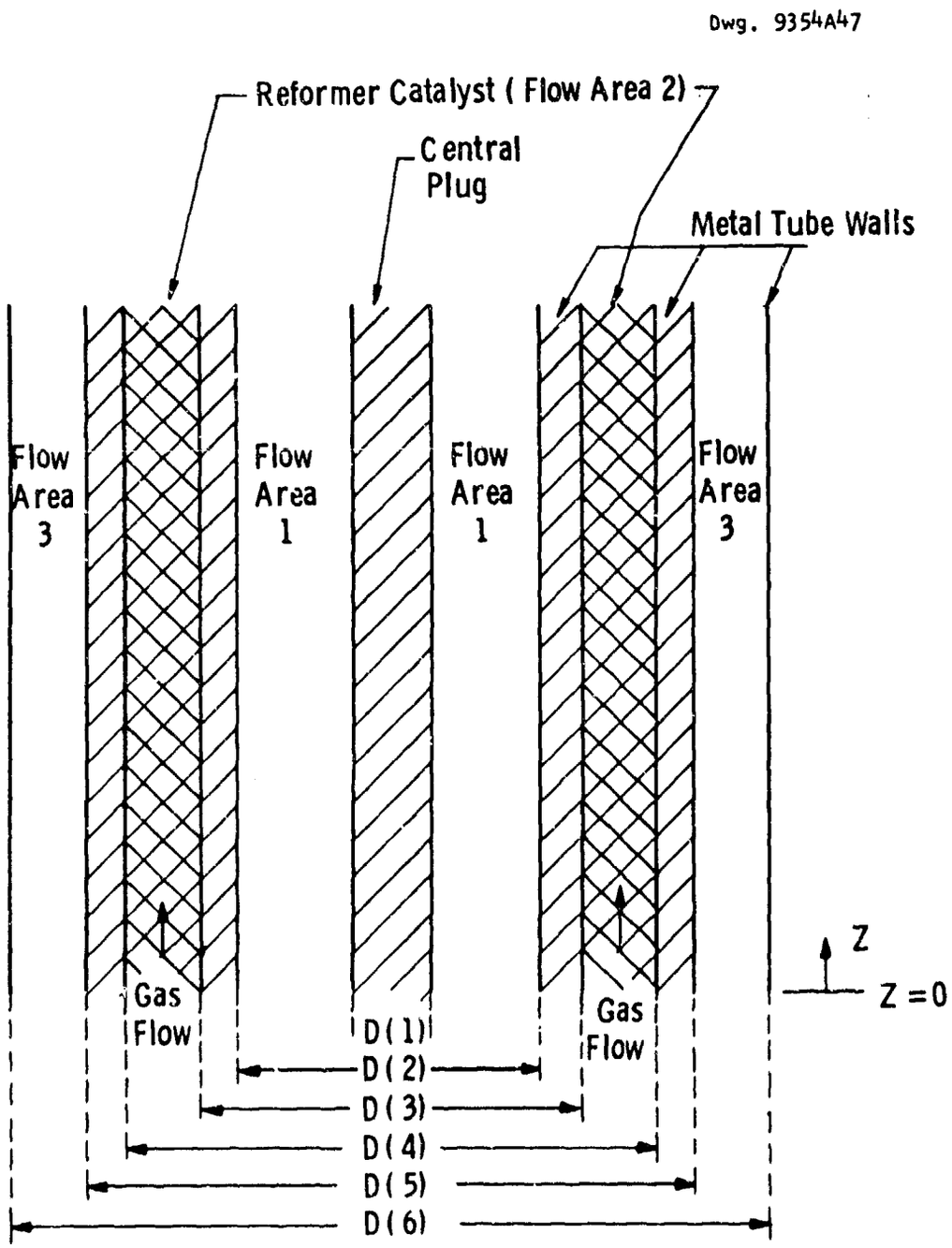

Figure 5.16 -- PLUTO Model Dimensions (Tubular Geometry-Cross Section)

Curve 751920-A

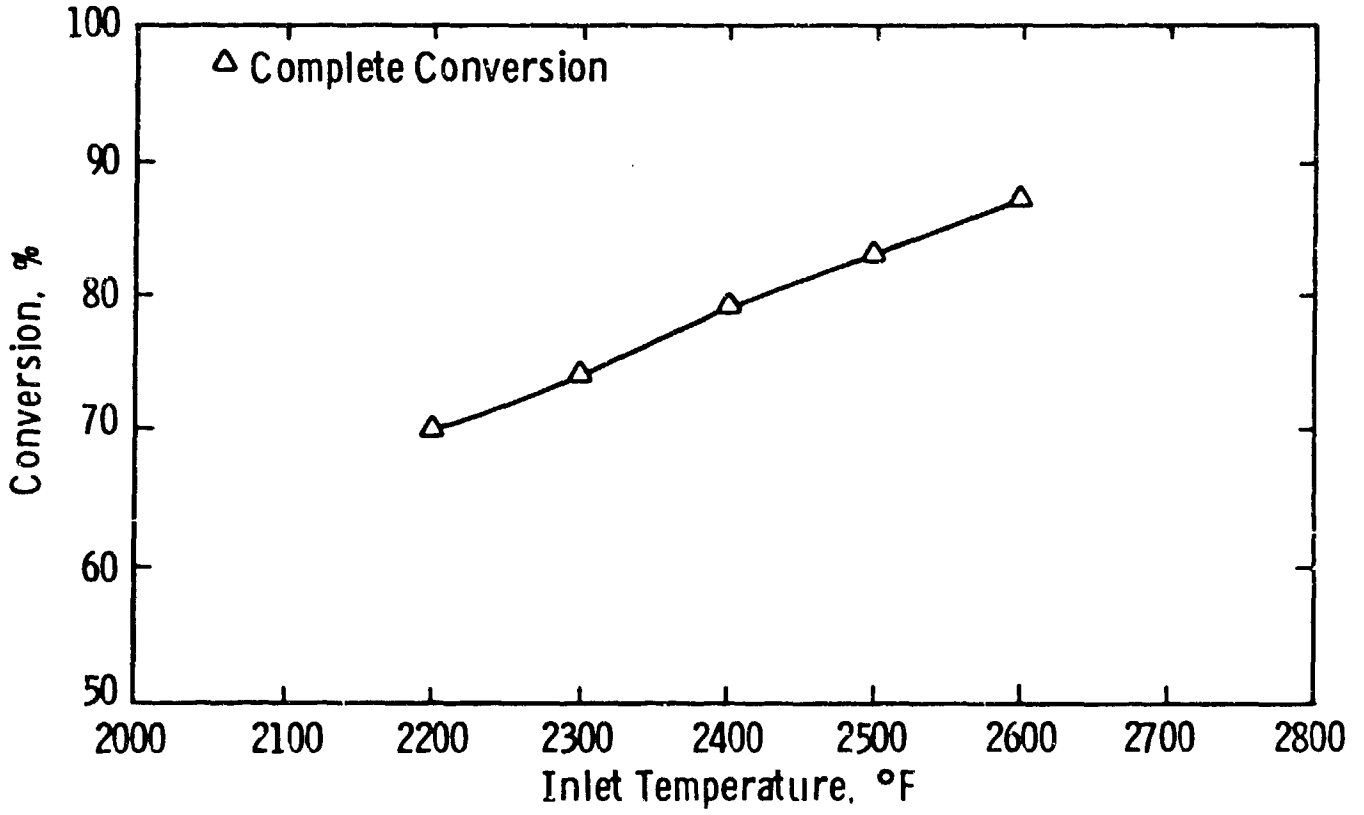

Figure 5.17 — Kinetic Program Calculation of Experimental System Conversion

Figure 5.18 shows the calculated exit temperatures: as expected, higher temperatures correspond to better conversions. Use of a higher activity catalyst (such as a 50-50 mixture of T12/T48) would increase conversion and reduce the exit temperature. Figures 5.19 and 5.20 depict calculated temperature and conversion axial profiles. These figures display the anticipated, co-current flow-like behavior. Therefore, the analyses imply:

- The experimental reformer design is probably adequate for 5 kW equivalent flow rates.
- High inlet temperatures (~2500°F) will be necessary, with correspondingly high reformer exit temperatures (>1500°F).
- A catalyst activity higher than T12 alone will be necessary.
- These calculations considered the autothermal/air cases, and over 60% nitrogen is present in the effluent. Consequently, the use of oxygen-enriched air will be mandatory.

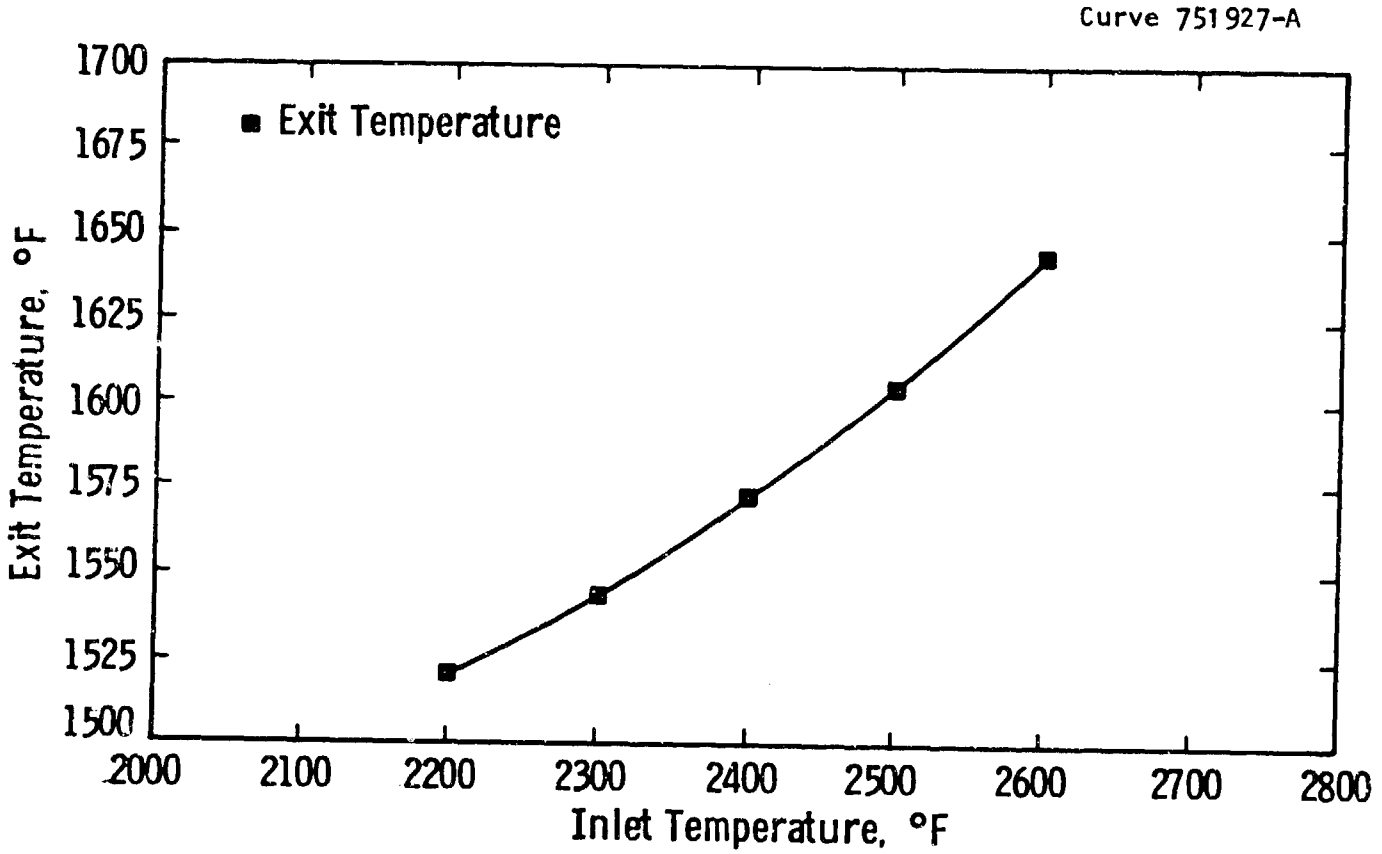

Figure 5.18 — Program Calculated Exit Temperatures

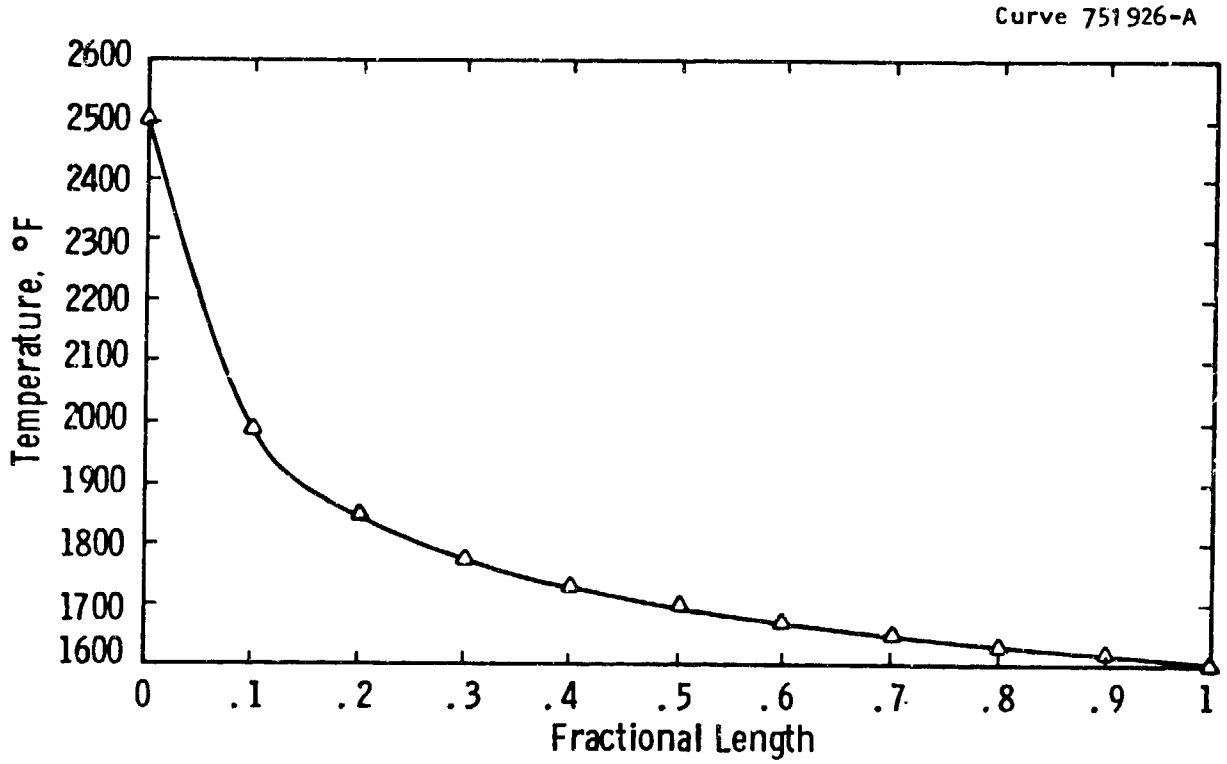

Figure 5.19 -- Calculated Autothermal Reformer, Axial Temperature Profile

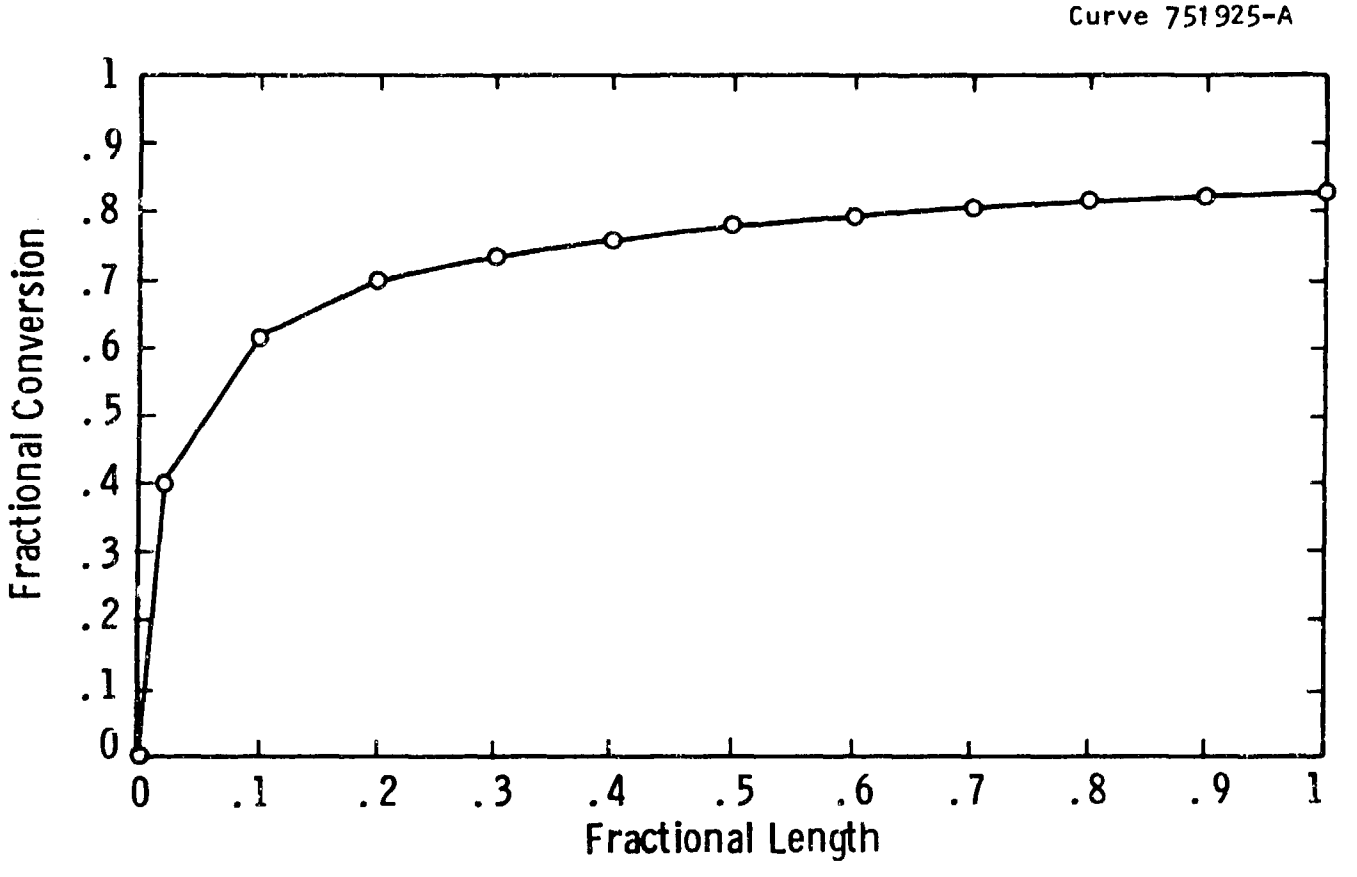

Figure 5.20 -- Calculated Autothermal Reformer, Axial Conversion Profile

6. Conceptual Advanced Fuel Processor Designs for a 5 KW, PAFC System

Several fuel processor designs have been formulated and analyzed. Figures 6.1-6.6 illustrate these designs, and Tables 6.1-6.6 present the corresponding state points. Stream and system integration are minimal in these preliminary designs, and, for uniformity, a fuel feed rate of 1.0 gph is assumed for all the designs. Figure 6.1 displays the basic fuel processor arrangement. Fuel is atomized at two locations in the burner: the primary nozzle and the secondary nozzle. The primary nozzle operates under oxidizing conditions, with a molar, air stoichiometric excess of ~100%.. The secondary nozzle introduces the additional fuel into the hot combustion gases, with the purpose of efficient volatilization without carbon formation. It operates under reducing conditions. Ultrasonic type nozzles are recommended for both locations because of their fine atomization, infinite turndown ratio, low power consumption, and their large diameter throat, although a less expensive, air atomizing nozzle could be used at the primary location. Preheated air is introduced to partially combust the fuel, and high temperatures are attained (>1800°F). The hot steam/fuel mixture enters the autothermal reformer, and a hydrogen/carbon oxides mixture is produced. The exit stream is cooled from ~1400°F to ~400°F in the let-down heat exchanger, using air as the coolant. The cooler sections of the let-down heat exchanger are packed with a high temperature shift catalyst (iron based), which accomplishes part of the shift conversion of carbon monoxide, and helps to suppress methane formation over the low temperature shift catalyst.

The cooled gases pass through a zinc oxide bed to remove hydrogen sulfide, and then pass into the shift reactor. This contains a low temperature shift catalyst, and is cooled by air. It completes the shift conversion. The effluent contains below 3% carbon monoxide, and

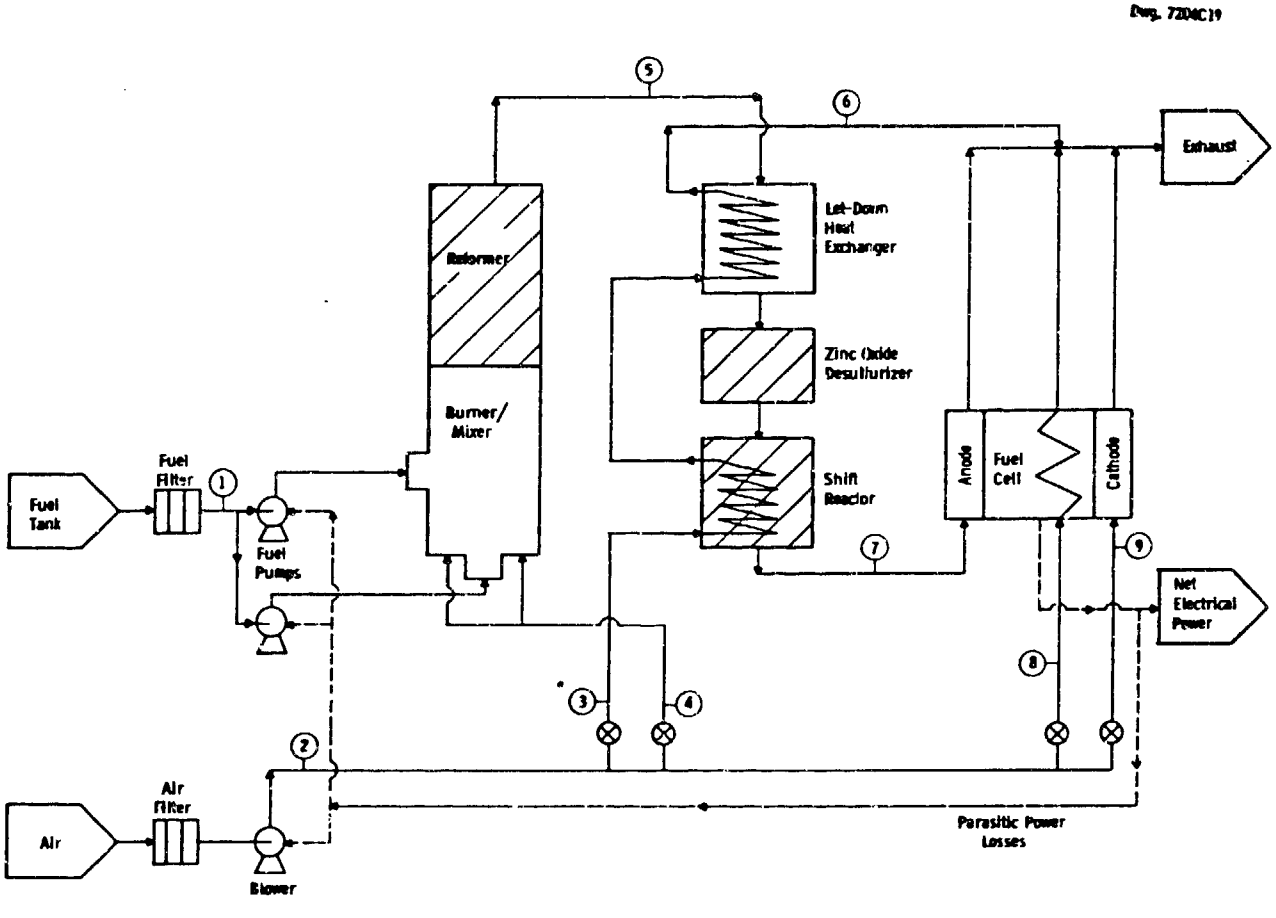

Figure 6.1 -- Standard Autothermal Fuel Processor Using Air

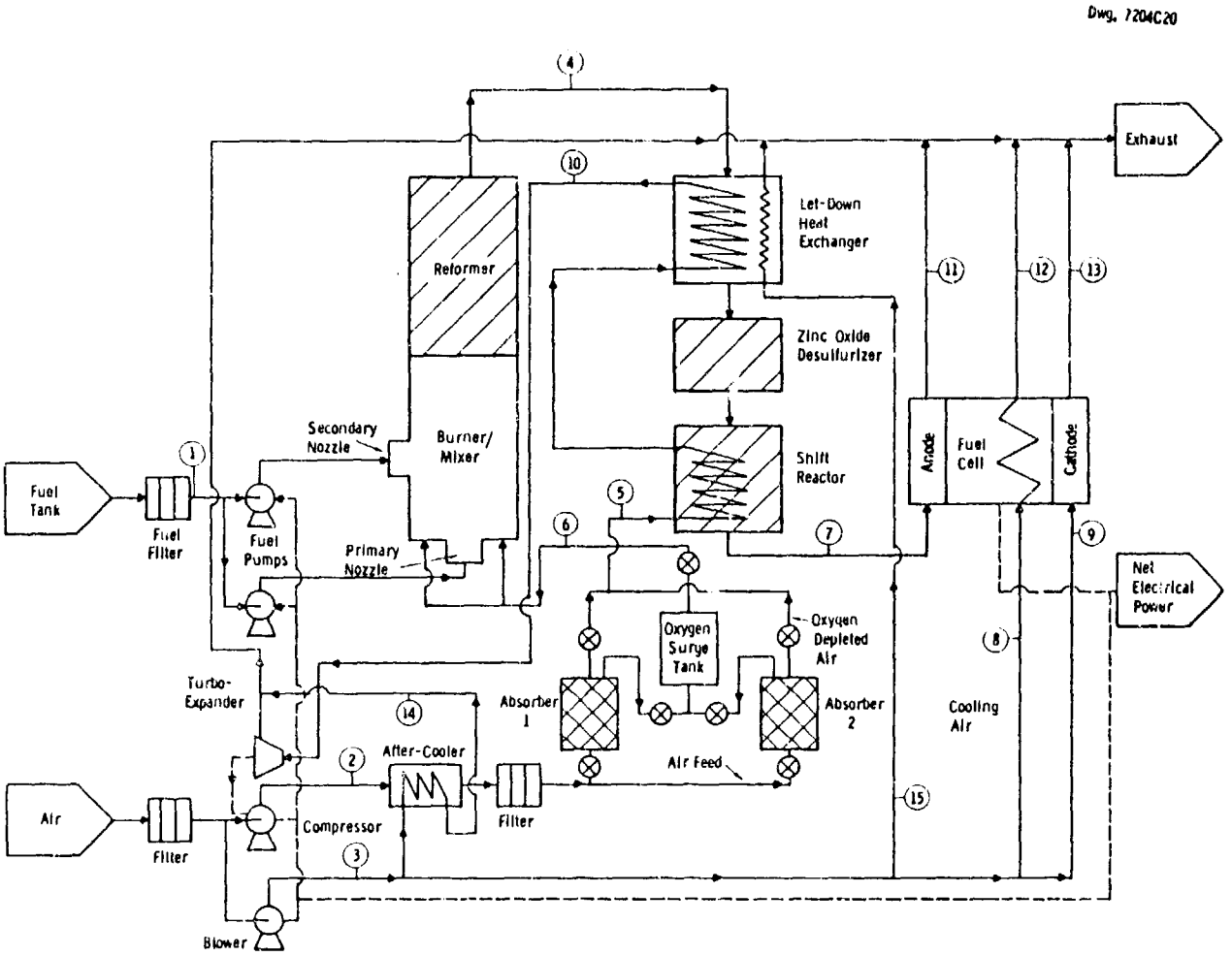

Figure 6.2 -- Autothermal Fuel Processor Using Oxygen Enriched Air

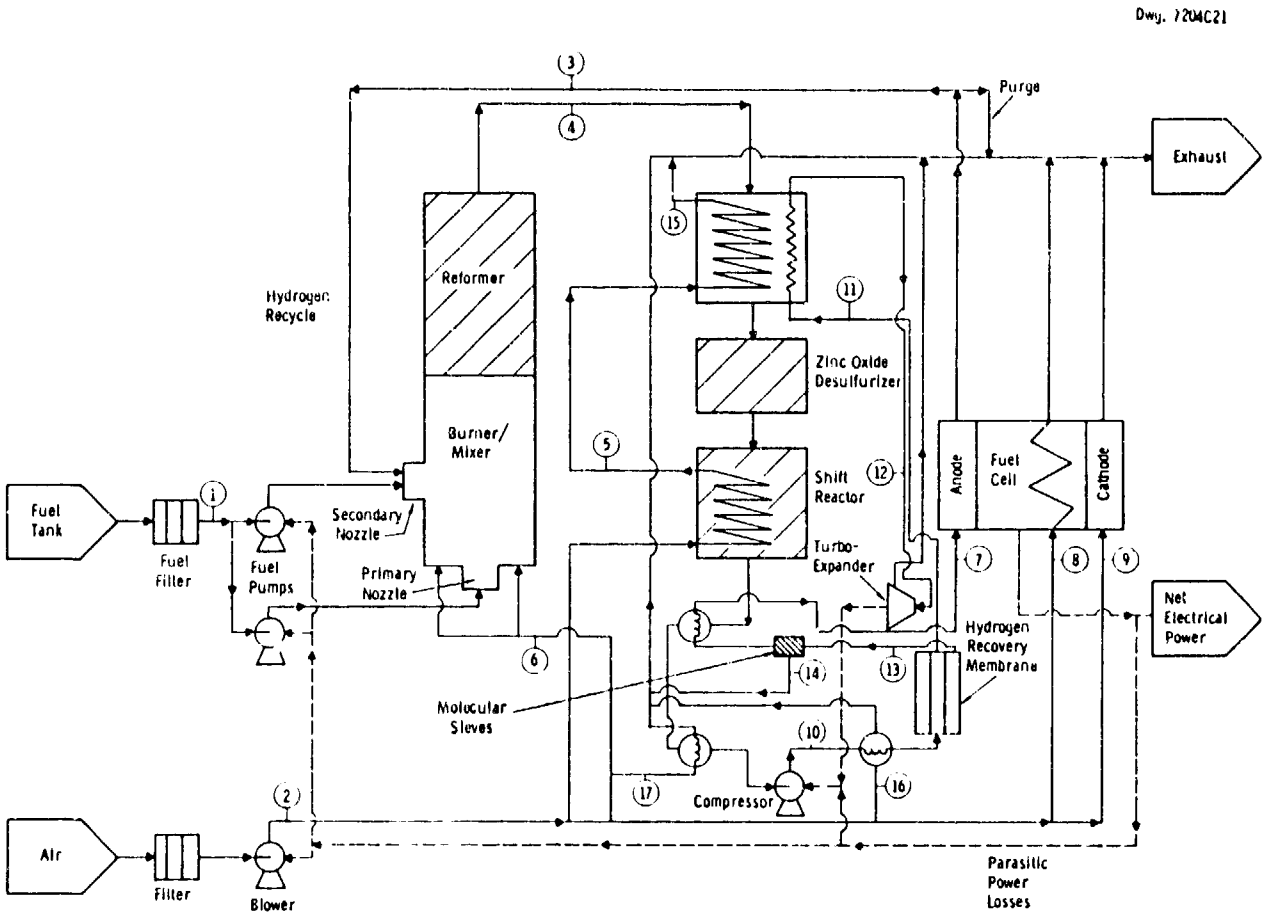

Figure 6.3 -- Autothermal Fuel Processor with Hydrogen Enrichment Prior to Fuel Cell

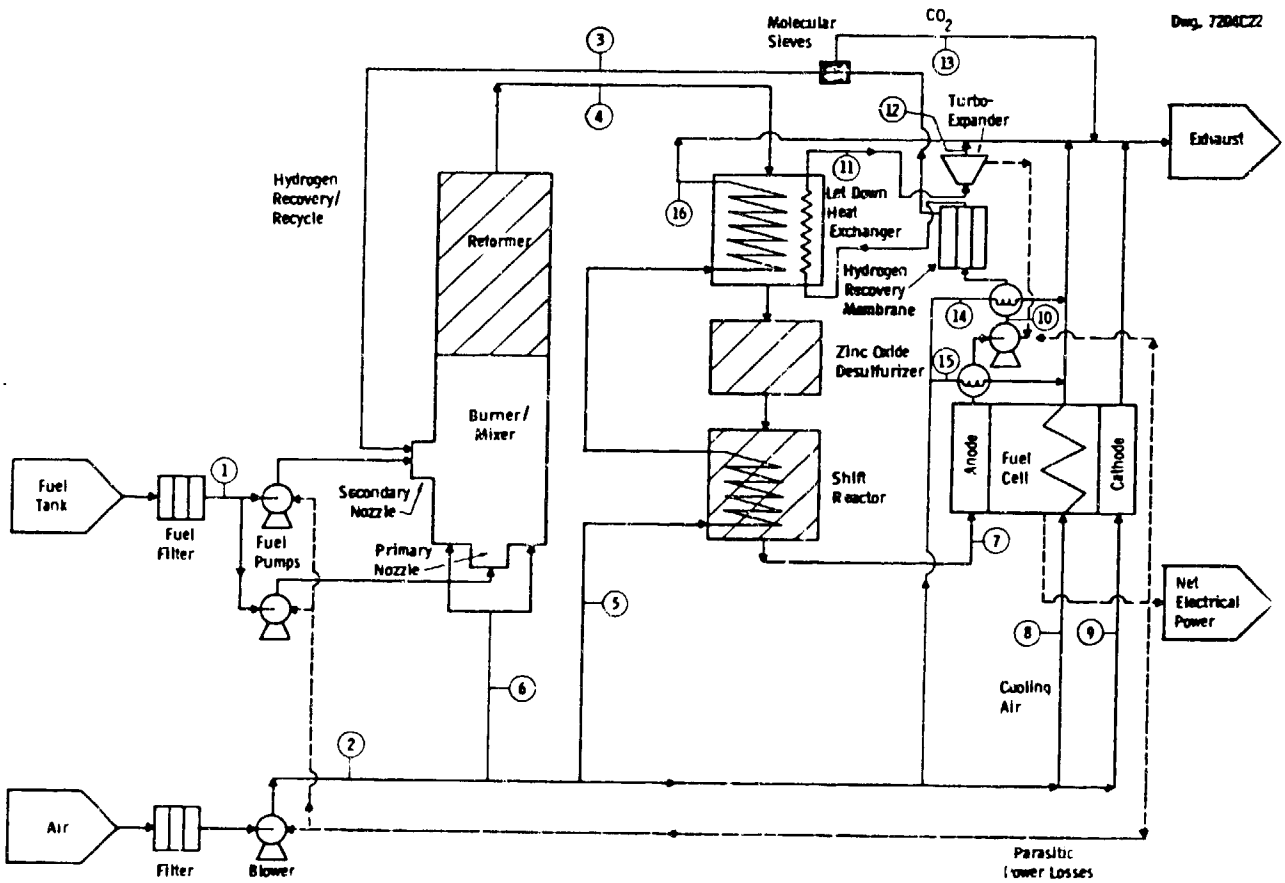

Figure 6.4 -- Autothermal Fuel Processor Using Anode Hydrogen Recovery and Recycle

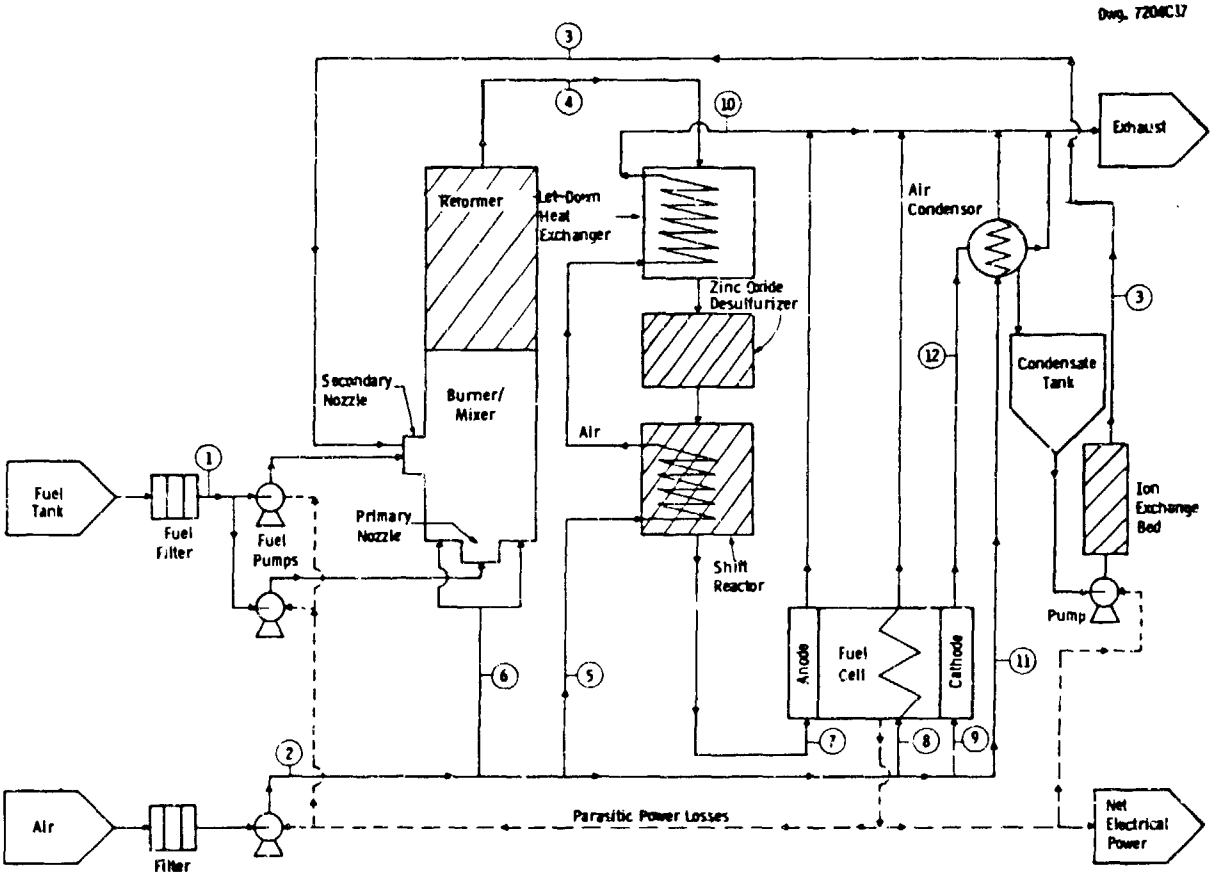

Figure 6.5 -- Autothermal Fuel Processor with Cathode Water Recovery and Recycle

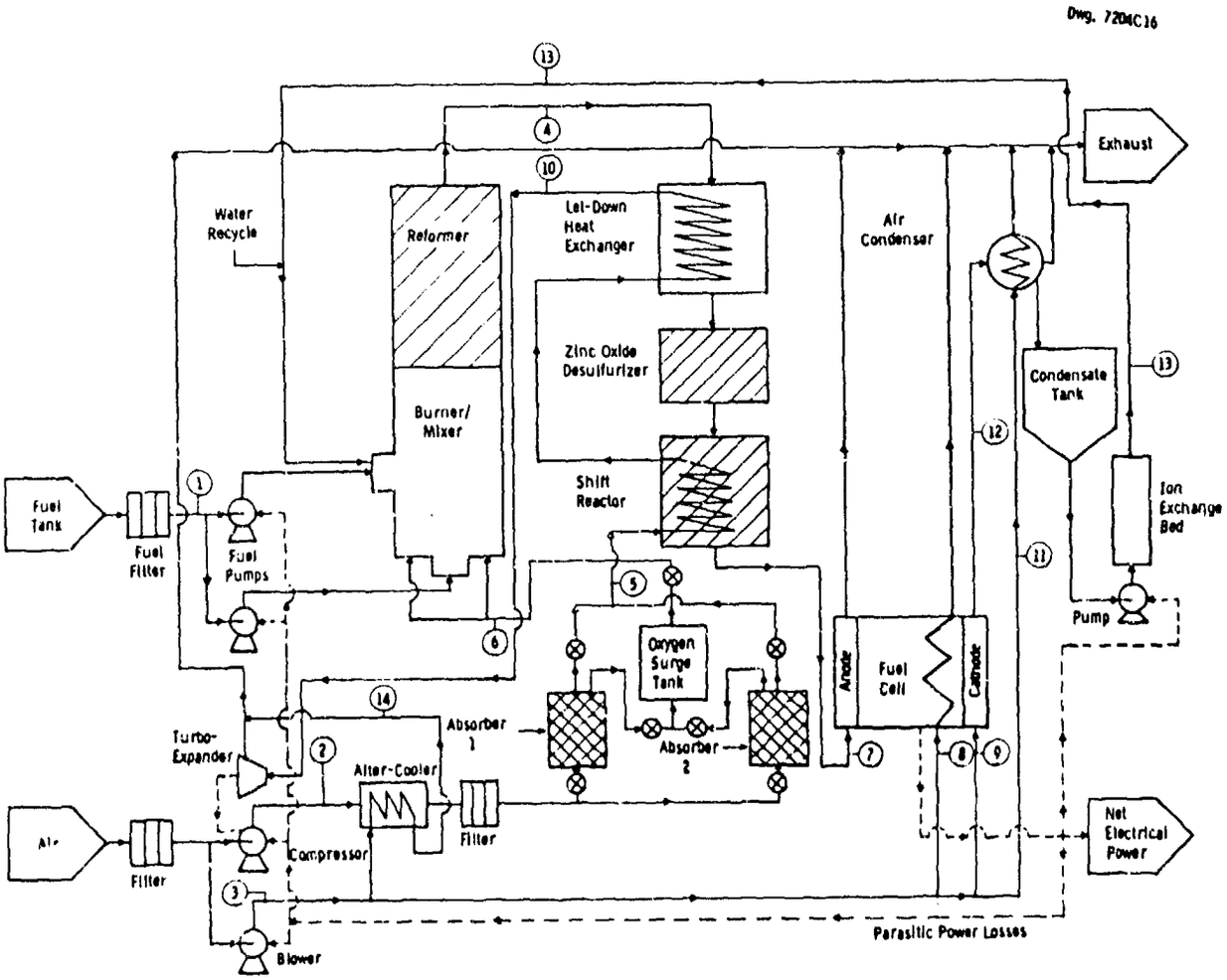

Figure 6.6 -- Autothermal Fuel Processor with Oxygen Enrichment and Cathode Water Recovery and Recycle

Table 6.1 -- Stream Flow Rates for Design 1

Component	Stream Number 1 Lb/Hr	1 LbMol/Hr	2 Lb/Hr	2 LbMol/Hr	3 Lb/Hr	3 LbMol/Hr	4 Lb/Hr	4 LbMol/Hr	5 Lb/Hr	5 LbMol/Hr	6 Lb/Hr	6 LbMol/Hr	7 Lb/Hr	7 LbMol/Hr	8 Lb/Hr	8 LbMol/Hr	9 Lb/Hr	9 LbMol/Hr
Diesel Fuel	7.1	.051																
CO									11.42	.408								
CO_2									4.488	.102			22.4	.51				
H_2O									7.344	.408								
H_2									.104	.052			.92	.46				
O_2			223.5	6.985	140.4	4.387	16.28	.5088			140.4	4.387			50.5	1.58	16.3	.51
N_2			735.7	26.28	462.1	16.50	53.60	1.914	53.76	1.92	462.1	16.50	53.76	1.92	166.5	5.94	53.2	1.90
H_2S									.021	6.62 E-4								
Total Flow	7.1	.051	959.2	33.26	602.5	20.89	69.89	2.423	77.14	2.891	602.5	20.89	77.08	2.89	217	7.52	69.5	2.41
SCFM	(-)		199		125		14.5		17.30		125		17.3		45		14.4	
Temp., °F	80		80		80		80		3561		600		400		80		80	
Pres., PSIG	1		.5		.5		.5		.5		.5		.5		.5		.5	

Table 6.2 -- Stream Flow Rates for Design 2

Component	Stream Number 1 Lb/Hr	1 LbMol/Hr	2 Lb/Hr	2 LbMol/Hr	3 Lb/Hr	3 LbMol/Hr	4 Lb/Hr	4 LbMol/Hr	5 Lb/Hr	5 LbMol/Hr	6 Lb/Hr	6 LbMol/Hr	7 Lb/Hr	7 LbMol/Hr	8 Lb/Hr	8 LbMol/Hr	9 Lb/Hr	9 LbMol/Hr
Diesel Fuel	7.1	.051																
CO							11.42	.408										
CO_2							4.488	.102					22.4	.51				
H_2O							7.344	.408										
H_2							.104	.052					.92	.46				
O_2			50.82	1.588	275.6	8.612			34.50	1.078	16.3	.51			50.5	1.58	16.3	.51
N_2			177.86	6.352	907.1	32.40	14.3	.51	163.58	5.842	14.3	.51	14.3	.51	166.5	5.94	53.2	1.90
H_2S							.021	6.62 E-4										
Total Flow	7.1	.051	228.68	7.94	1183	41.01	37.68	1.581	198.08	6.92	30.6	1.02	37.62	1.48	217	7.52	69.5	2.41
SCFM	(-)		47.5		245.4		9.5		41.4		6.1		8.86		45		14.4	
Temp., °F	80		272		80		5871		80		80		400		80		80	
Pres., PSIG	1		127		.5		.5		127		.5		.5		.5		.5	

Table 6.2 -- (Continued)

Component	Stream Number 10 Lb/Hr	10 LbMol/Hr	11 Lb/Hr	11 LbMol/Hr	12 Lb/Hr	12 LbMol/Hr	13 Lb/Hr	13 LbMol/Hr	14 Lb/Hr	14 LbMol/Hr	15 Lb/Hr	15 LbMol/Hr
Diesel Fuel												
CO												
CO_2			22.4	.51								
H_2O							6.624	.368				
H_2			.18	.09								
O_2	34.50	1.078			50.5	1.58	10.432	.326	115.0	3.593	93.88	2.934
N_2	163.58	5.842	14.3	.51	166.5	5.94	53.2	1.9	378.5	13.52	309.0	11.04
H_2S												
Total Flow	198.08	6.92	36.88	1.11	217	7.52	70.256	2.594	493.6	17.11	403.0	13.97
SCFM	41.4		6.64		45		15.52		102.4		83.6	
Temp., °F	600		400		300		400		252		80	
Pres., PSIG	127		.5		.5		.5		.5			

Table 6.3 -- Stream Flow Rates for Design 3

Component	Stream Number 1		2		3		4		5		6		7		8		9	
	Lb/Hr	LbMol/Hr	Lb/Hr	LbMol/Hr	Lb/Hr	LbMol/Hr	Lb/Hr	LbMol/Hr	Lb/Hr	LbMol/Hr	Lb/Hr	LbMol/Hr	Lb/Hr	LbMol/Hr	Lb/Hr	LbMol/Hr	Lb/Hr	LbMol/Hr
Diesel Fuel	7.1	.051																
CO							11.42	.408										
CO_2							4.488	.102										
H_2O							7.344	.408										
H_2					.144	.0722	.248	.124					.836	.418				
O_2			227.8	7.119					125.1	3.91	16.28	.5088			50.5	1.58	16.3	.51
N_2			749.9	26.78	2.63	.094	56.39	2.014	411.9	14.71	53.60	1.914	2.772	.099	166.5	5.94	53.2	1.90
H_2S							.021	6.62 E-4										
Total Flow	7.1	.051	983.5	33.9	2.774	.1662	79.91	3.057	537.0	18.62	69.89	2.423	3.608	.517	217	7.52	69.5	2.41
SCFM	(-)		203		.99		18.3		111.4		14.5		3.09		45		14.4	
Temp., °F	80		80		400		3561		80		80		400		80		80	
Pres., PSIG	1		.5		.5		.5		.5		.5		.5		.5		.5	

Table 6.3 -- (Continued)

Component	Stream Number 10 Lb/Hr	10 LbMol/Hr	11 Lb/Hr	11 LbMol/Hr	12 Lb/Hr	12 LbMol/Hr	13 Lb/Hr	13 LbMol/Hr	14 Lb/Hr	14 LbMol/Hr	15 Lb/Hr	15 LbMol/Hr	16 Lb/Hr	16 LbMol/Hr	17 Lb/Hr	17 LbMol/Hr
Diesel Fuel																
CO																
CO_2	22.4	.51	10.69	.243	10.69	.243	11.79	.268	11.79	.268						
H_2O																
H_2	1.064	.532	.228	.114	.228	.114	.836	.418								
O_2											125.1	3.91	2.72	.085	18.96	.53
N_2	56.39	2.014	53.45	1.909	53.45	1.909	2.772	.099			411.9	14.71	8.98	.321	56.19	2.01
H_2S																
Total Flow	79.85	3.056	64.37	2.266	64.37	2.266	15.40	.785	11.79	.268	537	18.62	11.7	.406	73.15	2.54
SCFM	18.3		13.6		13.6		4.70		1.60		111.4		2.43		15.2	
Temp., °F	334		94		600		94		80		600		314		80	
Pres., PSIG	.5		147		147		.5		.5		.5		.5		.5	

Table 6.4 -- Stream Flow Rates for Design 4

Component	Stream Number 1		2		3		4		5		6		7		8		9	
	Lb/Hr	LbMol/Hr	Lb/Hr	LbMol/Hr	Lb/Hr	LbMol/Hr	Lb/Hr	LbMol/Hr	Lb/Hr	LbMol/Hr	Lb/Hr	LbMol/Hr	Lb/Hr	LbMol/Hr	Lb/Hr	LbMol/Hr	Lb/Hr	LbMol/Hr
Diesel Fuel	7.1	.051																
CO							11.42	.408										
CO_2							4.488	.102					22.4	.51				
H_2O							7.344	.408										
H_2					.156	.078	.26	.13					1.076	.538				
O_2			274	8.564					126.9	3.966	16.28	.5088			50.5	1.58	16.3	.51
N_2			902.1	32.22	4.9	.175	58.66	2.095	417.8	14.92	53.60	1.914	58.66	2.095	166.5	5.94	53.2	1.90
H_2S							.021	6.62 E-4										
Total Flow	7.1	.051	1176	40.78	5.056	.253	82.17	3.143	544.7	18.89	68.89	2.423	82.18	3.143	217	7.52	69.5	2.41
SCFM	(-)		244		1.51		18.8		113		14.5		18.8		45		14.4	
Temp., °F	80		80		94		3561		80		80				80		80	
Pres., PSIG	1		.5		.5		.5		.5		.5				.5		.5	

Table 6.4 -- (Continued)

Component	Stream Number 10 Lb/Hr	10 LbMol/Hr	11 Lb/Hr	11 LbMol/Hr	12 Lb/Hr	12 LbMol/Hr	13 Lb/Hr	13 LbMol/Hr	14 Lb/Hr	14 LbMol/Hr	15 Lb/Hr	15 LbMol/Hr	16 Lb/Hr	16 LbMol/Hr
Diesel Fuel														
CO														
CO_2	22.44	.51	10.69	.243	10.69	.243	11.75	.267						
H_2O														
H_2	.184	.092	.028	.014	.028	.014								
O_2									42.85	1.339	21.42	.6695	126.9	3.966
N_2	53.76	1.92	48.86	1.745	48.86	1.745			141.0	5.037	70.52	2.519	417.8	14.92
H_2S														
Total Flow	76.38	2.522	59.58	2.002	59.58	2.002	11.75	.267	184	6.376	91.94	3.188	544.7	18.89
SCFM	15.1		12.0		12.0		1.60		38.2		19.1		113	
Temp., °F	334		600		80				80		80		600	
Pres., PSIG	147		147		.5				.5		.5		.5	

Table 6.5 -- Stream Flow Rates for Design 5

Component	Stream Number 1		2		3		4		5		6		7		8		9	
	Lb/Hr	LbMol/Hr	Lb/Hr	LbMol/Hr	Lb/Hr	LbMol/Hr	Lb/Hr	LbMol/Hr	Lb/Hr	LbMol/Hr	Lb/Hr	LbMol/Hr	Lb/Hr	LbMol/Hr	Lb/Hr	LbMol/Hr	Lb/Hr	LbMol/Hr
Diesel Fuel	7.1	.051																
CO							11.42	.408										
CO_2							4.49	.102					22.4	.51				
H_2O					10.17	.565	7.344	.408										
H_2							1.232	.616					2.048	1.024				
O_2			523	16.35					31.45	.983	7.325	.229			129.4	4.043	41.56	1.299
N_2			1723	61.52			24.08	.86	103.5	3.70	24.11	.861	24.08	.86	425.8	15.21	136.8	4.885
H_2S							.021	6.62 E-4										
Total Flow	7.1	.051	2246	77.88	10.17	.565	48.53	2.394	135.0	4.68	31.33	1.09	48.53	2.394	555.3	19.25	178.3	6.184
SCFM	(-)		466		(-)				28		6.5		14.32		115.2		37	
Temp., °F	80		80		100		1394		80		80		440		80		80	
Pres., PSIG	1		.5		.5		.5		.5		.5		.5		.5		.5	

Table 6.5 -- (Continued)

Component	Stream Number 10 Lb/Hr	10 LbMol/Hr	11 Lb/Hr	11 LbMol/Hr	12 Lb/Hr	12 LbMol/Hr
Diesel Fuel						
CO						
CO_2						
H_2O					14.75	.8192
H_2						
O_2	31.45	.983	313.4	9.792	28.46	.8894
N_2	103.5	3.70	1031.5	36.84	136.8	4.885
H_2S						
Total Flow	135.0	4.68	1344.8	46.63	180.1	6.594
SCFM	28		279		39.45	
Temp., °F	600		80		440	
Pres., PSIG	.5		.5		.5	

Table 6.6 -- Stream Flow Rates for Design 8

Component	Stream Number 1 Lb/Hr	1 LbMol/Hr	2 Lb/Hr	2 LbMol/Hr	3 Lb/Hr	3 LbMol/Hr	4 Lb/Hr	4 LbMol/Hr	5 Lb/Hr	5 LbMol/Hr	6 Lb/Hr	6 LbMol/Hr	7 Lb/Hr	7 LbMol/Hr	8 Lb/Hr	8 LbMol/Hr	9 Lb/Hr	9 LbMol/Hr
Diesel Fuel	7.1	.061																
CO							11.42	.408										
CO_2							4.49	.102					22.4	.51				
H_2O							7.344	.408										
H_2							1.232	.616					2.048	1.024				
O_2			23.86	.7455	535.7	16.74			16.56	.5175	7.296	.228			129.4	4.043	41.56	1.299
N_2			78.53	2.805	1763	62.98	6.384	.228	72.16	2.577	6.384	.228	6.384	.228	425.6	15.21	136.6	4.885
H_2S							.021	6.62 E-4										
Total Flow	7.1	.051	102.4	3.550	2299.2	79.72	30.89	1.763	88.72	3.095	13.68	.456	30.83	1.762	555.3	19.25	178.3	6.184
SCFM	(-)		21.24		477		10.55		18.5		2.73		10.54		115.2		37	
Temp., °F	80		272		80		1776		100		100		440		80		80	
Pres., PSIG	1		127		.5				127		.5		.5		.5		.5	

Table 6.6 -- (Continued)

Component	Stream Number 10 Lb/Hr	10 LbMol/Hr	11 Lb/Hr	11 LbMol/Hr	12 Lb/Hr	12 LbMol/Hr	13 Lb/Hr	13 LbMol/Hr	14 Lb/Hr	14 LbMol/Hr
Diesel Fuel										
CO										
CO_2										
H_2O					14.75	.8192	10.17	.565		
H_2										
O_2	16.56	.5175	313.4	9.792	28.46	.8894			51.66	1.614
N_2	72.16	2.577	1031.5	36.84	136.8	4.885			170.06	6.074
H_2S										
Total Flow	88.72	3.095	1344.8	46.63	180.01	6.594	10.17	.565	221.72	7.688
SCFM	18.5		279		39.45		(-)		46	
Temp., °F	867		80		440		100		252	
Pres., PSIG	127		.5		.5		.5		.5	

is suitable for PAFC use. In this standard case, the anode, cathode, and cooling air effluents are exhausted without any recycle or recovery of components and heat. This standard case is not suitable for fuel oil feedstocks, because the anode feed stream hydrogen concentration is too low.

Figure 6.2 introduces a variation of the standard case that has an oxygen enrichment system. Such systems, using molecular sieves and pressurized swing adsorption (PSA), have become highly developed in the past decade, and several skid mounted variations are available.[11-14,20-23,27] A typical system utilizes two molecular sieve beds in parallel; one absorbing oxygen from the air, the other releasing oxygen to a surge tank (Figure 6.7). A compressor pressurizes the incoming air to ~120 psig. The pressurized air passes through the molecular sieve bed, and the oxygen is preferentially absorbed. The exit gases contain ~5% oxygen. In present systems, this exhaust stream passes through a throttling valve and is discharged into the atmosphere. For this application, it makes sense to utilize a turbo-expander to recover the pressurization energy,[30] and use the exhaust as the coolant for the let-down heat exchanger, as illustrated in Figure 6.2. After a 2-3 minute absorption cycle, valves switch automatically, and reduce the pressure over the bed. The pressure drop initiates evolution of oxygen from the molecular sieves, and the product goes to a surge tank prior to use. Typical oxygen purities exceed 90% with delivery pressures around 20 psig. As with the standard case, all fuel cell exit streams are exhausted.

As Table 6.2 indicates, the oxygen-lean exhaust stream is relatively large, and, consequently, compressor energy consumption is relatively high. This can be reduced by the aforementioned turbo-expander. It can also be significantly reduced by absorbent operation at a lower pressure. PSA systems are being developed and tested at absorbent pressures of 15-50 psig, with the associated reduced energy consumption,[12] although prototypical units are not yet available.

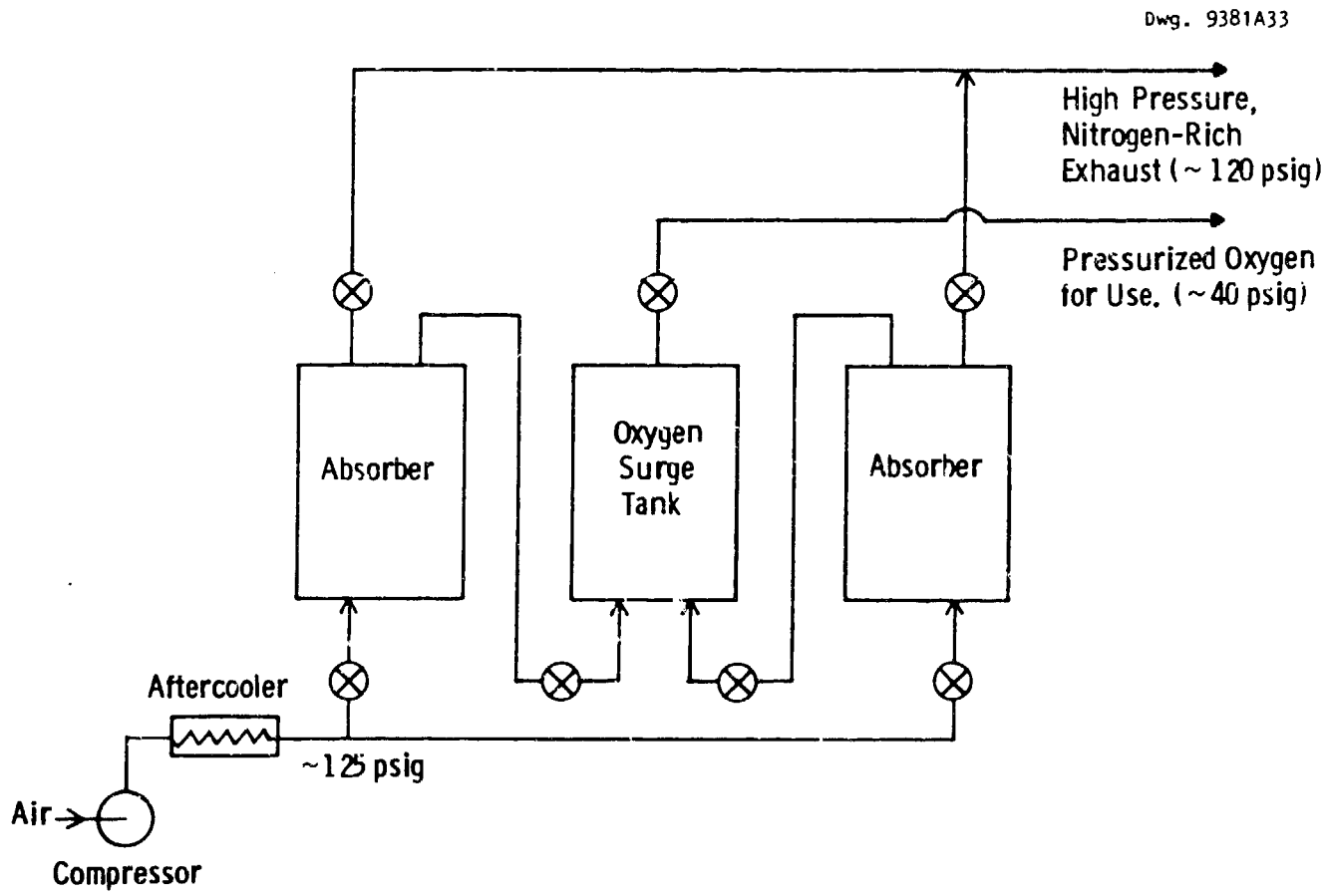

Figure 6.7 — Pressurized Swing Adsoprtion System for Oxygen Enrichment

The oxygen enrichment approach of Figure 6.2 has several significant advantages over the base case:

- improved ignition and combustion;
- better reformer reaction kinetics because of higher temperatures and higher reactant concentrations;
- lower flow rates by ~50%, which reduces equipment size and cost;
- higher hydrogen partial pressure in the anode feed, which translates into better fuel cell operation;
- reduced ammonia concentrations in the anode feed gases.

The disadvantages are:

- higher temperatures (~2500°F) imply materials concerns and the use of ceramic linings;
- the oxygen enrichment system increases the size, complexity, maintenance, and parasitic power losses of the fuel processor.

Figure 6.3 outlines an alternate approach. The approach is identical to the standard case through the shift reactor. Then, the shift reactor gases are pressurized and treated for hydrogen recovery. This can be either a membrane-diffusion method[15,16,24-26,31-33] or a PSA molecular sieve system. Greater than 90% recovery is obtained on simple system variations, with a high purity product (>90% hydrogen). This stream is fed directly to the anode, and, because of the high hydrogen content, the spent anode gases are recycled to the burner. The PSA system, exhaust gases contain principally nitrogen, and are pressurized. A turbo-expander partially recovers the compression energy, and the gases are exhausted. This approach has similar advantages and disadvantages as the enriched oxygen system. Its principal advantage is the high hydrogen content of the anode feed stream.

The key to successful, waterless fuel processor operation is effective management and balancing of the system's hydrogen and water streams. Figure 6.4 displays an example where hydrogen is recovered from the spent anode stream, and recycled. Again, either a membrane or a PSA system would be effective. Each would contain a compressor, separation system, and a turbo-expander. The recovered hydrogen is recycled to the burner. Again, this approach has similar advantages and disadvantages to the enriched oxygen system. Its additional advantage is that hydrogen recovery is relatively easy on the anode exhaust stream. Its principal disadvantage is with diesel fuel feedstocks, where the anode feed hydrogen concentration is ~20%, and fuel cell utilization would be poor.

The fuel cell produces water during normal operation. Consequently, as Figure 6.5 illustrates, this water can be condensed, purified, and recycled to the burner. This approach considerably eases fuel processor operation, and reduces the fuel fraction combusted, with an associated efficiency increase. The disadvantages are the additional weight and complexity of the condensor/condensate system, and the logistic requirement of resins for the ion exchange bed. Addition of an oxygen enrichment system (Figure 6.6) improves diesel fuel compatibility and fuel processor operation, with negligible efficiency penalties.

The preceding discussions imply that combination of two of the approaches appears to be the best, steady-state operational route. Table 6.7 summarizes the advantages and disadvantages of the different approaches.

The foregoing analyses illustrate the increased size and complexity of the waterless, fuel processor route. Now, it is necessary to quantify each approach in terms of size, weight, and operating parameters (efficiency, reliability, etc.). Table 6.8 lists the

Table 6.7 -- Fuel Processor Design Summary

	Design	Advantages	Disadvantages
1.	Basic Autothermal (Figure 6.1)	1. Simple 2. Once-through system 3. Least equipment	1. High temperatures (>3000°F) 2. Low efficiency 3. No hydrogen/water recovery 4. Low anode hydrogen concentration
2.	Autothermal with PSA/ oxygen enrichment (Figure 6.2)	1. Acceptable anode hydrogen concentration 2. Low diluent effects	1. High temperatures (>3000°F) 2. Low efficiency 3. No hydrogen/water recovery
3.	Autothermal, with hydrogen enrichment (Figure 6.3)	1. High anode hydrogen concentration	1. High temperatures (>3000°F) 2. Low efficiency 3. Complex system 4. Expensive
4.	Autothermal, with hydrogen recovery and recycle (Figure 6.4)	1. Recover hydrogen	1. High temperatures (>3000°F) 2. Low efficiency 3. Complex system 4. Expensive
5.	Autothermal, with cathode water recovery/ recycle (Figure 6.5)	1. Reasonable efficiency 2. Reasonable hydrogen concentration 3. More reasonable temperatures	1. More complex system
6.	Autothermal, with PSA/ oxygen enrichment and cathode water recovery/ recycle (Figure 6.6)	1. Good efficiency 2. Good anode hydrogen concentration	1. Complex system 2. Higher parasitic power losses

Table 6.8 -- Fuel Processor System Standard Components, Weights, and 1985 Prices

Component	Weight, lbs	Price, $
Main Burner, consists of:		
2 ultrasonic nozzles	10	5000
3' pipe section, 6" dia.*	57	105
1 6" slip-on flange	19	110
1 11" to 1" reducer flange	31	250
1 2" slip-on flange	5	30
1 2" to 1" reducer flange	5	54
1 burner assembly (cons.)	10	100
6" L, 2" pipe section	1.9	~10
Total Main Burner:	138.9	56[illegible]
Reformer, consists of:		
1.5' L, 6" dia. pipe section	28.5	53
1 6" slip-on flange	19	110
1 11" to 1" reducer flange	31	250
.5 ft^3 catalyst (~100 lbs./ft^3)	30	240
Total Reformer:	108.5	653
Desulfurizer, consists of:		
3' L pipe section, 6" dia.	57	105
1 6" slip-on flange	19	110
2 11" to 1" reducer flange	62	500
.5 ft^3 zinc oxide (64 lbs./ft^3)	32	~70
Total Desulfurizer:	170	785

*Pipe and flanges are Schedule 40, Type 304 stainless steel. Burner and reformer are welded together.

Table 6.8 -- (Continued)

Component	Weight, lbs	Price, $
Shift Reactor, consists of:		
6' pipe section, 6" dia.	114	210
1 6" slip-on flange	19	110
2 11" to 1" reducer flanges	62	500
1 5' high, 4" dia. cooling coil	~10	290
1 ft^3, copper/zinc oxide shift catalyst	85	500
Total Shift Reactor:	290	1610
Let-down heat exchanger, 316 S.S., spiral design	300	5380
Supporting Frame:		
~100' Kendorf @ 1.43 lbs./ft	143	~50
Enclosure: 72 ft^2, of 1/8" thick aluminum plate (1.76 lbs./ft^2)	127	~50
Connecting Piping ~10', make it 20' to include fittings, valves	34	92
Insulation:		
Castable alumina ceramic	~50	60
Ceramic fiber insulation	~30	63
Fiberglass	~10	22
Total Insulation:	90	145
Total Basic Fuel Processor:	1401	14424

Table 6.8 -- (Continued)

Component	Weight, lbs	Price, $
5 kW Fuel Cell Assembly, with invertor ($2000/kW)	~350	10,000
PSA Oxygen System: X-75 model, with compressor, ~1380 SCFH air feed	363	3995
Turbo-expander for above, ~1300 SCFH, 125 psi ——> 3 psi	~50	17000
Cathode Water Recovery:		
*Cool-down heat exchanger (24.1 ft^2)	58	2000
*Condensing heat exchanger (4.9 ft^2)	15	500
Condensate pump	5	300
Ion exchange column	10	50
109 SCFM blower (~1 hp)	80	~1000
10 gallon water tank (polyethylene)	5	~20
Total Cathode Water Recovery:	173	3870
Fuel Tank (50 gallons)	~40 with frame	120
Hydrogen recovery system:		
1 6' pipe section, 6" dia.	114	210
2 6" slip-on flange	38	220
2 11" to 1" reducer flanges	62	500
1 Compressor	50	1000
2 5' high, 2.5" dia. membrane modules	30 (est.)	30000
1 Turbo-expander	50	17000
Total Hydrogen Recovery System:	344	48930

*Whitlock heat exchanger sizes and dimensions.

components, estimated weights, and 1985 prices of individual components in the fuel cell system.

The fuel processor is the heaviest subsystem, with a total weight of ~1400 lbs. The heaviest components are the let-down heat exchanger and the shift reactor. The relatively high subsystem weight accrues from two areas: the wall thicknesses required by the high temperatures, and the use of Schedule 40 piping materials (i.e., the lowest weight and rating material routinely available). Clearly, this is not optimized. Sub-standard piping and flanges are available from manufacturers, once a detailed equipment design has been specified. The latter is beyond the scope of this program. However, it should be possible to use Schedule 10 materials, which weigh ~50% less, and would reduce the weight to ~1124 lbs. For a standard comparative basis between different systems, the weight values of Table 6.8 will be used.

Table 6.9 presents the assumptions and cost factors for the analyses. Diesel fuel is a mixture of paraffinic, naphthenic, and aromatic compounds, with a "typical" structure containing nine to sixteen carbon atoms. Table 6.9c lists a representative composition. The calculations assume a diene-like structure of $C_{10}H_{18}$, containing .3% sulfur. The combustion reaction enthalpy is ~1460 Kcal/mole (LHV), which corresponds to approximately 19,009 BTU/lb. Consequently, a 1 gph feed rate represents a fuel power equivalent of 39.5 KW-hr. In contrast, a 1 gph methanol feed rate denotes a fuel power equivalent of only 16.1 KW. The fuel cell utilization assumptions are standard.[1,17] A 5 kW nominal electrical power size is assumed. Air represents the cathode gas, flowing at three times stoichiometric (33% utilization). The anode hydrogen utilization is ~80% for most concentrations, and .4 lb.mol/hr is required for a 5 kW fuel cell unit. Higher hydrogen concentrations increase fuel cell utilization and power by about 10% at a .75 inlet mole fraction.

Table 6.9a -- Engineering Analysis Assumptions

1. Diesel Fuel Composition:

   empirical formula = $C_1H_{1.8}$, with .3% sulfur

   chemical formula = $[C_1H_{1.8}S_{1.298E-3}]_{10}$

   = $C_{10}H_{18}S_{1.298E-2}$

2. Molecular Weight: 138.4

3. Fuel Cell Utilization: 5KW nominal power.
   cathode oxygen (from air) = 33%
   anode hydrogen = 80% (.4 lb.mol/hr required) at .3-.5 hydrogen mole fraction, 88% at .75 mole fraction

4. Fuel Cell Cooling Air:
   inlet temperature = 80°F
   outlet temperature = 300°F
   heat removed = 11900 BTU/hr
   air flow = 45 SCFM (217 lb/hr)

5. Fuel Feed Rate: 1 gph diesel fuel (S.G.=.85) equivalent to 7.1 lbs/hr or .051 lb.mol/hr

6. Air is 21% oxygen, 79% nitrogen, with a molecular weight of 28.82.

7. PSA system compressor and turbo-expander operate at 90% of adiabatic efficiency. Compressor operates at 125 psig, and uses two stages with intercooler and aftercooler air heat exchangers.

Table 6.9b -- Equipment Assembly Cost Factors*

Component	Range, % of Total Cost	Assumed Values, %	Normalized** Value
Direct Costs			
Purchased Equipment	15-40	33	100
Equipment Installation	6-14	14	42
Instrumentation/Controls	2-8	8	24
Piping (installed)	3-20	20	61
Electrical (installed)	2-10	10	30
Yard Improvements	2-5	0	0
Service Facilities (installed)	8-20	0	0
Land	1-2	0	0
Total Direct Cost:	-	-	257
Indirect Costs			
Engineering/Supervision	4-21	21	64
Construction Expense	4-16	4	12
Contractor's Fee	2-6	6	18
Contingency	5-15	10	30
Total Indirect Cost:	-	-	124

Total Fixed Capital Cost = 381% of Purchased Equipment Cost

*From reference 18.
**With respect to equipment cost.

Table 6.9c -- Typical Number 2 Fuel Oil Composition*

Gravity, API	38.83	
Specific Gravity	.8307	
CHx	$CH_{1.78}$	
Hydrogen (wt%)	12.8	
Carbon (wt%)	86.8	
Sulfur (wt%)	.322	
Oxygen	--	
Nitrogen	--	
Halogens (ppm-wt)	<50	
Paraffins (vol%)		31.2
Olefins (vol%)		.8
Naphthenes (alicyclical ring compounds (vol%))		40.8
Aromatics (vol%)		27.3
Distillates: Initial Boiling Point		130°F
	10%	340°F
	50%	495°F
	70%	545°F
	90%	597°F
	95%	615°F
	98%	625°F

*From reference 3.

The PSA system is modelled after commercial units. It includes a compressor and a turbo-expander, both of which operate at 90% of adiabatic efficiency. This represents the upper performance range for these units, and, therefore, is somewhat optimistic. The molecular sieves operate at 125 psig. Newer systems are under development that operate at 15-40 psig, with the associated lower power penalties. These developments were not considered in the design.

Table 6.9b presents cost estimation factors from a standard source.[18] These are used to estimate the assembled unit cost from the equipment prices, and should give a good estimate of brassboard/early prototype fabrication cost.

Table 6.10 lists the pertinent features of the basic autothermal fuel processor. The total weight is 1791 lbs., with an estimated cost of $93,500. Parasitic power losses are estimated from vendor and literature data.[1,17] The net, electricity output is 4.75 kW. For methanol, one calculates a 29.5% efficiency. However, diesel fuel utilization reduces this to ~12% efficiency, with an unacceptably low, anode hydrogen concentration of 16%. The disparity as compared to methanol accrues from two important points: diesel fuel has 2.5 times the energy content of methanol on a mass basis, and a much lower hydrogen content.

Table 6.11 displays the fuel processor with an oxygen enrichment system. Typical PSA systems produce a minimum 90% oxygen stream from air, and, consequently, 50-90% oxygen enrichment is practical. This approach increases the anode hydrogen concentration to an acceptable 31%, using a 50% oxygen stream. Parasitic power consumption rises, although the turbo-expander recovers most of the compression energy. Net power output becomes 4.37 kW. Again, methanol system efficiency is reasonable (27%), but diesel fuel system efficiency is unacceptably low (11%), and unreasonably high temperatures are calculated.

Table 6.10 -- Design 1: Basic Autothermal Fuel Processor (Figure 6.1 System)

	Weight, lbs	Price, $
Fuel Processor	1401	14424
Fuel Cell/Invertor	350	10000
Fuel Tank	40	120
Total	1791	24544

Estimated Assembled Cost: $93,500

Gross Power Output (kWe): 5.9

Parasitic Power Consumption (kWe):

Air blower (199 SCFM @ .5 psig) =	1.31 (1.75 hp)
2 Ultrasonic nozzles, with pumps =	.10
Thermocouples/controls/valves (estimate) =	.30
Total	1.71

Net Power Output (kWe): 4.2

Fuel Feed: 1 gph diesel fuel = 7.1 lbs/hr

Hydrogen Produced: .473 lb.mol/hr = .95 lb/hr

Anode Feed Gas, Hydrogen Content: ~16%

System Efficiency:
Diesel fuel: 11%
Methanol: 29.5%

Comments: Anode feed hydrogen concentration is too low with diesel fuels, and will result in decrease of fuel cell performance. Unreasonably high gas temperatures will be encountered. However, the approach is feasible for neat methanol fuel (~41% anode feed gas, hydrogen concentration).

Table 6.11 -- Design 2: Autothermal Fuel Processor with PSA Oxygen Enrichment System (Figure 6.2 System)

	Weight, lbs	Price, $
Fuel Processor	1401	14424
Fuel Cell/Invertor	350	10000
Fuel Tank	40	120
PSA/Oxygen System	363	3995
Turbo-Expander	50	17000
Total	2204	45,539

Estimated Assembled Cost: $173,500

Gross Power Output (kWe): 5.9

Parasitic Power Consumption (kWe):

Air blower (245 SCFM @ .5 psig) =	1.83
2 Ultrasonic nozzles, with pumps =	.10
Thermocouples/controls/valves (estimate) =	.30
PSA system compressor (9.04 hp) =	6.75
PSA turbo-expander recovery =	7.13
Total	1.85

Net Power Output (kWe): 4.14

Fuel Feed: 1 gph diesel fuel = 7.1 lbs/hr

Hydrogen Produced: .473 lb.mol/hr = .95 lb/hr

Anode Feed Gas, Hydrogen Content:
31% with 50% oxygen
45% with 90% oxygen

System Efficiency:
Diesel fuel: 15%
Methanol: 27%

Comments: Ultrahigh temperatures involved. Hydrogen output limited by low hydrogen content of the diesel fuel. 57% anode hydrogen content with neat methanol fuel and 50% oxygen.

Tables 6.12 and 6.13 analyze Designs 3 and 4, which, respectively, utilize a membrane system to enrich the anode feed gases or recover hydrogen from the anode exhaust. The approach also requires molecular sieve use for carbon dioxide removal. Unfortunately, this greatly increases system complexity, without ameliorating the high temperatures or increasing system efficiency. Consequently, hydrogen enrichment or recovery are not feasible approaches.

Designs 5 and 6 investigate the autothermal/cathode water recovery combination. As pointed out in Section 5, the fuel cell generates sufficient cathode gas water vapor to allow a recycle at the 2:1 steam/carbon level. This implies only minimal combustion of the incoming fuel (say, ~8%). However, based on an 80°F ambient temperature for cooling air, a saturation temperature of ~100°F can be obtained. This corresponds to condensation and recovery of 69% of the spent cathode water vapor, and only 55% recovery of the anode feed hydrogen. Reducing the saturation temperature to 80°F only increases the values to 80% and 64%, for water and hydrogen recovery, respectively. Increasing the cathode oxygen utilization to 50% has about the same effect. Therefore, using the 69% recovery factor, 31% of the feed fuel requires combustion in order to provide the remaining water. This also allows direct recycle of the liquid water without a separate boiler. The theoretical, maximum system efficiency for the autothermal/cathode recycle approach is 33%.

Table 6.14 provides the air autothermal/cathode water recovery combination results. The fuel processor weighs ~2400 pounds. Gross power output is 12.8 kWe, with a net power output of ~9 KW, based upon a 1 gph diesel fuel flow rate. Most of the parasitic power derives from the relatively large blower requirements; some 60% of which is necessary for cathode water condensation. The hydrogen production rate is ~360 SCFH, at an anode concentration of 43%. System temperatures are more

Table 6.12 -- Design 3: Autothermal Fuel Processor with Hydrogen Enrichment Prior to the Fuel Cell (Figure 6.3 System)

	Weight, lbs	Price, $
Fuel Processor	1401	14424
Fuel Cell/Invertor	350	10000
Fuel Tank	40	120
Hydrogen Recovery System Turbo-Expander (includes turbo-expander and molecular sieves)	544	50930
Total	2375	75,474

Estimated Assembled Cost: $287,600

Gross Power Output (KWe): 5.75

Parasitic Power Consumption (KWe):

Air blower (203 SCFM @ .5 psig) =	1.31
2 Ultrasonic nozzles, with pumps =	.10
Thermocouples/controls/valves (estimate) =	.30
PSA system compressor =	2.77
PSA turbo-expander recovery =	2.14
Total	2.34

Net Power Output (KWe): 3.41

Fuel Feed: 1 gph diesel fuel = 7.1 lbs/hr

Hydrogen Produced: .418 lb.mol/hr = .836 lb/hr

Anode Feed Gas, Hydrogen Content: 80%

System Efficiency:
Diesel fuel: 9%

Comments: Unrealistically high temperatures. Membrane system requires 4 additional heat exchangers as well as a compressor, and provides no efficiency or operational advantages.

Table 6.13 -- Design 4: Autothermal Fuel Processor with Anode Hydrogen Recovery and Recycle (Figure 6.4 System)

	Weight, lbs	Price, $
Fuel Processor	1401	14424
Fuel Cell/Invertor	350	10000
Fuel Tank	40	120
Hydrogen Recovery System	544	50930
Total	2375	75474

Estimated Assembled Cost: $287,600

Gross Power Output (KWe): 6.725

Parasitic Power Consumption (KWe):

Air blower (2x120 SCFM @ .5 psig) =	1.49
2 Ultrasonic nozzles, with pumps =	.10
Thermocouples/controls/valves (estimate) =	.30
Compressor =	2.42
Turbo-expander =	2.14
Total	2.17

Net Power Output (KWe): 4.56

Fuel Feed: 1 gph diesel fuel = 7.1 lbs/hr

Hydrogen Produced: .538 lb.mol/hr = 1.076 lb/hr

Anode Feed Gas, Hydrogen Content: 17%

System Efficiency:
Diesel fuel: 12%

Comments: Unrealistically high temperatures and low anode hydrogen concentration. The membrane system requires 3 additional heat exchangers and a compressor, and provides no advantages.

Table 6.14 -- Design 5: Autothermal Fuel Processor with Cathode Water Recovery and Recycle (Figure 6.5 System)

	Weight, lbs	Price, $
Fuel Processor (2 extra blowers)	1561	16424
Fuel Cell/Invertor (12.8 kW)	615	25600
Fuel Tank	40	120
Cathode Water Recovery	173	3870
Total	2389	46,014

Estimated Assembled Cost: $175,300

Gross Power Output (KWe): 12.8

Parasitic Power Consumption (KWe):

Air blowers (466 SCFM @ .5 psig) =	3.54
2 Ultrasonic nozzles, with pumps =	.10
Thermocouples/controls/valves (estimate) =	.30
Total	3.84

Net Power Output (KWe): 8.96

Fuel Feed: 1 gph diesel fuel = 7.1 lbs/hr

Hydrogen Produced: 1.02 lb.mol/hr (366 SCFH)

Anode Feed Gas, Hydrogen Content: 43%

System Efficiency:
Diesel fuel: 23%

Comments: Water condensor requires large air flow (~58% of the total), which increases the parasitic power load by a comparable amount. However, water recycle reduces fuel combustion from >50% to ~31% of the feed.

reasonable, although the reformer effluent temperature may be too low to prevent methane slip (at the 1-3% level). The analysis estimates the system efficiency as 23%. For a 5 KW net power output, this system requires a fuel feed rate of .56 gph of diesel fuel.

Table 6.15 analyzes the oxygen autothermal/cathode water recovery combination. For this example, the fuel processor weighs ~2800 pounds. Gross power output is 13.2 KW. However, routing the PSA system exhaust via the let-down heat exchanger provides for effective power recovery by the turbo-expander, and the net power output becomes ~11 KW. System efficiency is approximately 28% of the fuel's LHV. The air blowers represent the principal, parasitic power consumers. The hydrogen production rate is ~360 SCFH, with an anode feed gas concentration of 58%. System temperatures are higher but still workable, and the reformer effluent temperature of ~1700°F should eliminate any methane slip concerns (i.e., unconverted fuel). For a 5 kW net power output, this system's fuel feed rate is .45 gph of diesel fuel. Therefore, this system has all the benefits of oxygen enriched air, without the efficiency penalties.

Table 6.16 summarizes the fuel processor design analyses, and compares them to the present, methanol premix 5 kW unit. Designs 5 and 6 have been normalized to the 5 kW net power level. The first half of the table compares the designs using calculations quantified under this program: the second half presents qualitative comparisons based upon literature information on the present, methanol premix systems.[1] The current, 5 kW system uses approximately 1.6 gph of a 58% (volume) methanol/water premix as the fuel, with an enthalpy content of only ~4983 BTU/lb. This system cannot be re-energized to operate on diesel fuel. Designs 1 to 6 represent the system arrangements discussed previously. It is surprising that the hydrogen recovery approaches (Designs 3 and 4) do not rank highly, given the relative ease of

Table 6.15 -- Design 6: Autothermal Fuel Processor with Oxygen Enrichment and Cathode Water Recovery and Recycle (Figure 6.6 System)

	Weight, lbs	Price, $
Fuel Processor	1561	16424
Fuel Cell/Invertor (12.8 kW)	615	25600
Fuel Tank	40	120
Cathode Water Recovery	173	3870
PSA Oxygen System	363	3995
Turbo-Expander	50	17000
Total	2802	67,009

Estimated Assembled Cost: $255,300

Gross Power Output (KWe): 13.2

Parasitic Power Consumption (KWe):

Air blowers (477 SCFM @ .5 psig) =	~3.54
2 Ultrasonic nozzles, with pumps =	.10
Thermocouples/controls/valves (estimate) =	.30
PSA system compressor (4.07 hp) =	3.04
Turbo-expander recovery (-6.51 hp) =	4.86
Total	2.12

Net Power Output (KWe): 11.08

Fuel Feed: 1 gph diesel fuel = 7.1 lbs/hr

Hydrogen Produced: 1.02 lb.mol/hr (366 SCFH)

Anode Feed Gas, Hydrogen Concentration: 58%

System Efficiency:
Diesel fuel: 28%

Comments: ~3% estimated increase in fuel cell power output because of higher hydrogen concentration. This, and the turbo-expander, balance oxygen PSA system power consumption.

Table 6.16 -- Fuel Processor Design Summary and Comparisons (5 kW Size)

	Fuel Requirements	Power kWe Gross	Power kWe Parasitic	Net	Efficiency, % Based on Fuel LHV	Max. Temp., °F	Projected Weight Lbs.	Estimated Prototype Cost, $
Design 0: Current System	1.6 gph, 58% Methanol-Water Premix	~5.4	~.4	5	24	~1200	500	(-) (least expensive)
Design 1: Autothermal	1 gph Diesel Fuel	5.9	1.71	4.2	11% (diesel) 27% (methanol)	>3000	1791	93,500
Design 2: PSA/O_2	"	5.9	1.85	4.14	11% (diesel) 27% (methanol)	>3000	2204	173,500
Design 3: H_2 Enrichment	"	5.75	2.34	3.41	9	>3000	2375	287,600
Design 4: H_2 Recovery	"	6.73	2.17	4.56	12	>3000	2375	287,600
Design 5:* Cathode Recovery	.56 gph Diesel Fuel	7.15	2.15	5	23	~2200	2389	175,300
Design 6:* Cathode Recovery + PSA/O_2	.45 gph Diesel Fuel	5.95	.95	5	28	~2600	2802	255,300

*Table 6.14 and 6.15 results scaled to 5 kWe net power output.

Table 6.16 -- (Continued)

	Anode H_2 Concentration, Mole %	Estimated Noise, Inaudible Distance, M	Relative Start-Up Control	Fuel Flexibility	Relative Infrared Signature	Special Logistical Requirements	Rank* (Points)
Design 0: Current System	~75	100	1.0	None (Methanol Premix Only)	1.0	Fuel, Catalysts	2 (51)
Design 1	16 Diesel (41 Methanol)	100	.8 (easier)	Diesel, Gasoline, Alcohols	1.2	Catalysts	3 (49)
Design 2	31	~125	1.2 (harder)	"	1.3	Catalysts, Sieves	6 (39)
Design 3	80	~125	1.2	"	1.2	Catalysts, Membranes	7 (28)
Design 4	17	~125	1.2	"	1.2	"	5 (40)
Design 5	43	~110	1.0	"	1.2	Catalyst, IX Resin	1 (52)
Design 6	58	~125	1.2	"	1.3	Catalyst, IX Resin, Sieves	4 (46)

*Based on 1-6 point rating system, 6 points for the best system in the category.

recovery. Designs 5 and 6 have the best fuel economy and efficiency of the proposed systems, and more reasonable temperatures (2200-2600°F). Qualitatively, all the designs are estimated to be slightly noisier, somewhat harder to start and control, and to possess a slightly larger, infra-red signature, as compared to the present system. The most favorable ranking is for the autothermal/cathode recycle approach (Design 5), followed by the present approach (Design 0), basic autothermal (Design 1), and autothermal/PSA/cathode recycle (Design 6) systems. Since the present system cannot use diesel fuel, and the basic autothermal route involves very high temperatures (>3000°F), the two most promising designs are:

- Design 5: autothermal reformer with cathode water recovery.
- Design 6: autothermal reformer, using PSA/50% oxygen, with cathode water recovery.

These two designs are estimated to be comparably favorable: Design 5 weighs less and is less expensive, while Design 6 will provide for better reformer operation.

Table 6.17 estimates size and costs for final prototype configurations of Designs 5 and 6. Weights and costs have been adjusted to the 5 KW level using the .6 exponent law. Further weight economies could be accomplished by using nonstandard flanges, smaller thickness materials (e.g., Schedule 10), and higher alloys (e.g., Inconel, Hastelloy); these approaches were not evaluated. The final Design 5 system weight is estimated to be 1388 lbs., with an assembled cost of ~$83,000. For Design 6, these values become 1718 lbs. and $113,000, using a multi-lot (>5 units) price for the turbo-expander.[19] The weight estimates are approximately triple the present, methanol system value of ~500 lbs. This is expected. The methanol system's fuel processor only uses a low temperature burner/reformer. In contrast, the

Table 6.17 -- Estimated Final Prototype Size and Cost

Design 5: Autothermal System, with Cathode Water Recovery and Recycle

	Weight, lbs	Price, $
Fuel Processor	900	9400
Fuel Cell/Invertor (5 KW)	350	10000
Fuel Tank	40	120
Cathode Water Recovery	98	2200
Total	1388	21,720

Estimated Assembled Cost: $82,800

Design 6: Autothermal System, Using PSA/50% Oxygen, with Cathode Water Recovery and Recycle

	Weight, lbs	Price, $
Fuel Processor	900	9400
Fuel Cell/Invertor (5 KW)	350	10000
Fuel Tank	40	120
Cathode Water Recovery	98	2200
PSA/Oxygen System	280	2995
Turbo-expander	50	5000
Total	1718	29,715

Estimated Assembled Cost: $113,200

Design 5 fuel processor uses three additional process vessels (let-down heat exchanger, desulfurizer, and shift reactor), along with a larger, high temperature reformer/burner assembly, and results in a ~750 lb. increase in weight over the methanol system's fuel processor.

Figure 6.8 presents a conceptualization of the size and configuration of an assembled Design 5/6 system. The overall dimensions are 6' L x 3' D x 5' H (~90 ft^3). This is also considerably larger than the present methanol system (approximately 6' L x 3' D x 2' H). The differences derive from the more complex fuel processor required for diesel fuels. Prototype fabrication and testing undoubtedly will reduce system size and weight below these estimates, but, in the final analysis, the diesel fuel system will remain considerably larger and heavier than its methanol fuel cell system counterpart.

Dwg. 9381A32

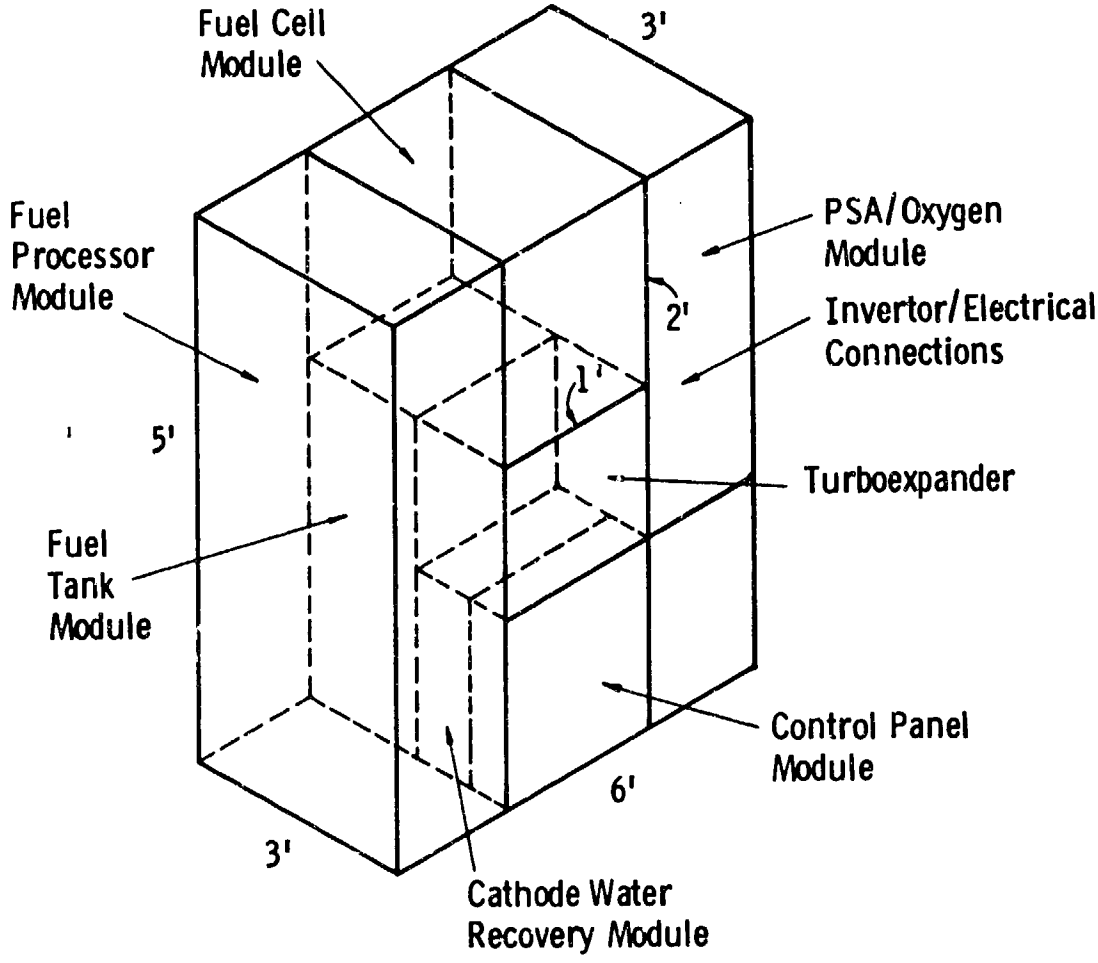

Figure 6.8 -- Conceptual View of Assembled, 5 kW, Diesel Fuel System (Design 6)

7. Experimental Fuel Processor Facility

The experimental fuel processor consists of seven major equipment pieces. All metals in contact with the process gases are Type 304 or Type 316 stainless steels. Figure 7.1 illustrates the equipment and the major processing steps, Figure 7.2 presents the complete fuel processor flow sheet. The major equipment operations are:

1. main burner - for fuel atomization, combustion, and mixing.
2. autothermal reformer - for fuel conversion to hydrogen/carbon oxides mixtures.
3. let-down heat exchanger - for cooling the reformer effluent gases.
4. desulfurizer - for hydrogen sulfide removal.
5. sample quencher - for quenching hot gas samples.
6. shift reactor - for water gas shift reaction conversion of carbon monoxide to hydrogen and carbon dioxide.
7. afterburner - for combusting the hydrogen rich gases produced by the experimental system.

The system is fabricated from Schedule 40 (150 psig) materials. Process vessels are 6" nominal pipe size, and most of the interconnecting, process plumbing is 1" pipe size. The maximum system working pressure is 20 psig: above this, three relief valves will open and direct process gases to the afterburner. The main burner, reformer, and afterburner are lined with castable ceramic materials, and are suitable for gas temperatures up to 2500°F. The rest of the system has a maximum working temperature of 1350°F, and, in normal operation, this does not exceed ~500°F. Table 7.1 summarizes other system specifications and limits.

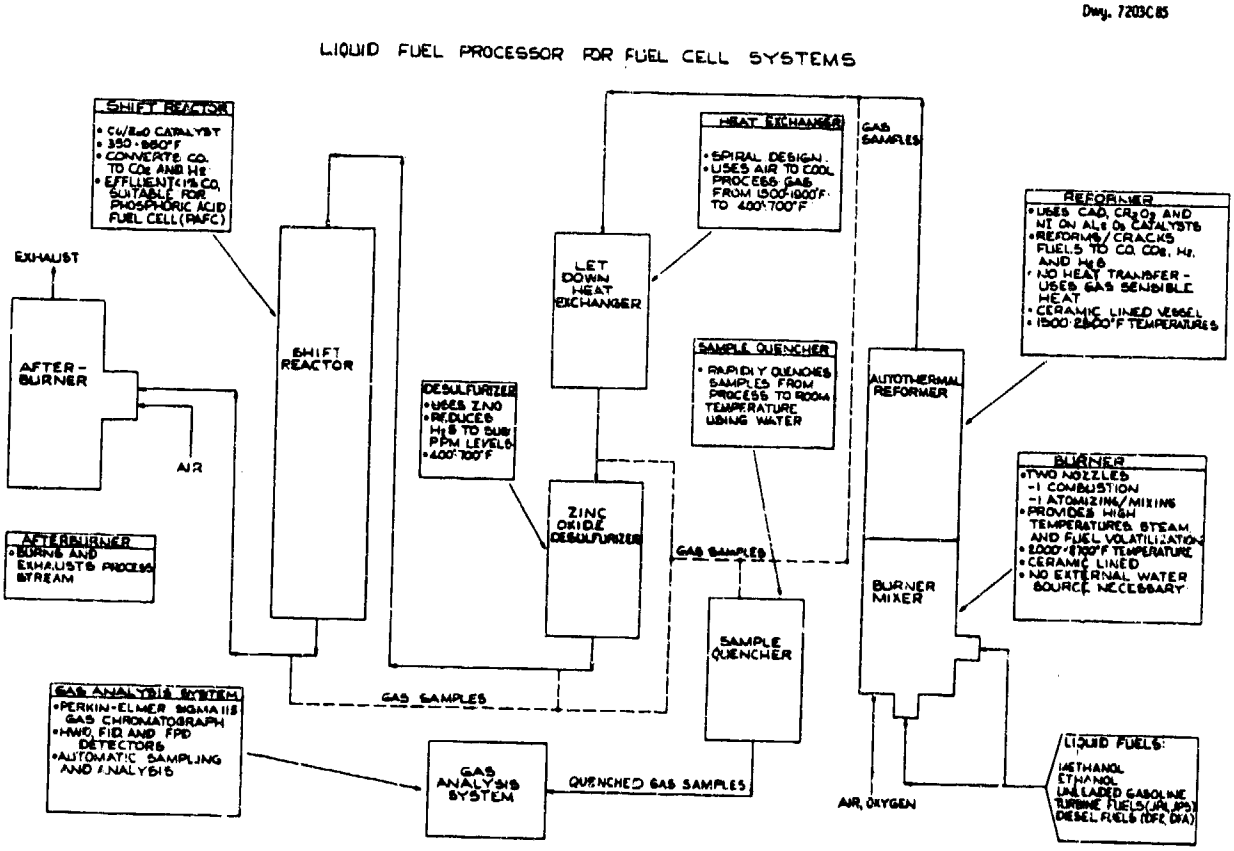

Figure 7.1 -- Major Processing Operations in the Experimental Fuel Processor System

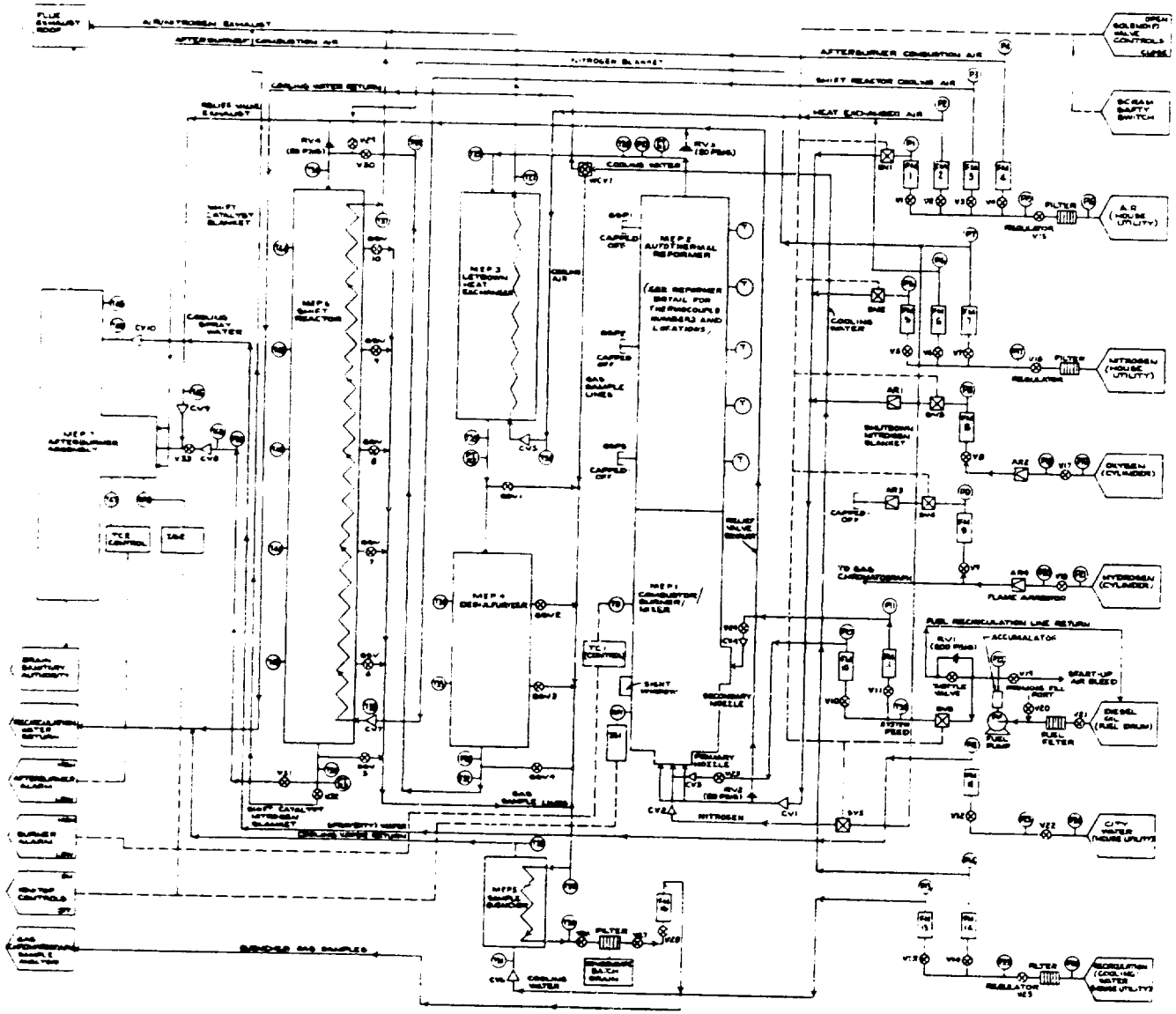

Figure 7.2 -- Waterless, Diesel Oil Fuel Processor: Process and Instrumentation Diagram for the Experimental System

Table 7.1 -- Experimental System Operating Parameters and Specifications

Criteria	Normal Operation	Maximum Limit
System pressure	3 psig	20 psig
System temperature (°F):		
ceramic lined vessels	2300-2400	2500
all others	400-500	1350
System flow rates:		
liquid fuel	1 gph	3 gph
combustion air	100-200 SCFH	700 SCFH
oxygen	100 SCFH	200 SCFH

Fabrication:
Main equipment vessels: 6", Schedule 40, 304 S.S. pipe.

Interconnecting plumbing: 1", Schedule 40, 304 S.S. pipe.

Minor amounts: 1/2", Schedule 40, 304 S.S. pipe and 4", Schedule 40, 304 S.S. pipe, and 316 S.S., 1/2" tubing.

Air and Fuel Lines: 1/2" copper tubing.

Sealants: high temperature doping compound, some teflon seals for areas <450°F

Gaskets: standard, flexitallic gaskets. (contain asbestos).

Figure 7.3 presents the laboratory arrangement and dimensions, and Figure 7.4 shows a photograph of the experimental system taken from the doorway area. The experimental system is organized into three test rigs:

1. Reformer Test Rig (Tag #5643)
2. Shift Reactor Rig (Tag #5649)
3. Control Panel Rig (Tag #5648)

Figure 7.5 displays the reformer test rig, which is 4' L x 3' D x 7' H. It contains the burner, reformer, let-down heat exchanger, desulfurizer, and sample quencher. Figure 7.6 depicts the shift reactor rig, which is also 4' L x 3' D x 7 H. It consists of the shift conversion reactor, afterburner, relief valve lines, and a nitrogen blanketing system. Figure 7.7 shows the control panel. Rotameters are used to measure all the flow rates, and a datalogger records all thermocouple and pressure transducer outputs (Table 7.2A). A separate display monitors vessel surface temperatures (Table 7.2B). As shown on the P&ID and on the control panel, there is a master on-off switch and an emergency shut down system. Four emergency shutdown ("SCRAM") switches are distributed around the laboratory (see Figure 7.3). This switch, or a power failure, causes solenoid valves to return to their unenergized positions. This shuts off the fuel flow, and purges the process system with nitrogen.

Figure 7.8 shows the burner in the laboratory. Figure 7.9 presents an axial cross-section of the main burner. Overall dimensions are 7" O.D. by 36" long. The main burner performs two functions: it combusts a set percentage (usually 30-60%) of the fuel to generate steam and high temperatures, and it atomizes additional fuel into the resultant hot gases. Consequently, the burner is divided into two sections. The primary nozzle area is a can-type burner, operating under oxidizing conditions (typically around two times stoichiometric). A

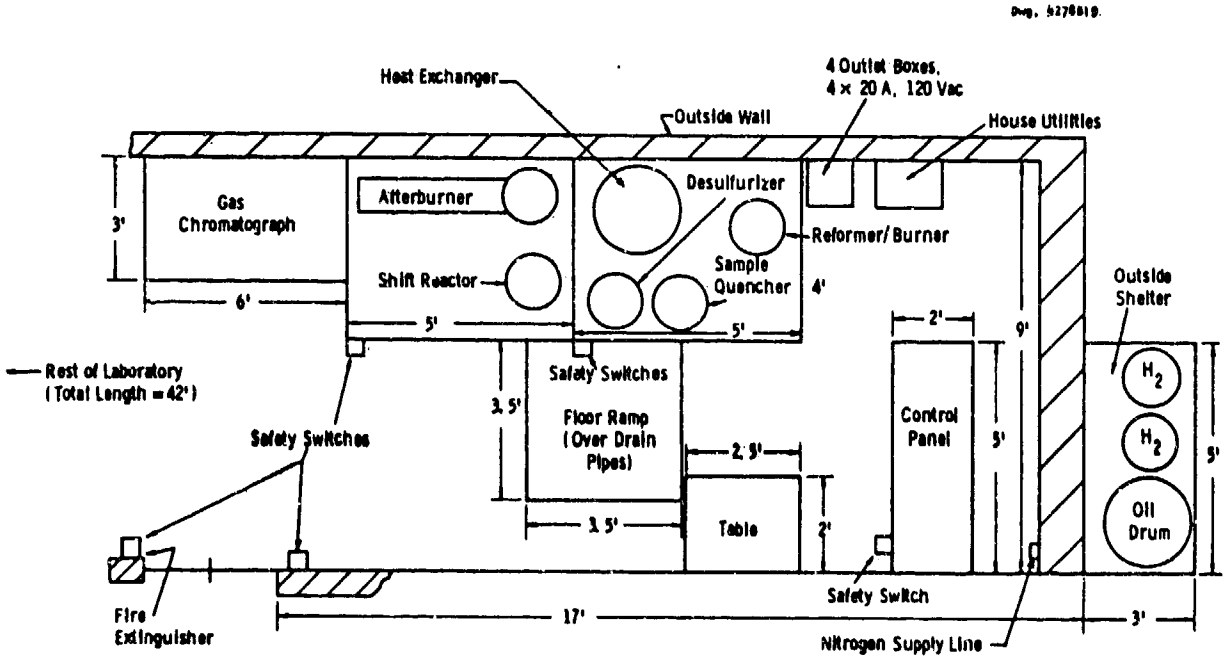

Figure 7.3 -- Experimental Fuel Processor Layout in the 301-1C3A Laboratory

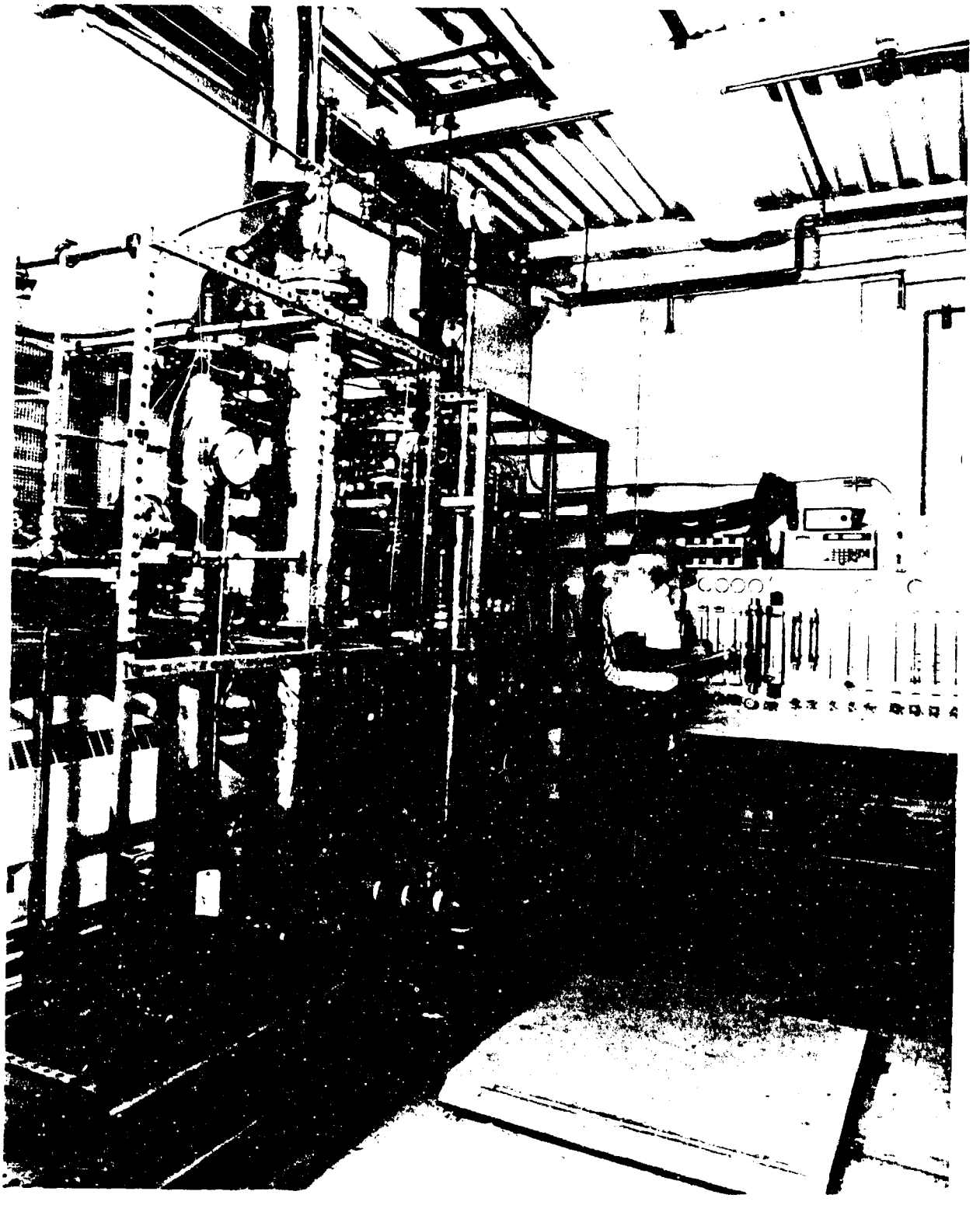

Figure 7.4 -- Experimental Fuel Processing System
(Insulation Removed)

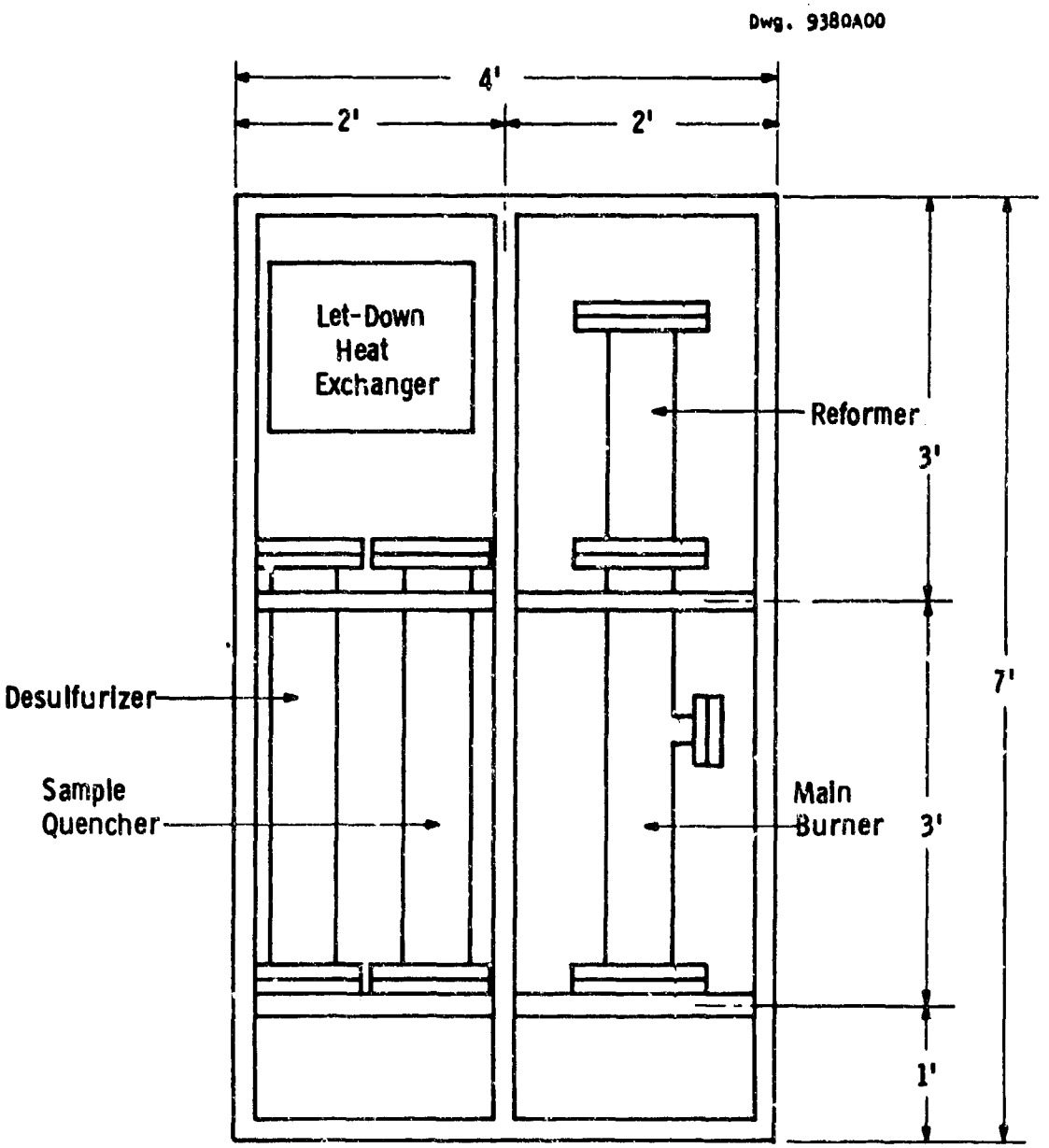

Figure 7.5A -- Reformer Test Rig Schematic

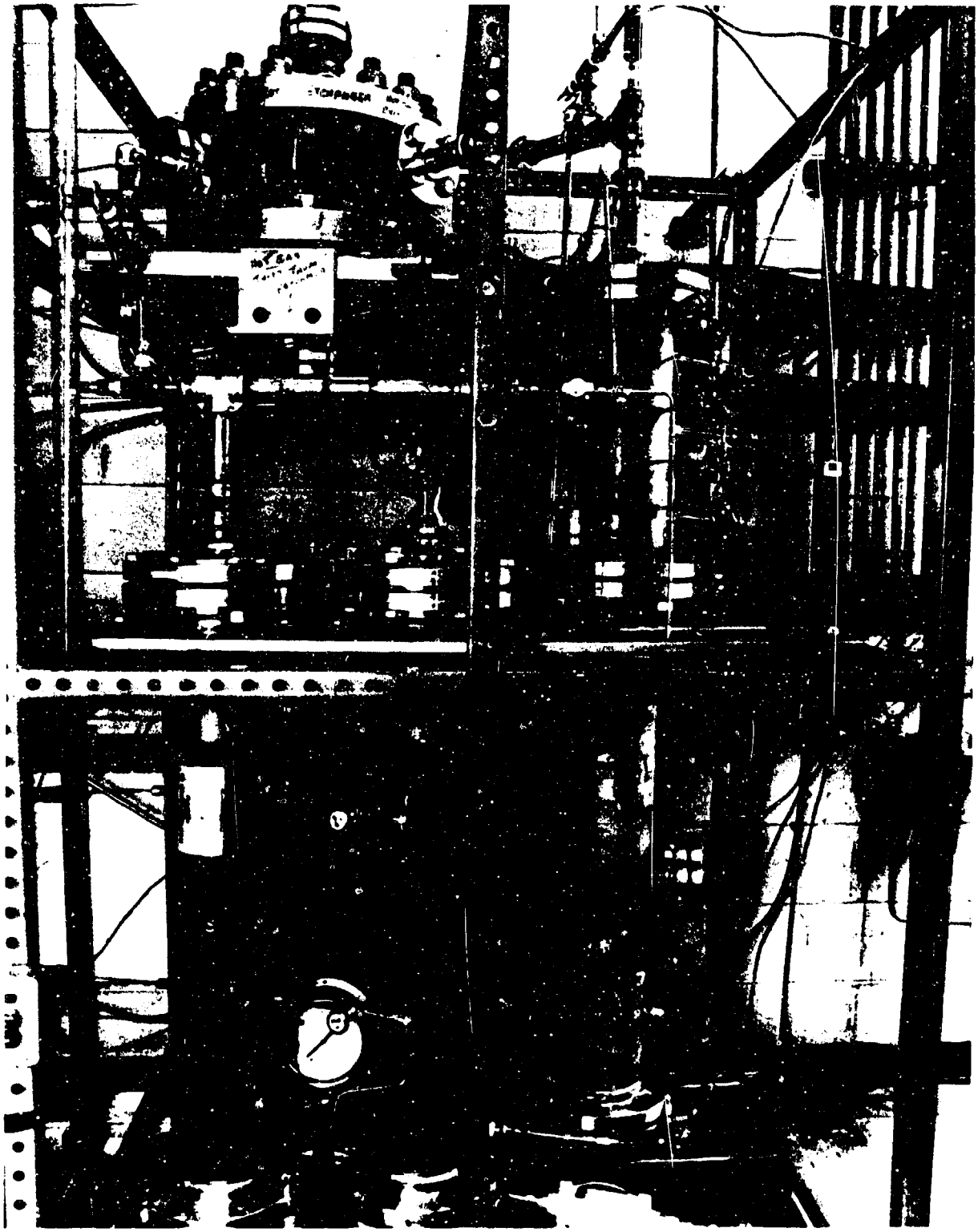

Figure 7.5B -- Photograph of the Reformer Test Rig

Dwg. 9380A01

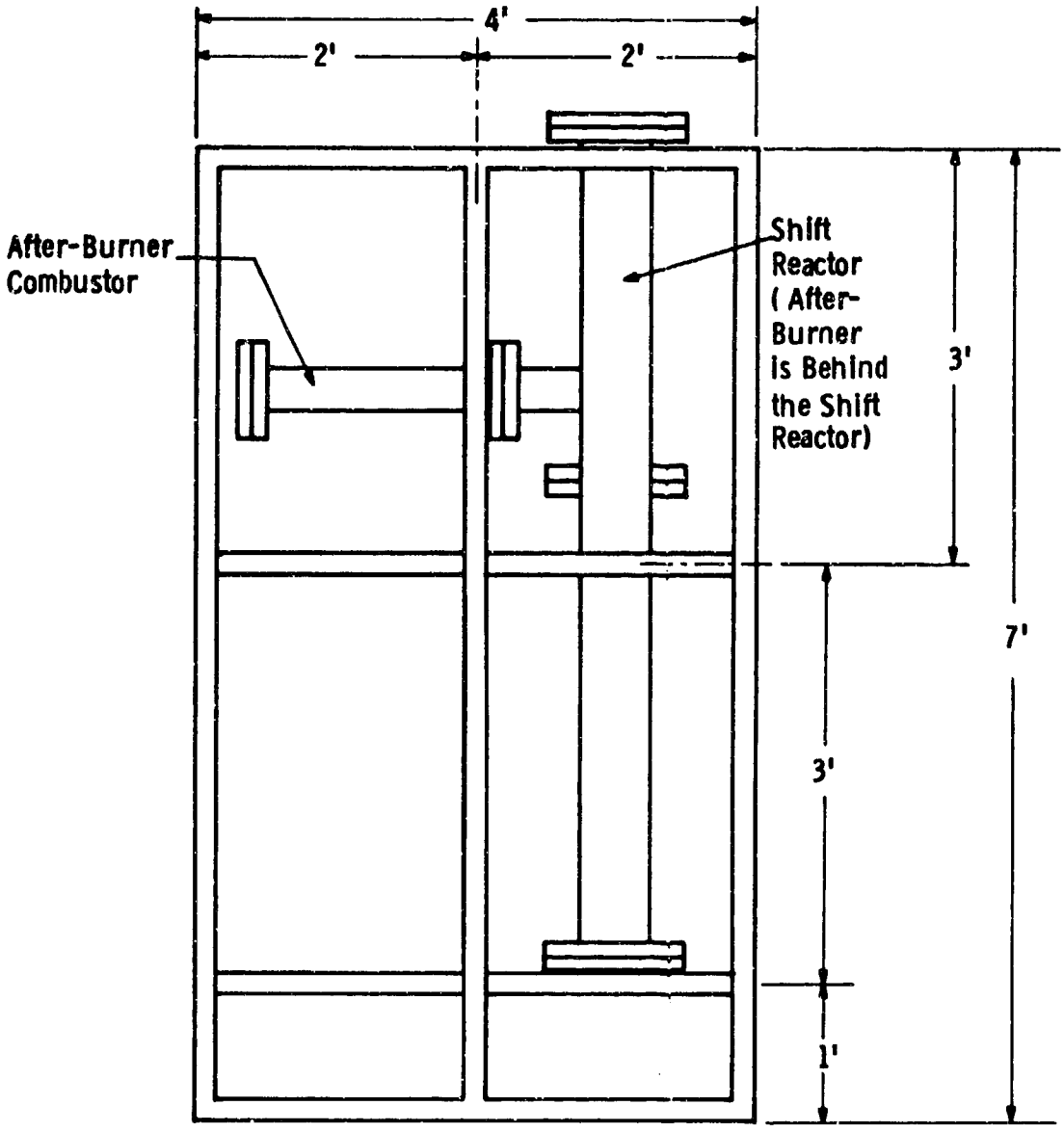

Figure 7.6A -- Shift Reactor Rig Schematic

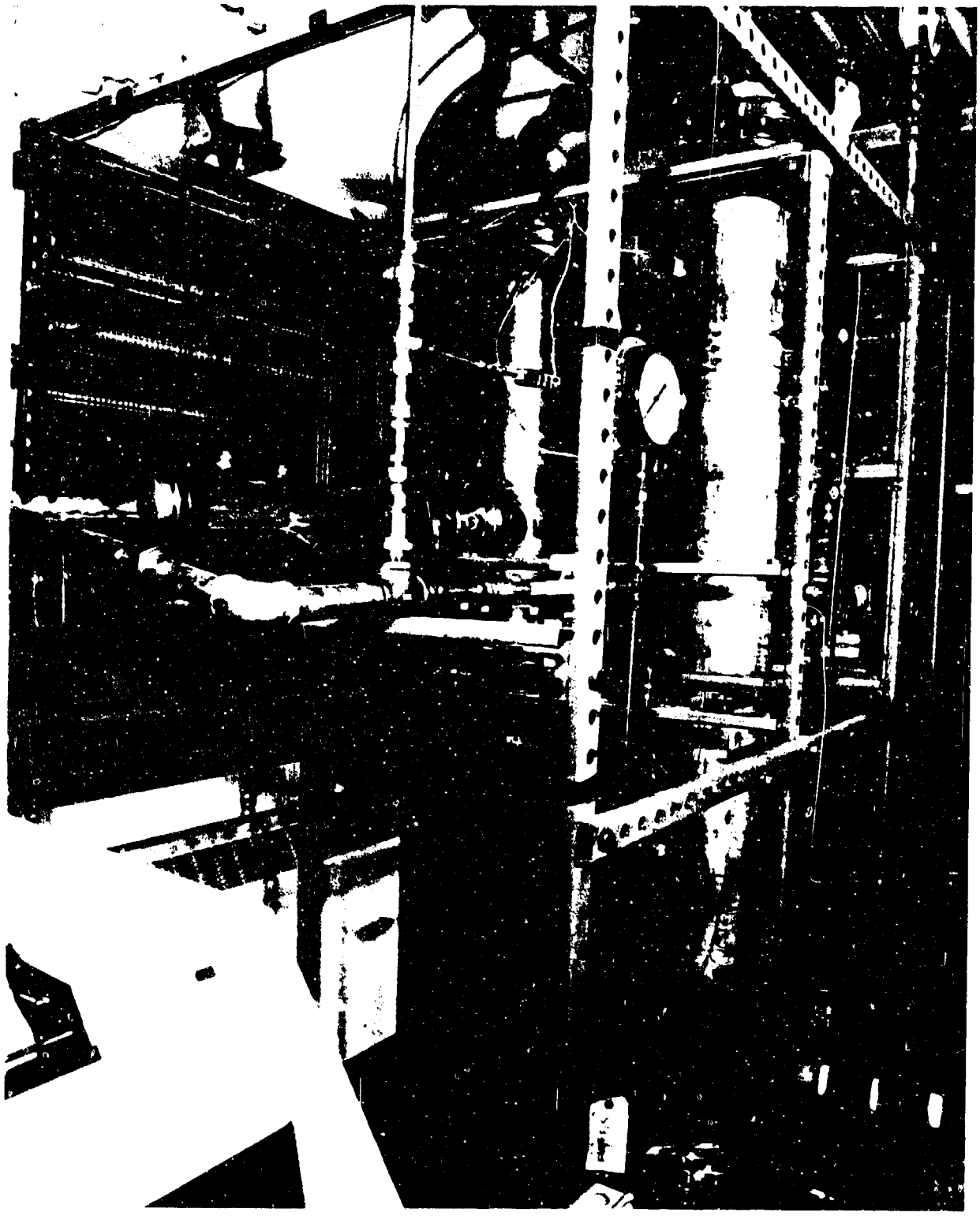

Figure 7.6B -- Shift Reactor Rig Photograph

Dwg. 4279813

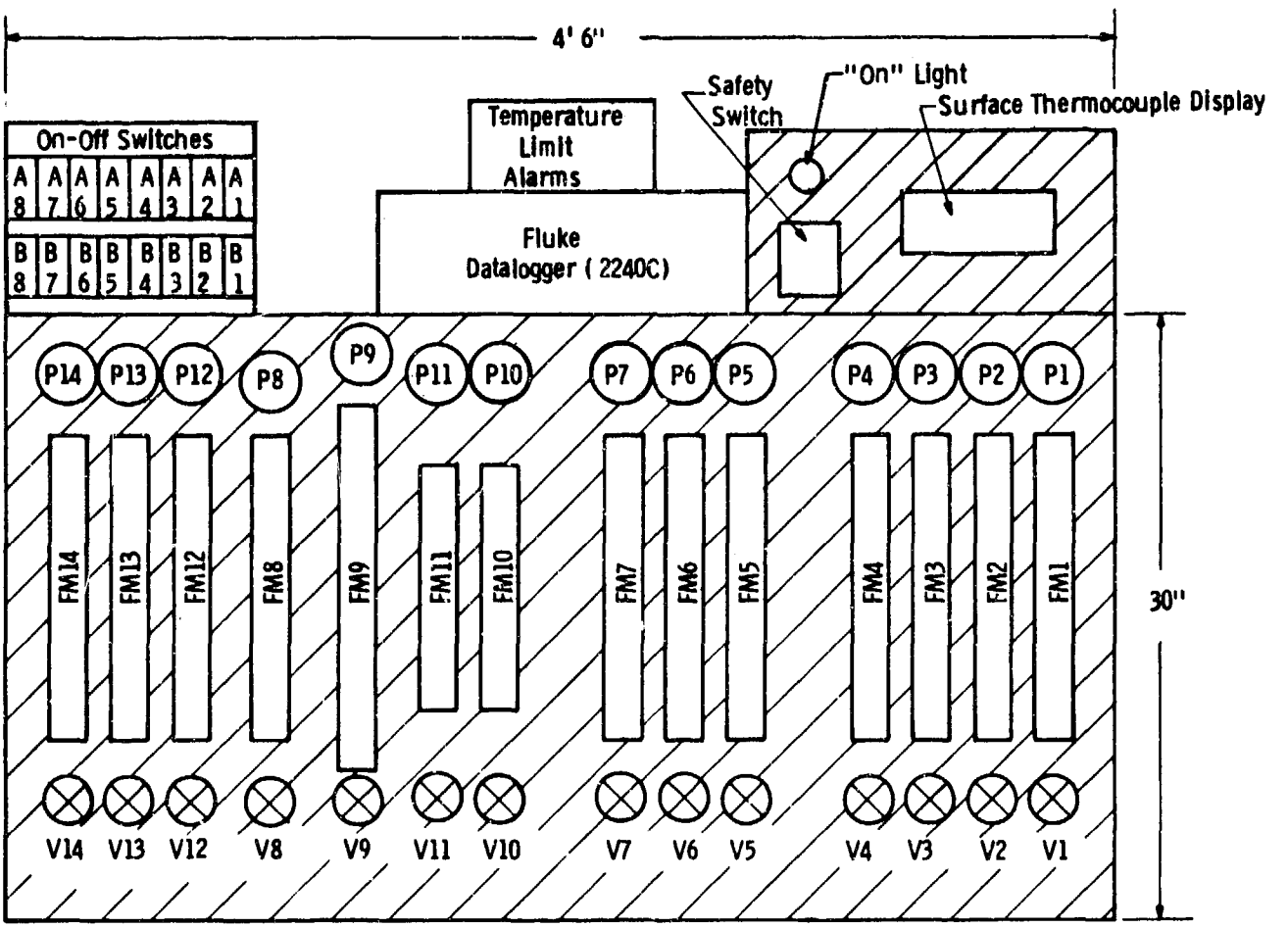

Figure 7.7A -- Control Panel Layout

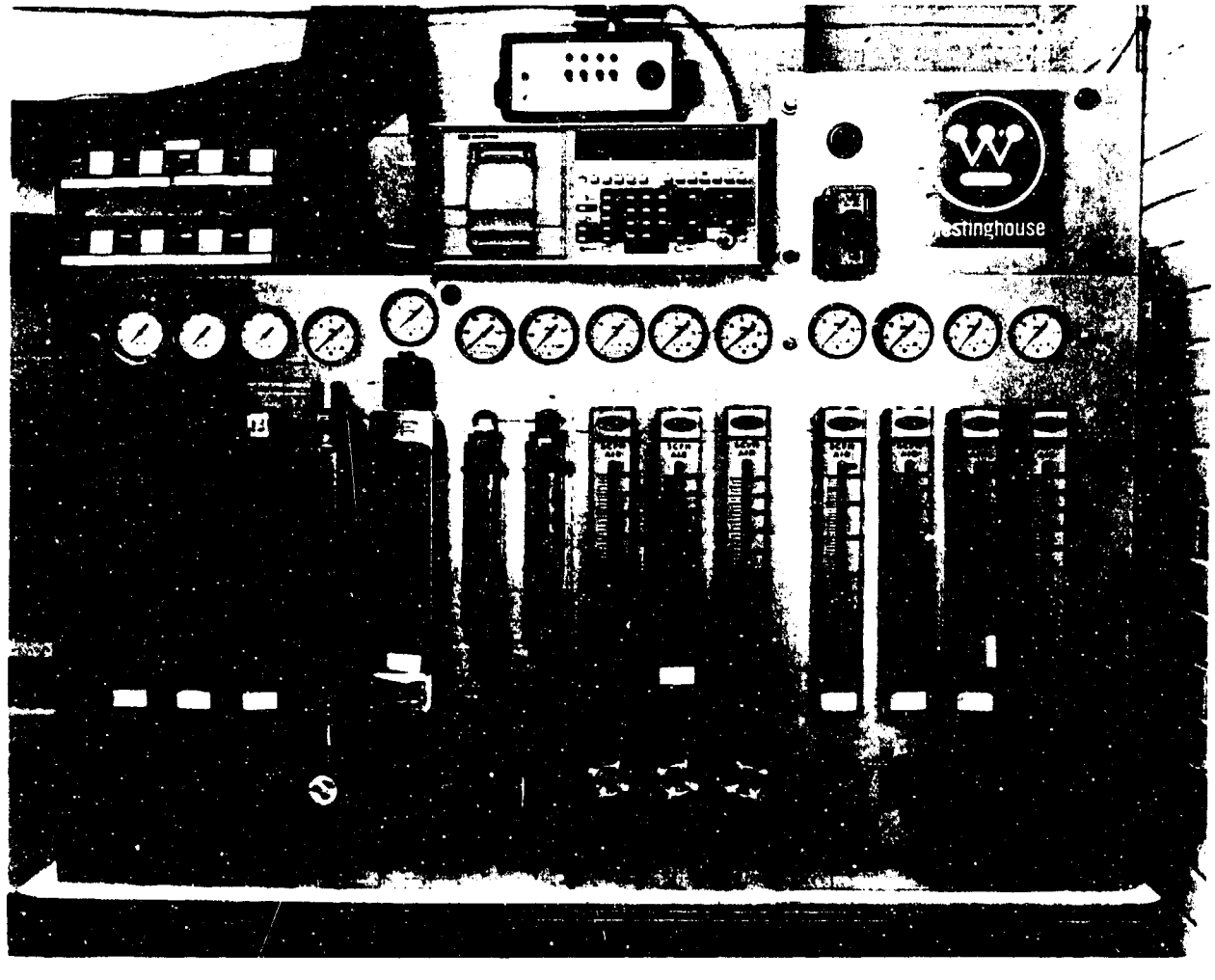

Figure 7.7B -- Control Panel

Table 7.2A -- Data Logger Channels and Thermocouple Locations*

Channel #	Description
0	Pt/Rh T-C, main burner
1, 2, 3, 4	Type K T-C, multi-fitting, reformer
5	Type K T-C, single fitting, reformer
6, 7, 8, 9	Type K T-C, multi-fitting, reformer
10	Type K T-C, single fitting, reformer
11, 12, 13, 14	Type K T-C, multi-fitting, reformer
15-24	Type K T-C, reformer
25	hot gas inlet on the heat exchanger
26	reformer exit line (top)
27	air exit on the heat exchanger
28	sample quencher (top) cooling water exit
29	sample quencher: gas sample line inlet
30	sample quencher: gas sample line exit
31	sample quencher: cooling water inlet
32	desulfurizer exit line
33, 34	desulfurizer
35	heat exchanger: process gas exit (to desulfurizer) 36 shift reactor inlet (top)
37	shift reactor: cooling air exit (top of coil

*all Type K thermocouples, unless noted otherwise.

Table 7.2A -- (Continued)

Channel #	Description
38	shift reactor: cooling air inlet (bottom of coil)
39	shift reactor exit (bottom)
40	bottom, left-side of shift reactor
41	left side of shift reactor
42	middle left side of shift reactor
43	left side of shift reactor (near top)
44	top, left side of shift reactor
45	process line, to afterburner
46	relief valve line to afterburner
47	Pt/Rh T-C, afterburner
48	spray cooler, gas exhaust (top)
49	city water to spray nozzles on afterburner
50	fuel oil feed to the system
51	heat exchanger, cooling air inlet
52	pressure transducer, shift reactor exit
53	pressure transducer, heat exchanger exit
54	pressure transducer, reformer exit

Table 7.2B -- Metal Surface Thermocouples (STC)

Display Number	Location*
0	ambient, control panel
1	16" from end of the afterburner
2	28" from bottom of the shift reactor
3	16" from bottom of the desulfurizer
4	9" from bottom of the reformer
5	4" from bottom of the reformer
6	32" from bottom of the main burner
7	10.5" from bottom of the main burner

All are Type K thermocouples

*all locations are measured from the gasket side of the flanges.

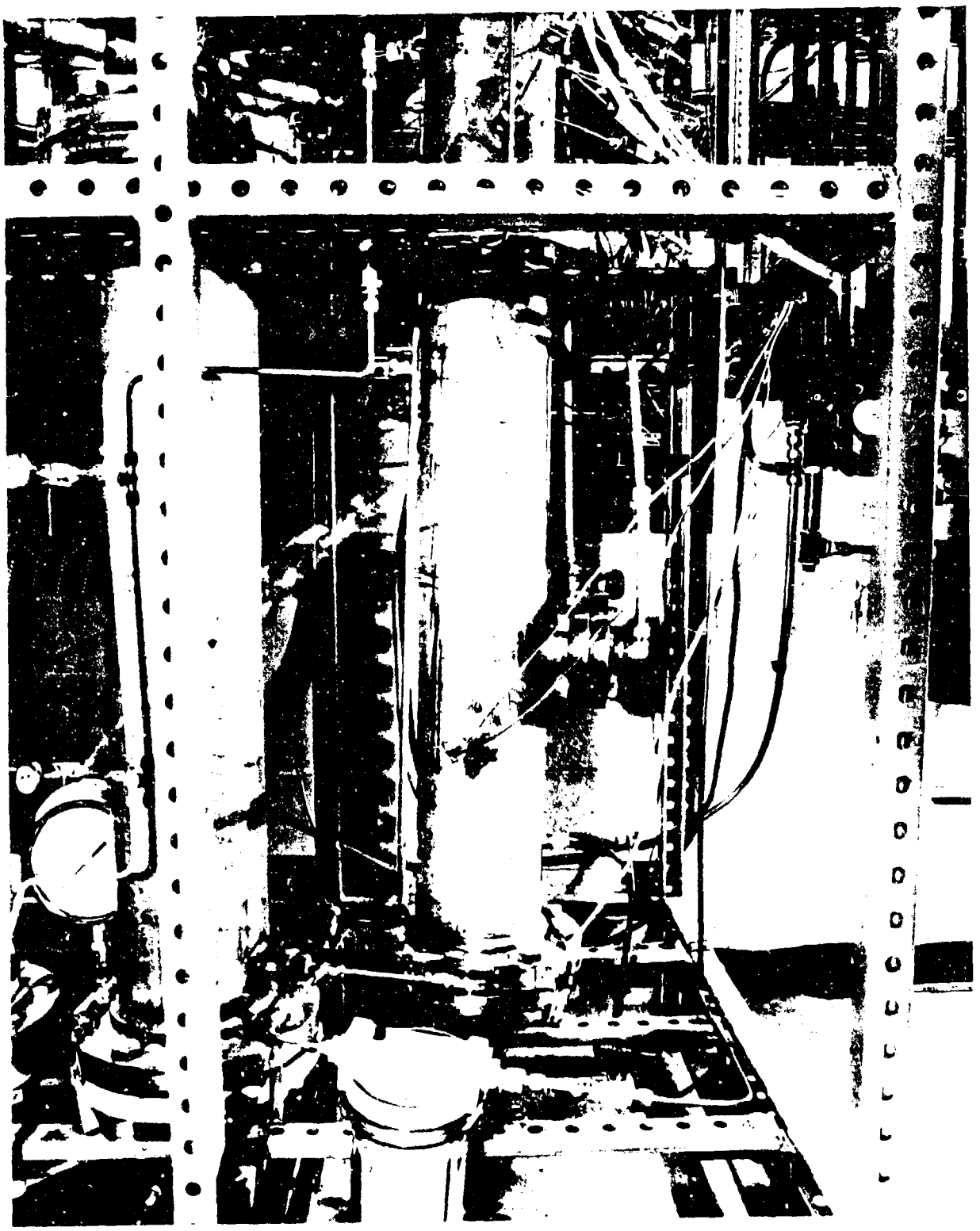

Figure 7.8 -- Main Fuel Processor Burner

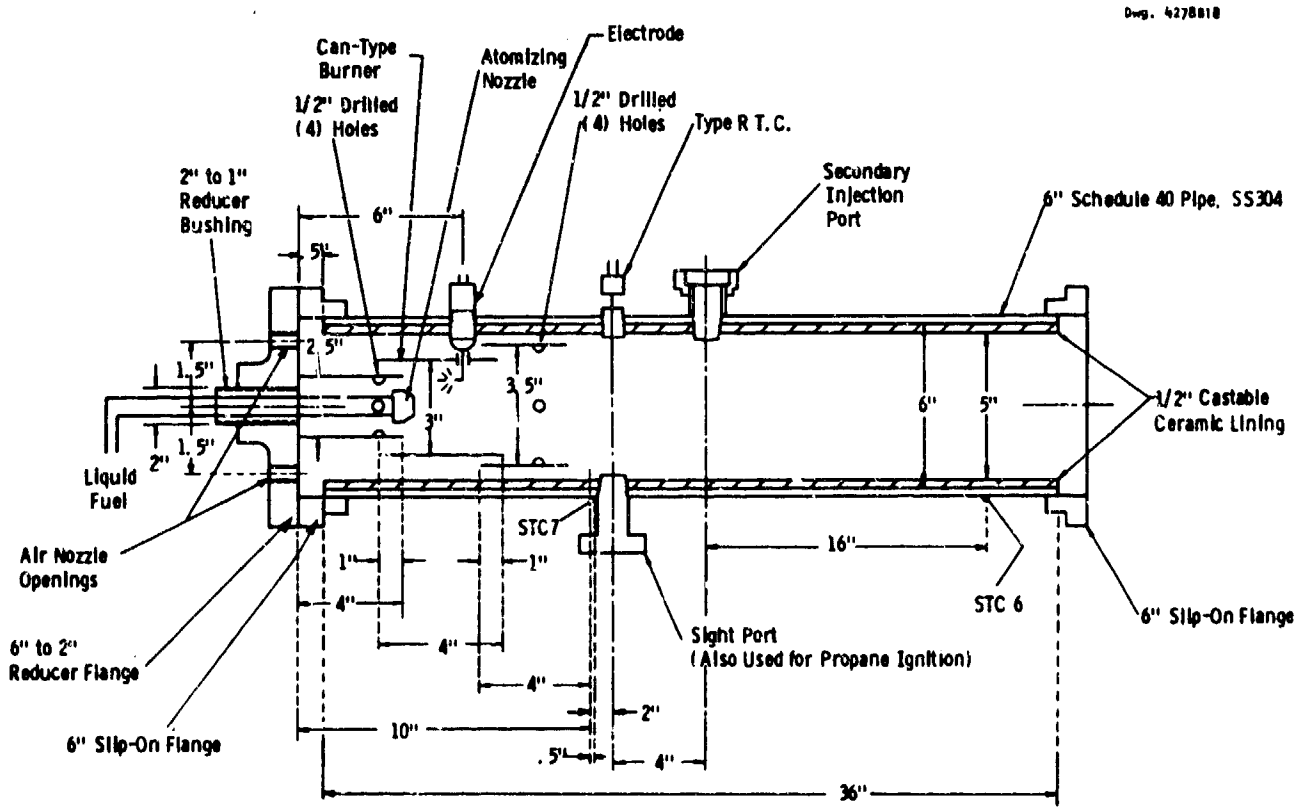

Figure 7.9 -- Axial Cross-Section of the Main Burner

pressure nozzle (~90 psig) atomizes the fuel into an air/oxygen stream, where ignition occurs from a high voltage electrode. Alternatively, ignition has been accomplished by connecting a propane torch ignition system installed in place of the sight window. Laminar air flow cools the stainless-steel, burner cans, and a Type R (13% rhodium/platinum) thermocouple monitors the flame temperature. The secondary nozzle uses pressure atomization to introduce additional fuel, and operates under reducing conditions. Figure 7.9 illustrates the secondary nozzle/injection port. Finally, the pressure vessel boundaries of the burner are protected by a 1/2" thick cast alumina ceramic (Puratab fine, manufactured by National Refractories) for protection against the high gas temperatures expected (2000-2500°F).

The reformer is attached on top of the burner via a flanged connection. As Figure 7.10 indicates, there are numerous thermocouple and gas sample ports. The reformer contains a catalyst that efficiently reacts the hot, atomized fuel/steam/gas mixture into hydrogen and carbon oxides. This design uses an autothermal (also called adiabatic) approach: the gas stream's sensible heat provides the enthalpy for the endothermic reformer reactions, and no external heat transfer or heat source is required. Consequently, high inlet gas temperatures are necessary. Figure 7.11 shows the reformer axial cross-section with the thermocouple and gas sample port locations. Figure 7.12 shows the top view. The approximate overall dimensions are 7" O.D. by 18" high, with an internal catalyst volume of approximately .176 cubic feet (5.00 1). The reformer was designed using methanol data at 600°F: a computer model verified the design for diesel fuels.[10] The vessel includes a cast, alumina ceramic lining (Puratab fine) because of the high temperatures involved. A catalyst screen support ring is welded inside the reformer vessel (Figure 7.11). The catalyst support assembly is manufactured out of inconel. Four inconel bolts connect the catalyst support assembly to the screen support ring inside the reformer, using access from below the unit. For the exit line at the top of the reformer, an inconel screen is simply placed on top of the catalyst,

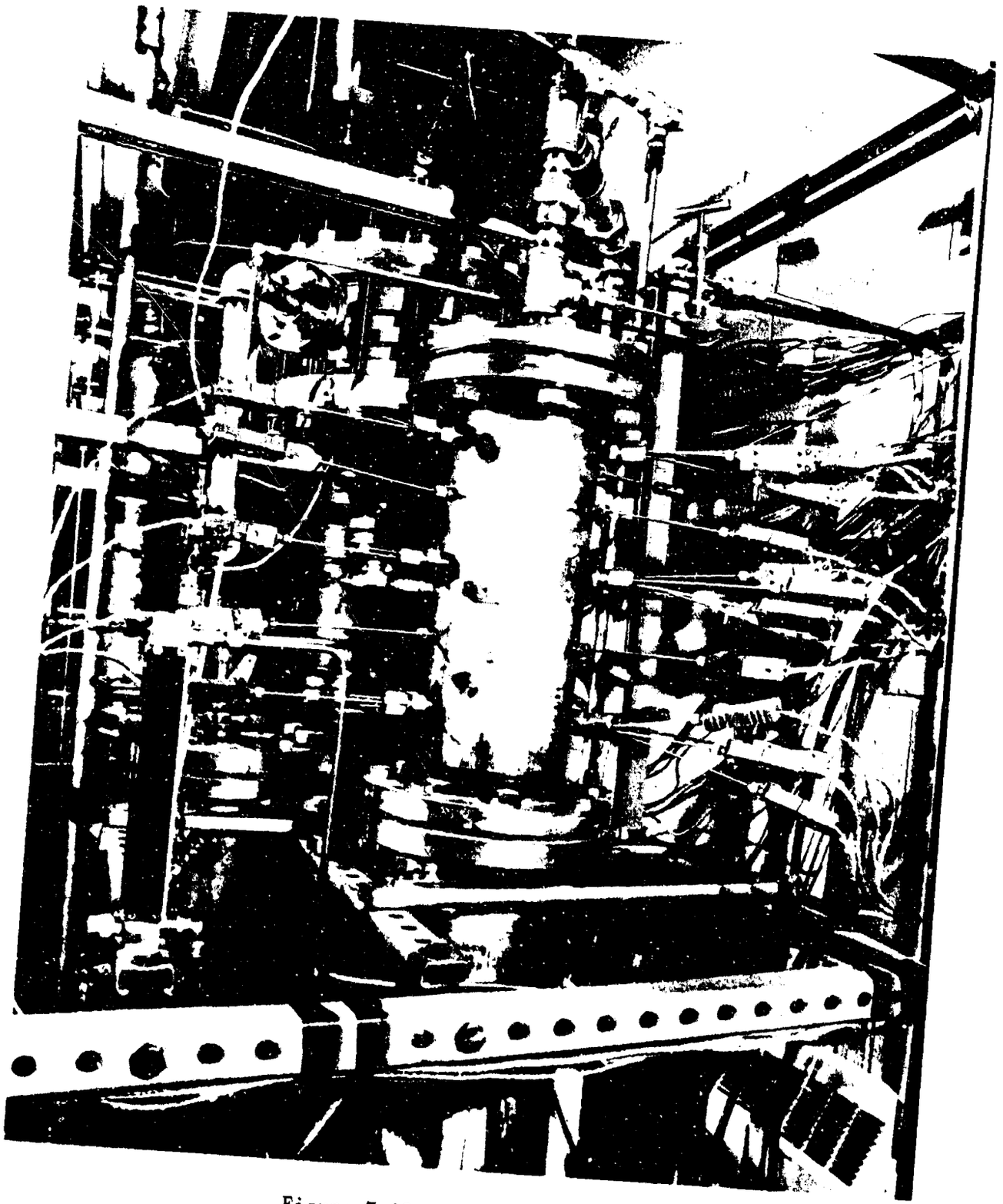

Figure 7.10 -- Reformer Vessel

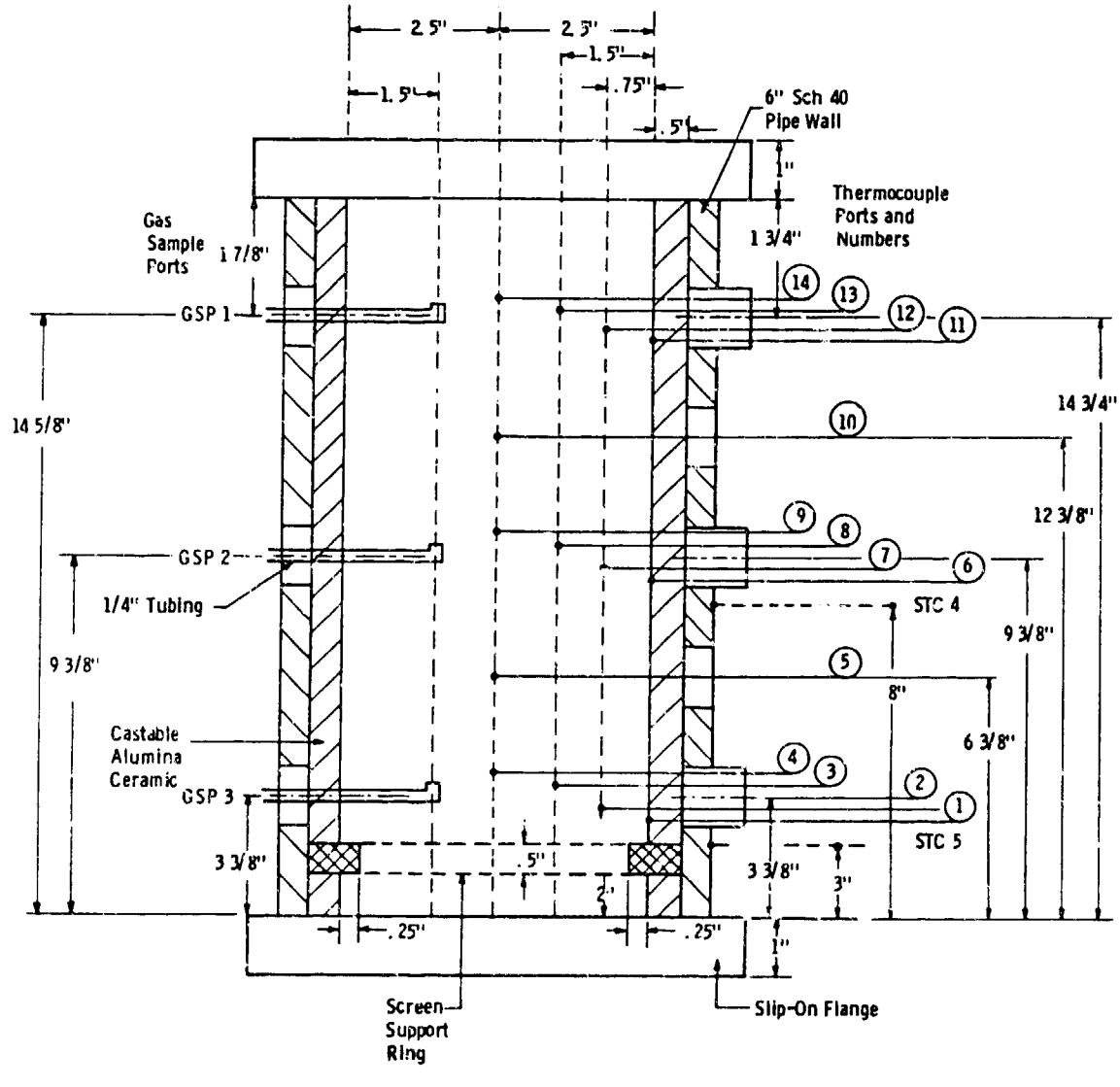

Figure 7.11A -- Reformer Thermocouple and Gas Sample Port Locations (Side View, STC = Surface Thermocouple)

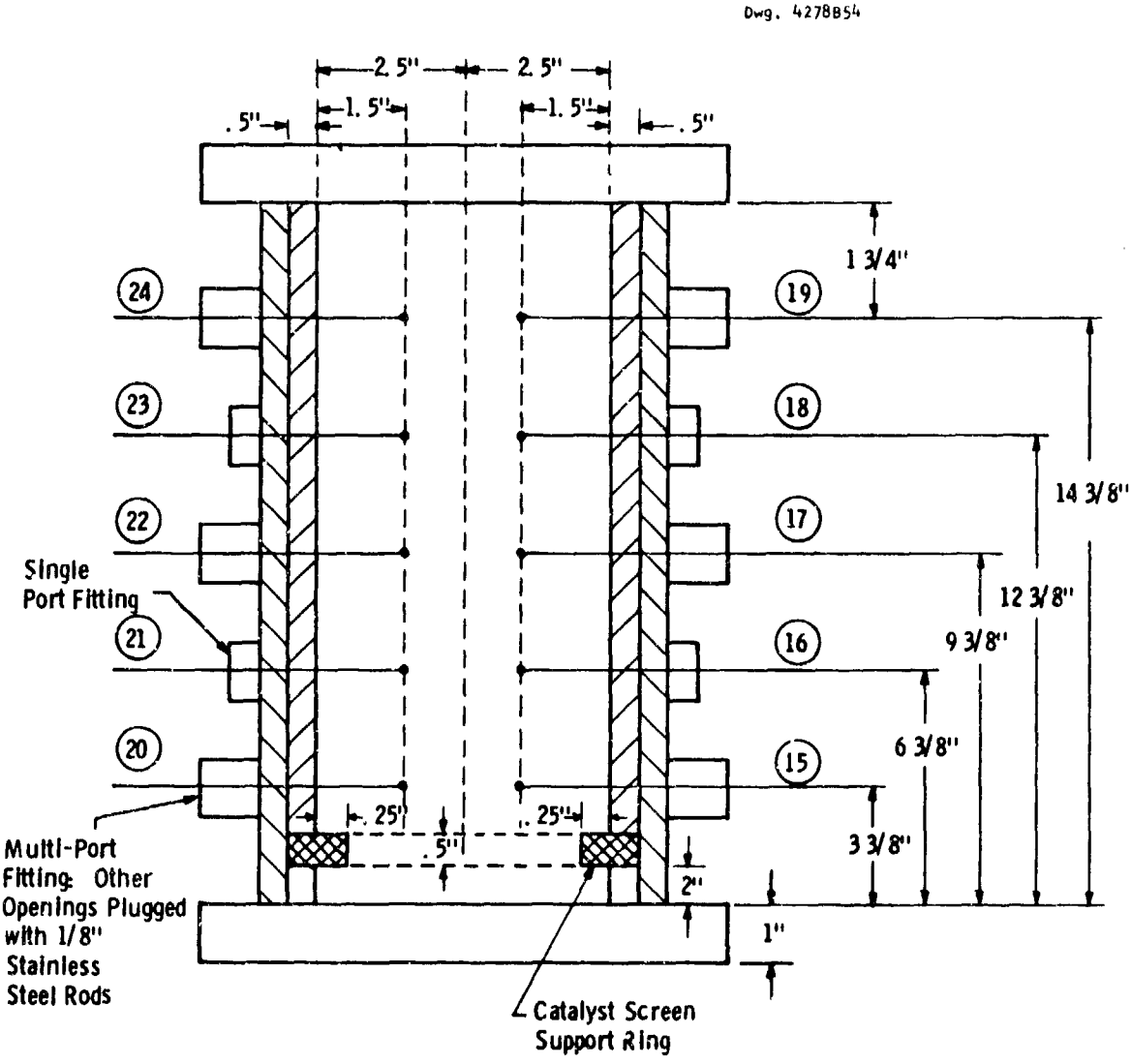

Figure 7.11B -- Reformer Side View - Other Thermocouple Locations

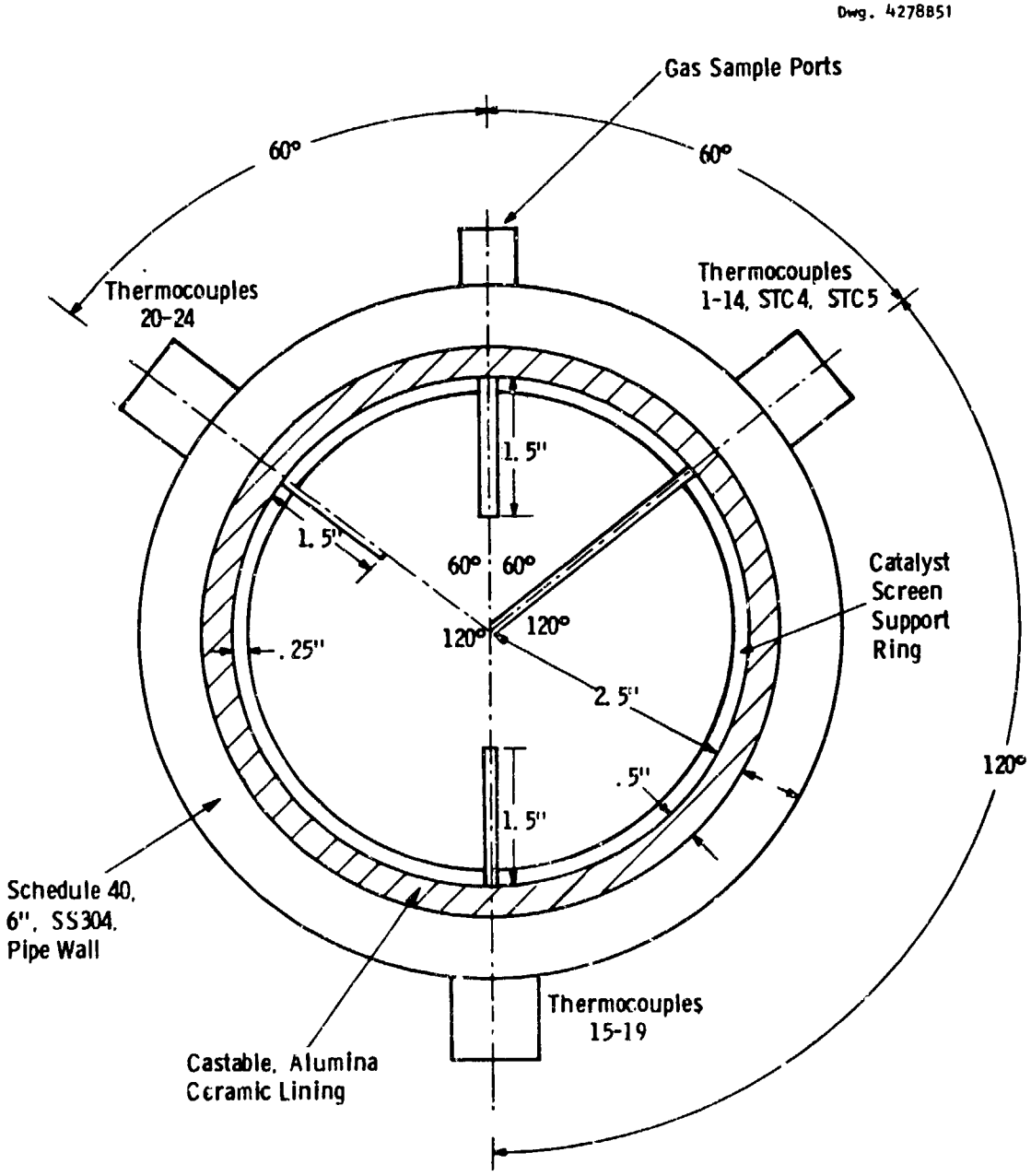

Figure 7.12 -- Reformer Thermocouple and Gas Sample Port Locations
Top View

inside the flange area. This prevents catalyst entrainment into the exit line. Inconel screens should behave acceptably in the reformer's high temperature inlet. Inconel should retain adequate strength even at ~2200°F, and it will be cooled by the endothermic reactions occurring on the catalysts it supports. Alternatively, the bottom support ring can be manufactured from ceramic materials, inserted from above the reformer, and supported by the screen support ring.

Figure 7.13 displays the let down heat exchanger. This is a commercial unit manufactured by Alfa Laval. It is a spiral heat exchanger design (AHRCO Type 1-V), with overall dimensions of 23 1/2" diameter by 22" high. The heat transfer surface area is 5 square feet, and the unit weighs approximately 310 pounds. The entire unit is manufactured out of Type 316 stainless steel, and has a maximum working pressure of 50 psig at 1350°F. This heat exchanger uses air to cool the hot (1300-1600°F), reformer effluent gases to 400-600°F for desulfurization and shift reaction conversion.

Figure 7.14 shows the desulfurization reactor and sample quencher. The desulfurizer uses zinc oxide to absorb hydrogen sulfide from the process gas. Figure 7.15 displays a detailed schematic. The support and retention screens are fabricated from Type 304 stainless steel, instead of Inconel. These are inserted from each end, and secured with four bolts, in the same manner as the reformer catalyst screen. The actual packing volume is ~.49 ft^3, and corresponds to ~119 hours of operation with 300 ppm(v) hydrogen sulfide in the process stream at 400°F. A tee-shaped manifold on the sealing flange provides for effective gas distribution.

The sample quencher uses recirculation (cooling) water to rapidly cool process gas samples from 400-1300°F down to ambient temperatures. Figure 7.16 presents a schematic. Overall dimensions are 7" O.D. by 36" high. The pipe walls and flanges are Type 304 stainless steel, while the coil is fabricated from 1/2", Type 316 stainless steel

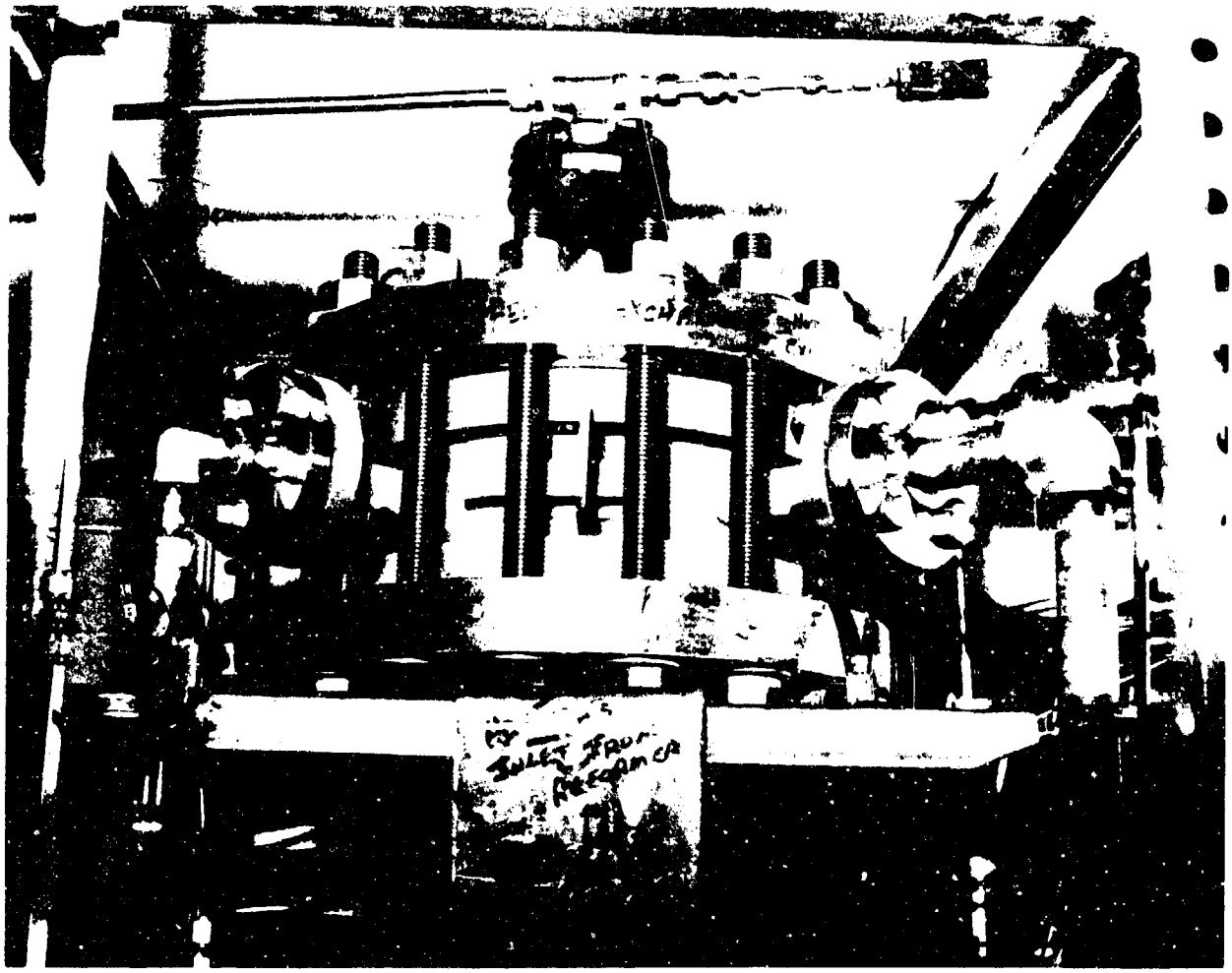

Figure 7.13 -- Let-Down Heat Exchanger

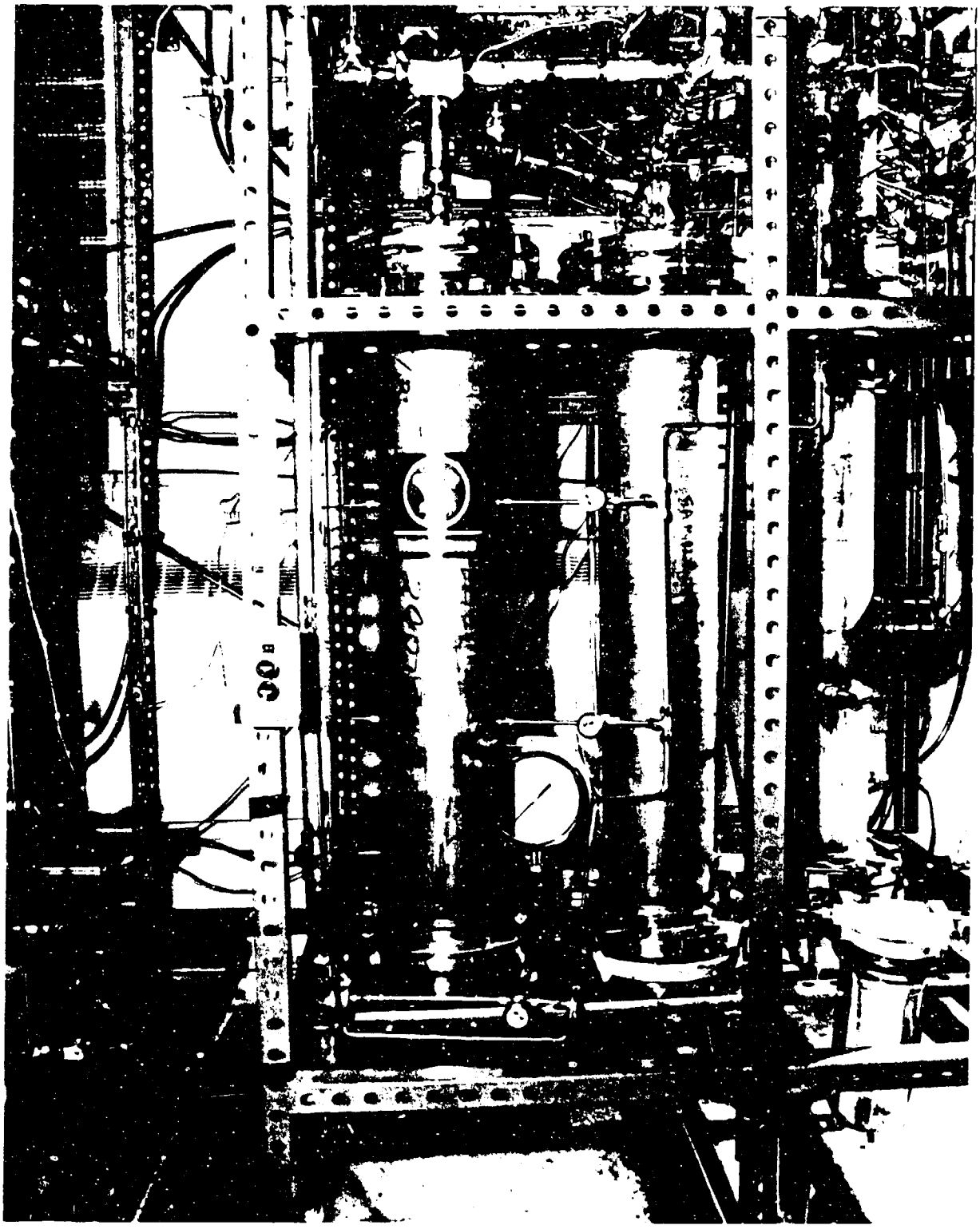

Figure 7.14 -- Desulfurization Reactor and Sample Quencher

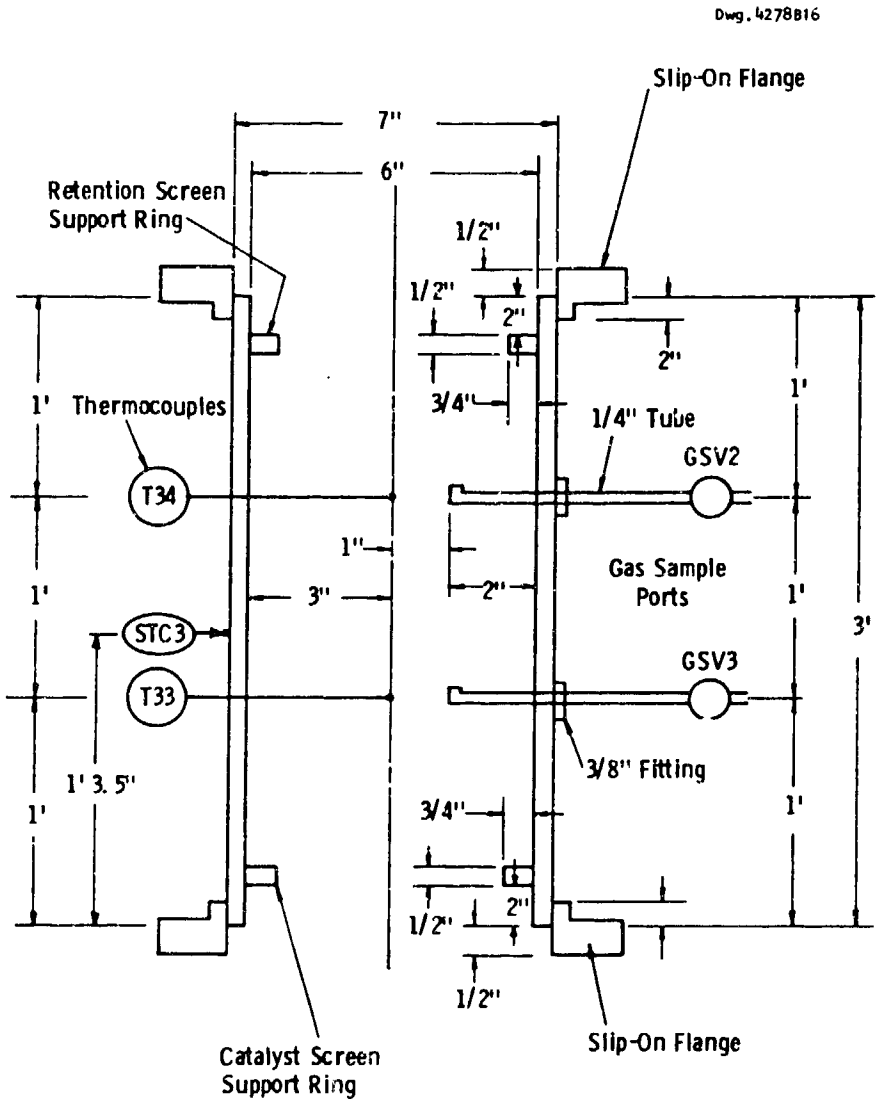

Figure 7.15 -- Desulfurization Reactor Schematic
(Pipe and Flanges are 6" Nominal, Schedule 40)

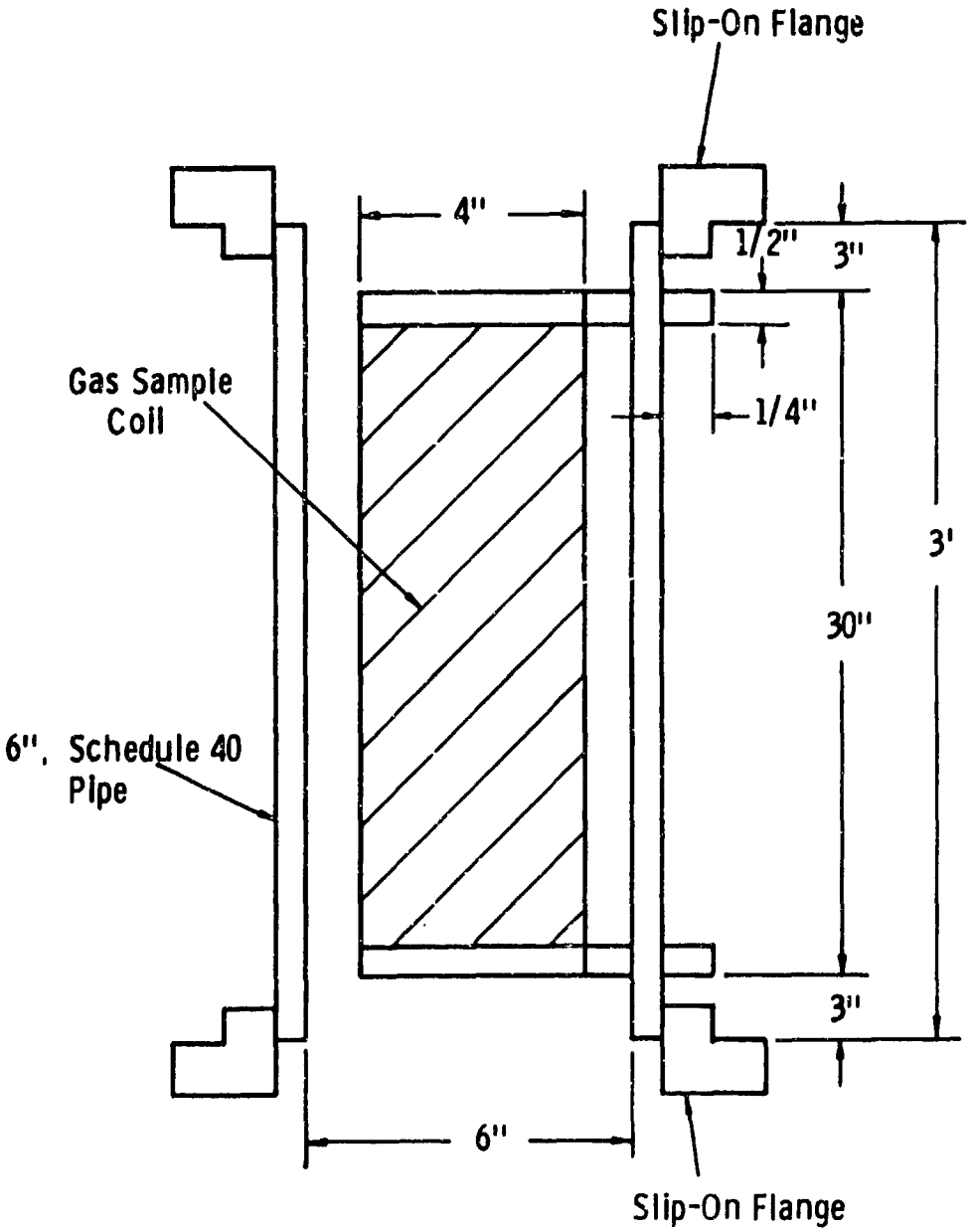

Figure 7.16 -- Gas Sample Cooler/Quencher

tubing (Figure 7.17). One inch pipe couplings are welded around the tube extensions on the outside of the vessel. Flanges with tee manifolds are bolted on the ends of the sample quencher. In operation, the hot gas sample enters at the top of the coil, and is cooled by the water flowing around the coil's exterior. The quenched sample exits through the lower coil port. A cartridge filter acts as a trap for condensates and particulates, and the quenched gas sample proceeds to the gas chromatograph for analysis.

Figure 7.18 shows the shift reactor and afterburner. The shift reactor has overall dimensions of 7" O.D. by 72" high, and is depicted in Figure 7.19. The reactor includes retention screens made from Type 304 stainless steel, which are dimensionally identical to the desulfurizer and reformer screens. The reactor is sized using the unidimensional design equation and assuming isothermal behavior. Literature kinetic data was used. The effective catalyst volume is 1.03 ft^3 (the coil volume is an additional ~.075 ft^3). The shift reaction is slightly exothermic and occurs over the 350-600°F range. Consequently, cooling air flows through the coil, and process gas flows through the vessel. A tee-manifold on the end flanges distributes the gas flow evenly.

Figure 7.20 displays the afterburner schematics. Overall dimensions are 7" O.D. by 72" high, with a horizontal tee section 5" O.D. by 36" long. The afterburner uses a horizontal, can-type combustor for burning the process gases (e.g., hydrogen and carbon monoxide) prior to exhaust via the stack. Ignition uses an electrode. Combustion will produce temperatures in the 1600-2000°F range, and, consequently, the vessels are lined with a cast magnesia-based ceramic (Permanete, from National Refractories). A type R thermocouple monitors flame temperatures. The vertical section constitutes a spray cooler, using city water flowing at ~1 gpm. A ~12" high water level trap prevents burner off-gases from entering the laboratory area, and directs the

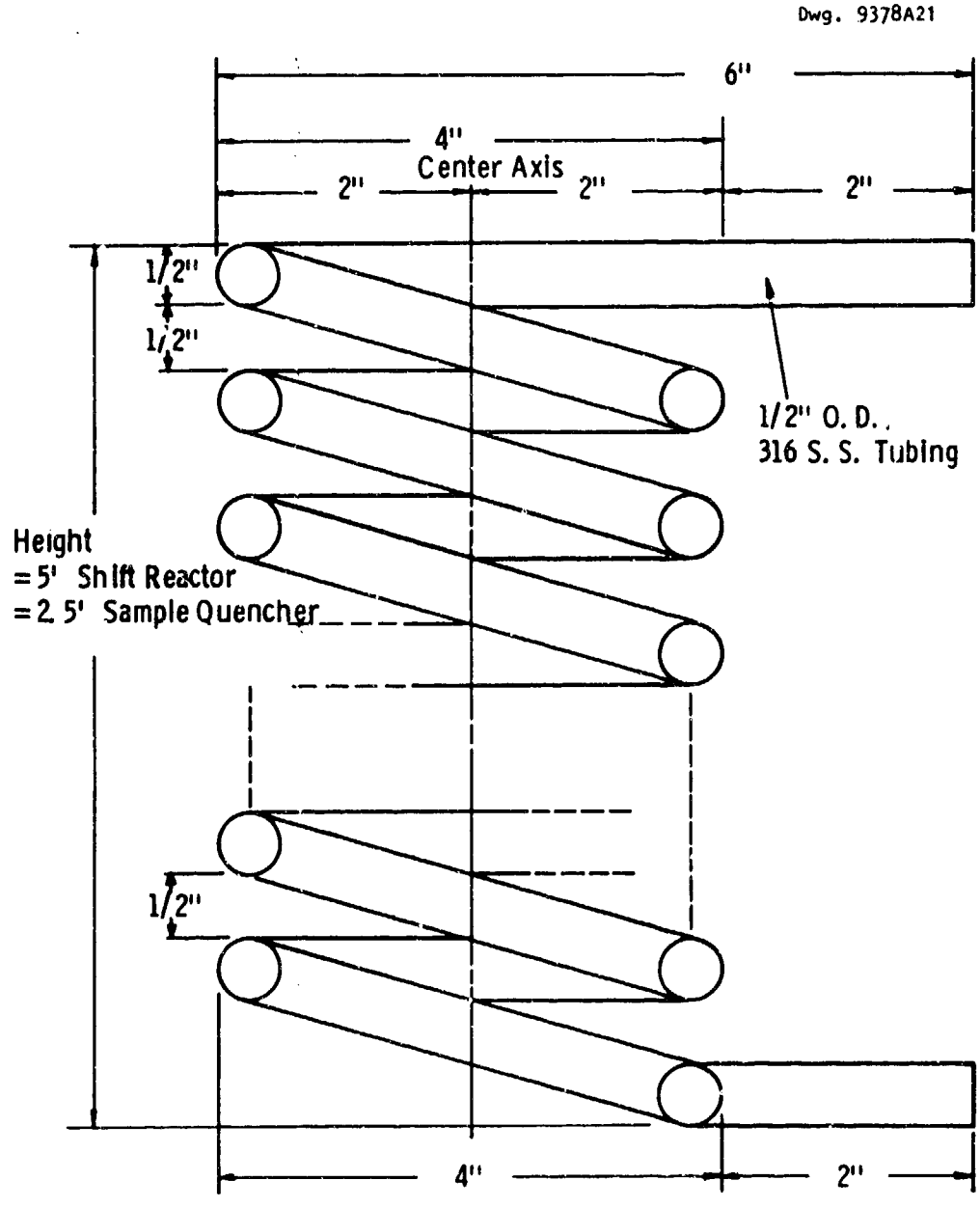

Figure 7.17 -- Cooling Coil Detail for Sample Quencher and Shift Reactor Side View

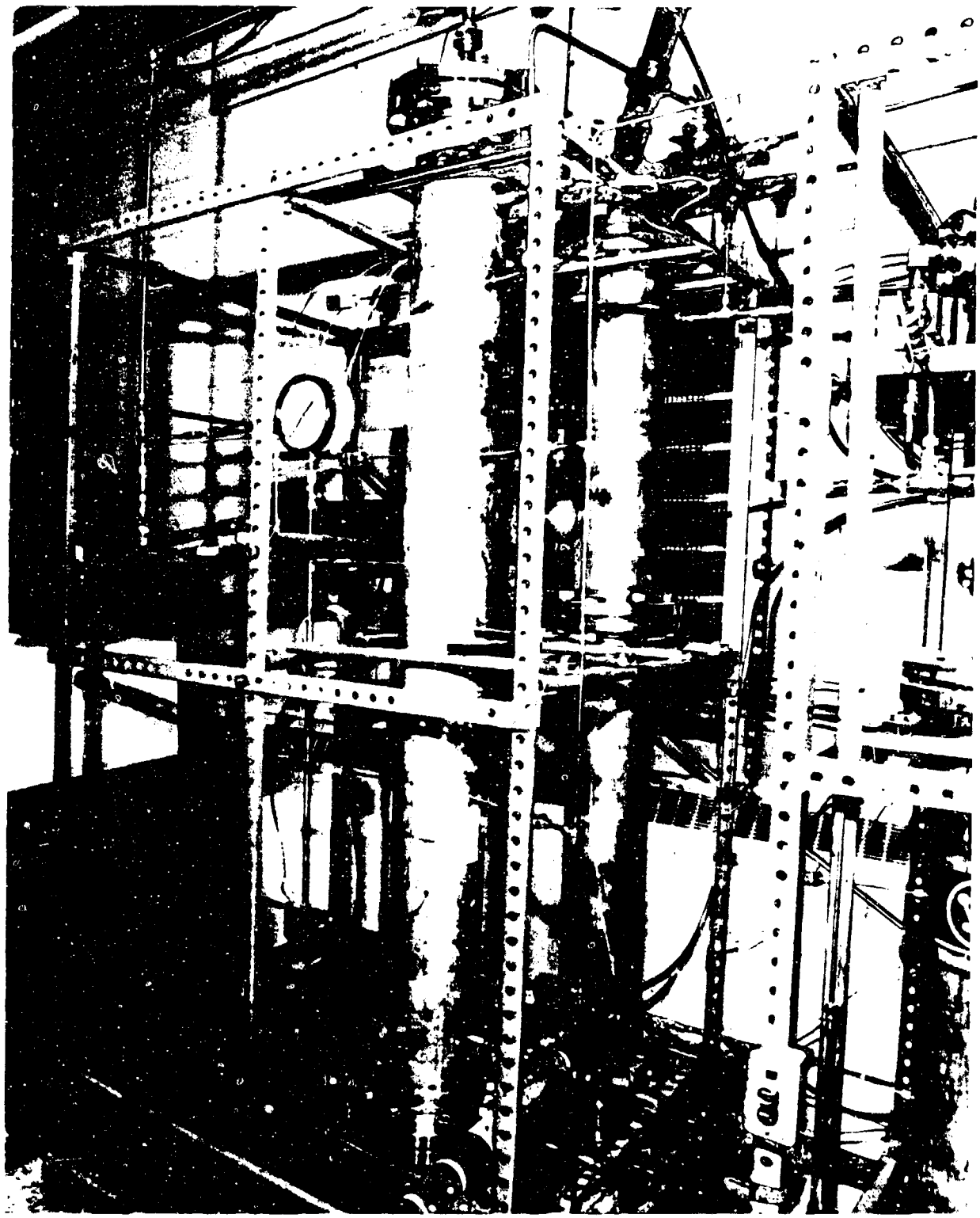

Figure 7.18 -- Experimental Fuel Processor Shift Reactor and Afterburner

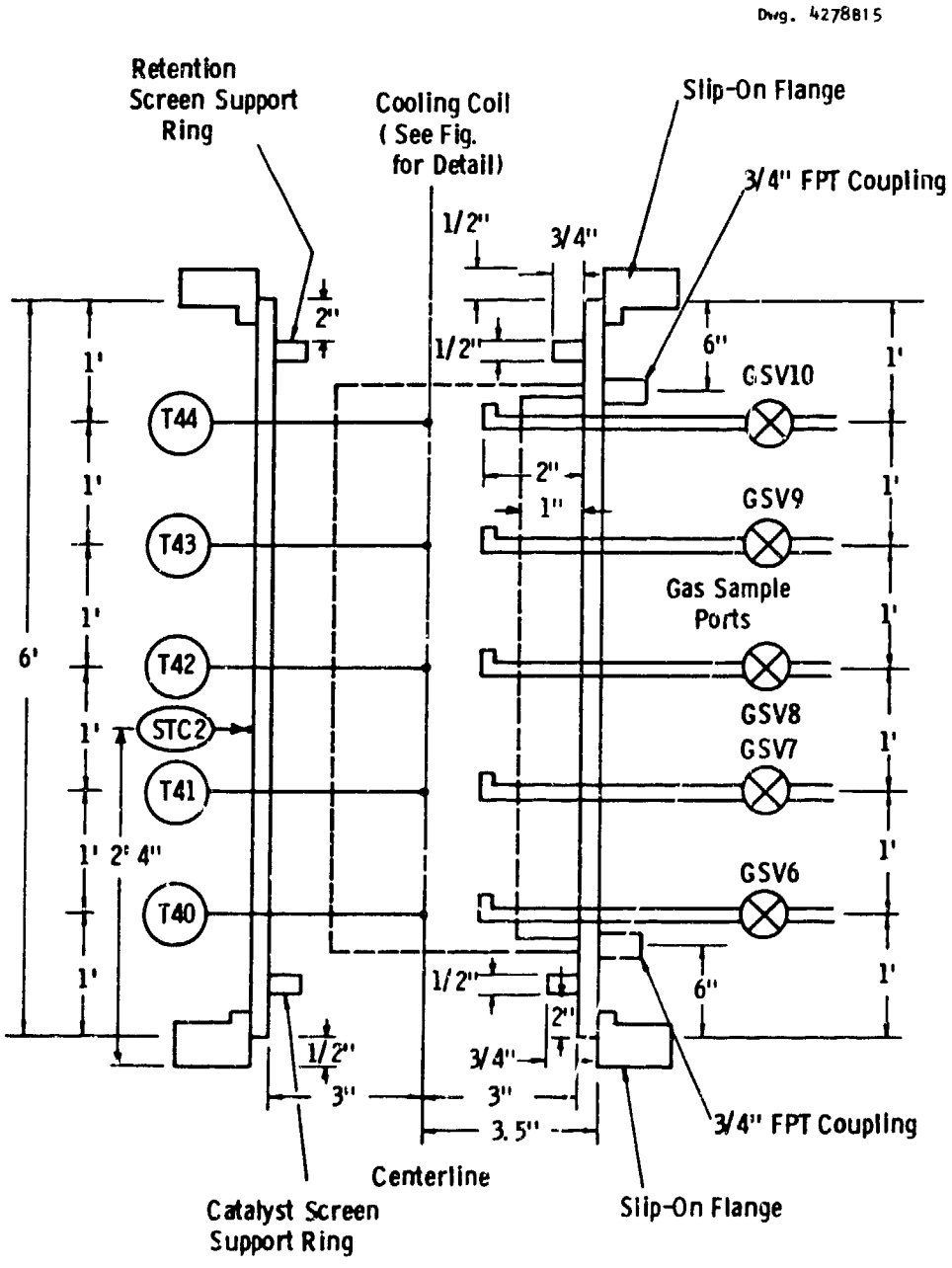

Figure 7.19 -- Water Gas Shift Reactor Detail (Pipe and Flanges are 6" Nominal, Schedule 40)

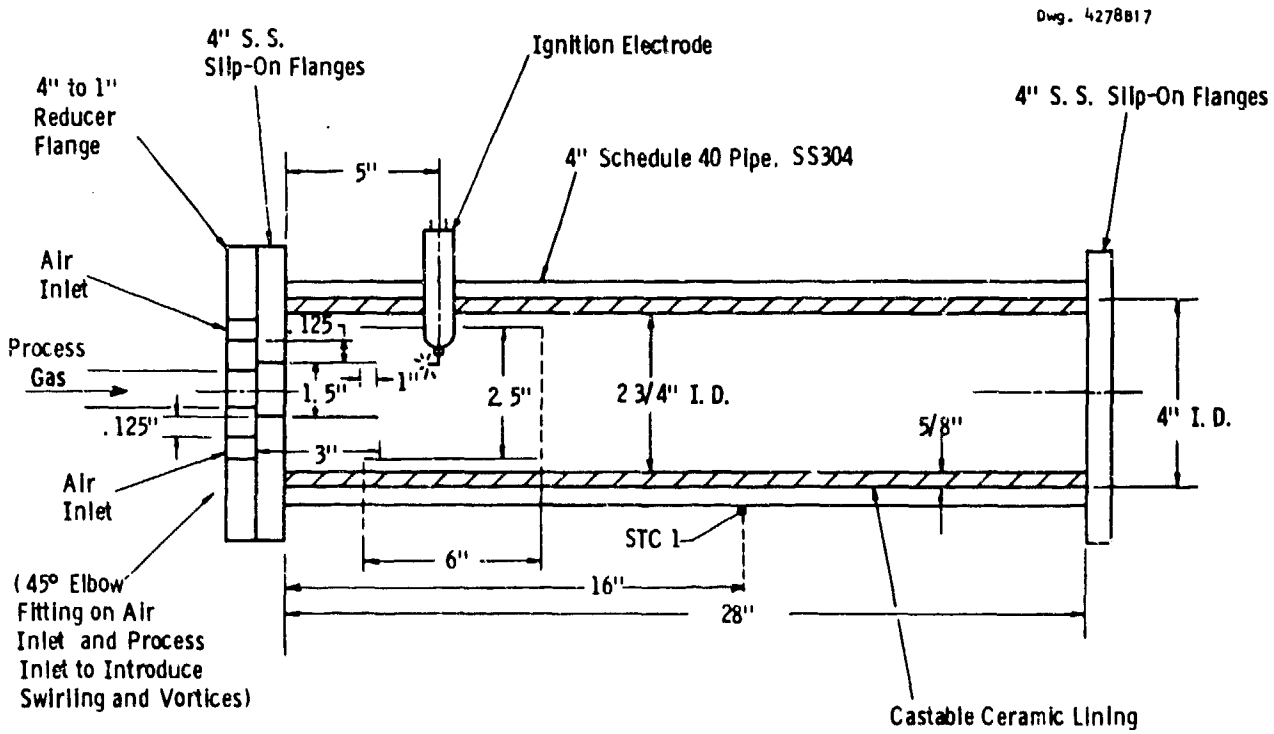

Figure 7.20A -- Combustor for the Afterburner

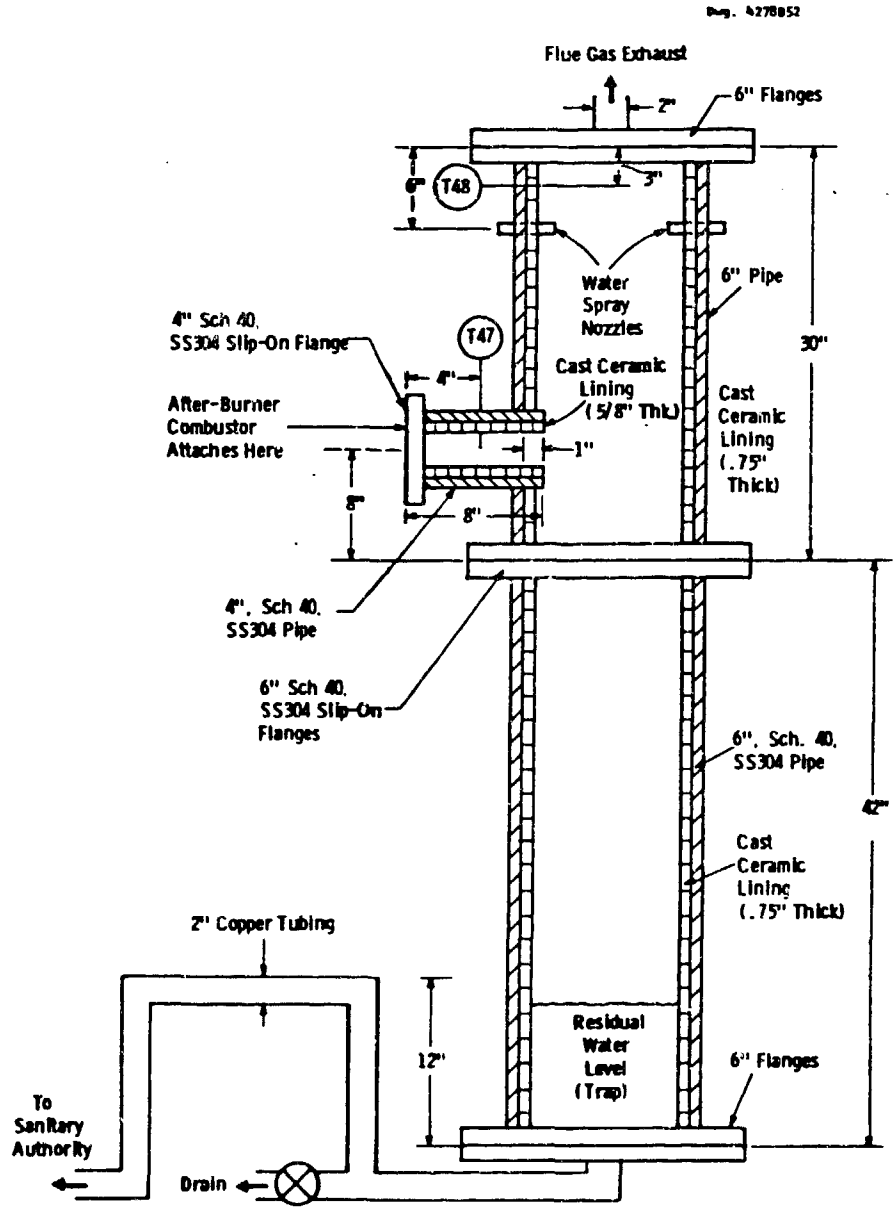

Figure 7.20B -- Afterburner Detail

gases towards the flue exhaust. The exhaust connects to a 6" diameter, stainless steel, metal-bestos duct, which ends in a roof stack.

A Perkin-Elmer, Sigma 115 gas chromatograph is used for the gas analyses (Figure 7.21), in a semi-continuous mode. This unit includes, a hot wire detector (HWD - thermal conductivity, for most gases), a flame photometric detector (FPD - for low level sulfur analysis), and a flame ionization detector (FID - for total hydrocarbons). The appropriate calibration (span) gases are also available. Initial operation of this unit proved unsatisfactory because of electronic/control problems. Consequently, the sample train has been modified to include discrete, gas sample taking via sample cylinders. This allows subsequent analysis using any of the other gas chromatographs at the R&D Center.

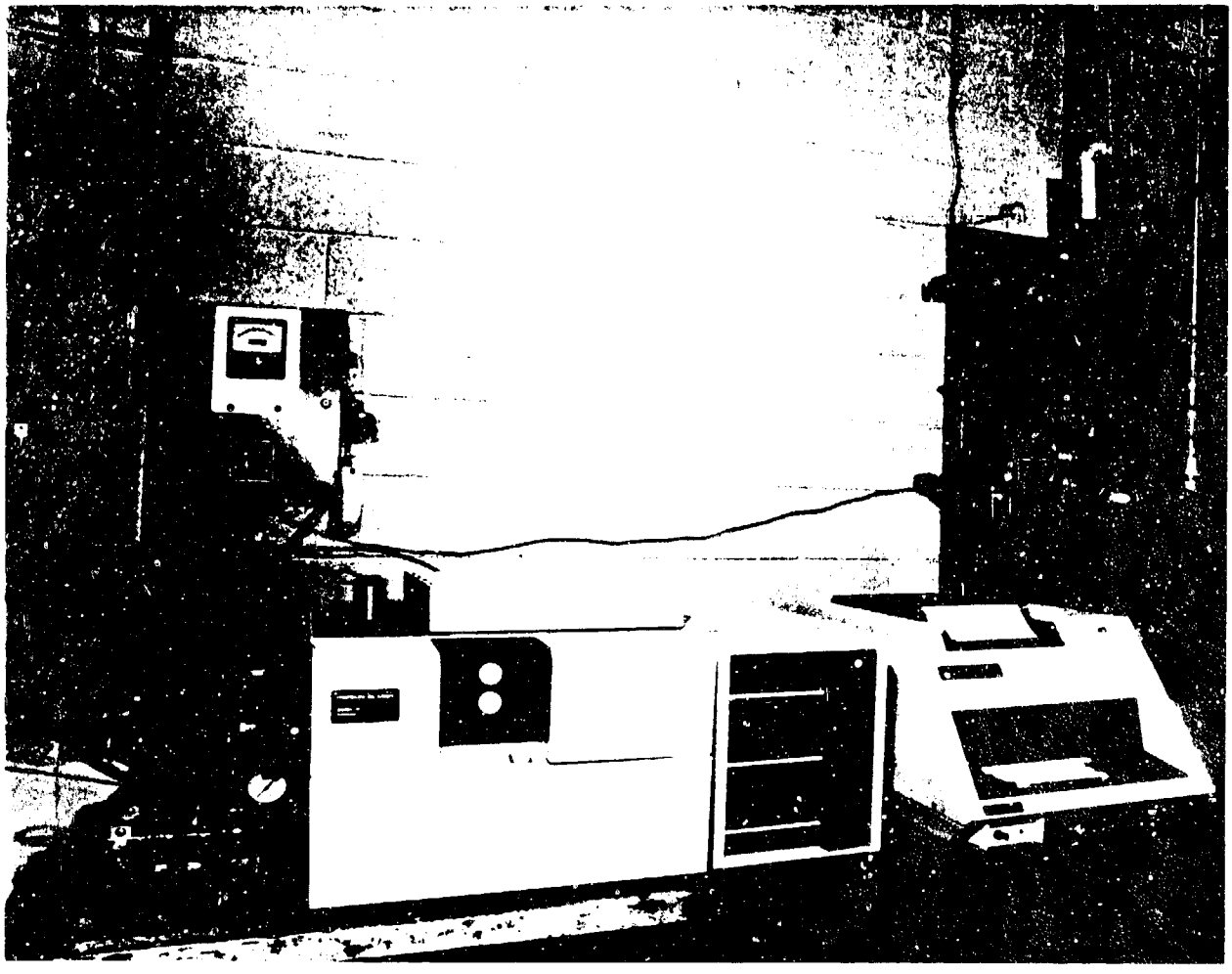

Figure 7.21 -- Gas Analysis System

8. Experimental Tests

Five tests were planned for the experimental system:

1. straight combustion
2. 5 KW flow rates reforming test (~ .5 gph diesel fuel), with the C15 chromia catalyst.
3. as test 2, but with 10 KW flow rates.
4. 5 KW flow rates, reforming test, with a 1:1 ratio of T12/T48 catalysts.
5. as test 4, but with 10 KW flow rates.

Two test series of five tests each were accomplished (Tables 8.1 and 8.2). Various equipment and experimental difficulties were encountered which precluded hydrogen production. However, valuable information and insight were obtained about system performance, which will be beneficial for future fuel cell programs. These tests are discussed in this section.

Series A experiments (Table 8.1) used pressure atomizing nozzles, operated at ~ 120 psig. These nozzles performed poorly, giving inadequate atomization and plugging frequently, apparently by coking in the nozzle's orifice. Although various modifications were made, only one of the five tests successfully ran for a short time. This test showed high temperatures were achievable in the test unit, both with and without cylinder oxygen addition. These tests also indicated that nozzle performance had to be improved, and that system heatup to operating temperatures was a potential problem.

The test system was modified for the Series B experiments. Two air atomizing nozzles were installed for diesel fuel atomization, and one water nozzle and injection line were added to simulate cathode water recycle. A small, additional control panel was also assembled for operating these nozzles. As Table 8.2 indicates, the system performed

Table 8.1 -- Experimental Tests - Series A*

Test	Date	Fuel Flow, GPH Main Nozzle	Fuel Flow, GPH Side Nozzle	Burner Oxidant Gas Flow (SCFH)	Comments
1	9/16/86	.22	0	~ 200	1. No insulation on burner, reformer or heat exchanger. 2. No fuel ignition by electrode system. 3. Nozzle not atomizing fuel - replaced.
2	9/23/86	.22	0	~ 200	1. Using propane torch for ignition. 2. Fuel ignited, but nozzle plugged after ~ 30 minutes, even at 200 psi - fuel pressure.
3	9/27/86	.222	0	268	1. New nozzle 2. Ignited, ran well for 1.5 hours 3. 1904°F average burner temperature, up to 2300°F for 10 minutes 4. Used 44% oxygen 5. Reformer only at 572°F
4	10/1/86	.22	0	~ 200	1. Insulation added on burner, reformer, and heat exchanger 2. Nozzle plugged 30 minutes after ignition
5	10/7/86	.22	0	~ 190	1. New nozzle 2. N_2 blow-out line added to nozzle 3. Ran for ~ ½ hour 4. Nozzle plugged 5. 30 PSI pressure drop across reformer 6. Inspection indicated severe carbon deposition.

*pressure atomizing nozzles.

Table 8.2 -- Experimental Tests - Series B*

Test	Date	Fuel Flow, GPH Main Nozzle	Fuel Flow, GPH Side Nozzle	Burner Oxidant Gas Flow (SCFH)	Comments
6	5/1/86	.22	0	103	1. 2 hour run 2. propane torch went out - system restarted well 3. 78% oxygen - although burner temperatures moderate (700°C)
7	5/7/86	.19	0	151	1. 4 hour run 2. 48% oxygen 3. high gas temperatures 4. high metal wall temperatures - 1550°F
8	5/9/86	.173	0	208	1. 5 hour run 2. all air - no oxygen added 3. good temperatures but slow heat-up 4. moderate wall temperatures (1200°F)
9	5/16/86	.159	0	367	1. 6.5 hour run 2. all air, no oxygen 3. good temperature, but slow heat-up 4. wall temperatures of 1534°F
10	5/22/86	.175	0	292	1. system shutdown after ~ 30 minutes because of nozzle plugging

*air-atomizing nozzles.

quite well, although, on the tenth test, the principal fuel nozzle did plug completely. Again, this appears to be due to carbon formation inside the nozzle.

Figure 8.1, 8.2 and 8.3 display the temperature profiles for Tests 7, 8 and 9, respectively. These indicate that burner thermal equlibrium requires 1-2 hours, and reformer thermal equilibrium requires an additional 1.5-2.5 hours. These temperatures are at the lower end of the calculated operational range (from Section 5), but are acceptable. Furthermore, the desulfurizer and shift reactor have not been effectively heated above ~85°C. This introduces the possibility of water condensation in the packing of these vessels. Figure 8.4 shows the pressure profiles for Run 9. Condensation does appear to be causing pressure drops during the test.

Secondary nozzle fuel introduction was not attempted on these experiments because of the low desulfurizer and shift reactor temperatures and the pressure oscillations. Consequently, hydrogen production was precluded. Complete system heat-up time is estimated to be ~10 hours, by extrapolation. The contract's technical effort period expired before a longer duration test could be conducted.

Curve 752323-A

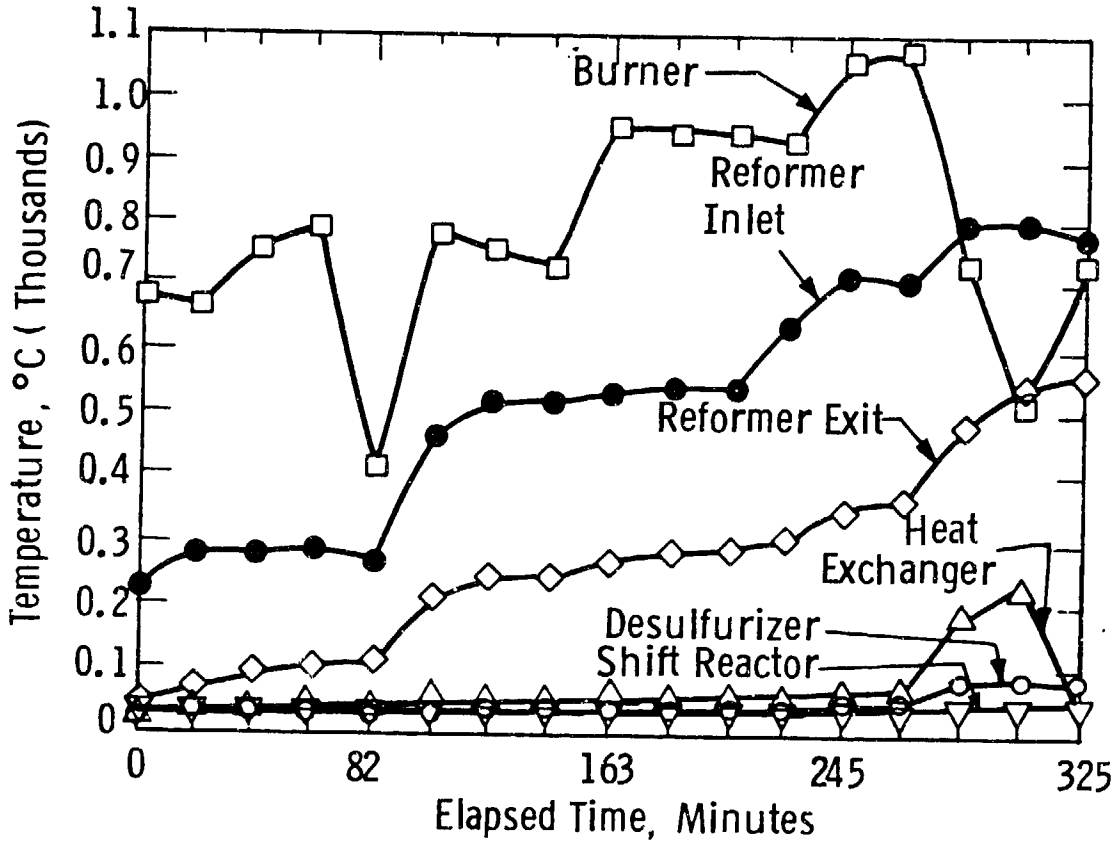

Figure 8.1 — Test 7 Temperature Profiles

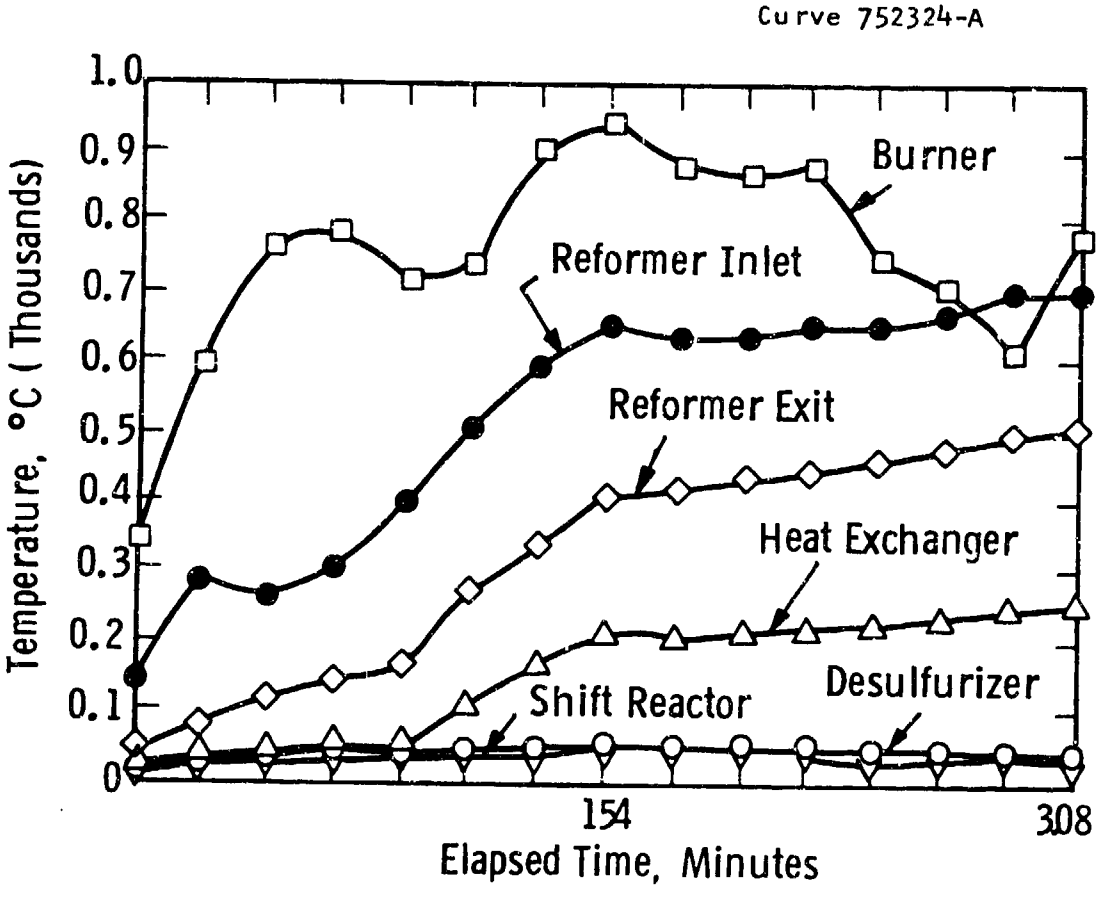

Figure 8.2 — Test 8 Temperature Profiles

Curve 752161-A

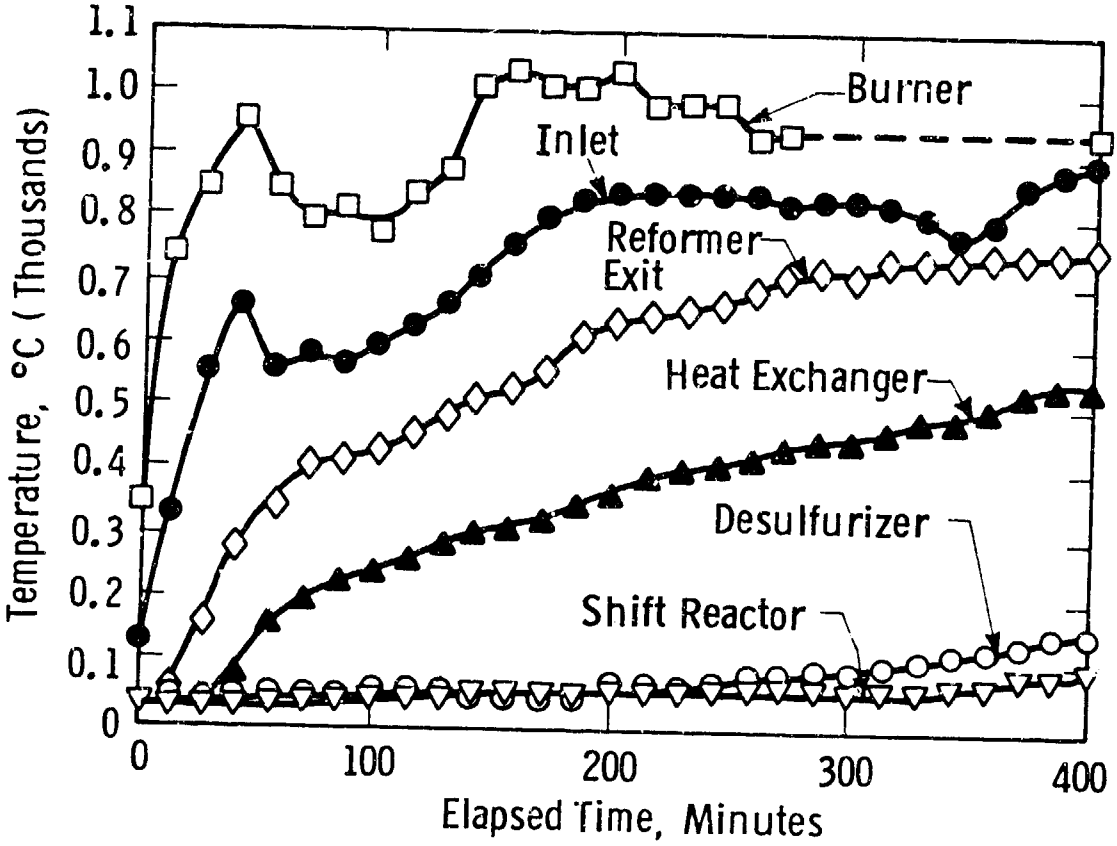

Figure 8.3 — Test 9 Temperature Profiles

Curve 752322-A

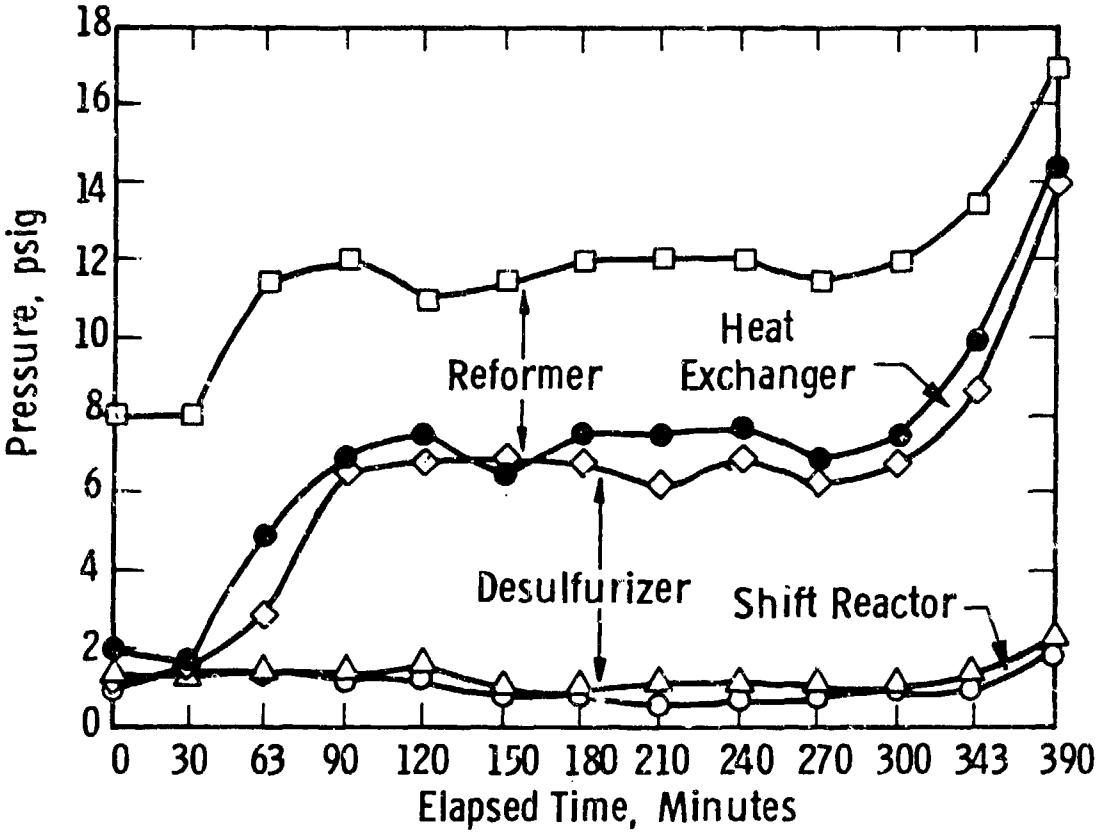

Figure 8.4 — Fuel Processor Pressure Profiles (Test 8)

9. Discussion

The relatively long, system heatup time is a concern, from both the experimental system and prototype design viewpoints. Table 9.1 presents an analysis of the experimental system's enthalpies. The largest, system heat capacity is the structural (vessel) steel. The system requires the heat equivalent of one full hour's flow, based upon complete combustion. Thus, using primary nozzle flow rates of ~ .15 gph, around three hours would be the expected, "thermodynamically ideal," heat-up time. The estimated time, based upon observation, is approximately triple this value (~ 10 hours) and implies system heat losses (through the insulation) and condensed water effects are much greater than anticipated. Obviously, for experimental testing, this infers preheating the system to > 300°F; for example, by using hot air. Table 9.1 also implies that a prototype, 5 KW system with a required start-up time of 15 minutes, would consume a <u>minimum</u> fuel flow of four times normal, for a total, fuel consumption of .44 gallons during this period.

System size and weight are obvious concerns. Table 9.2 compares calculated fuel cell system values to commercially available diesel electric generators in the same size range.[28,29] The fuel cell systems have slightly improved operating performance, but are significantly larger and heavier than the diesel-electric systems. It is unclear if the performance margin can be increased and the weight reduced sufficiently to make the fuel cell systems the obvious choice.

The three components that contribute the most weight are the heat exchanger, desulfurizer, and shift reactor. The experimental system's heat exchanger is a 316 stainless steel spiral design with 1.5" thick flanges, and weighs 350 pounds. Higher alloy use (such as 25/35 Cr/Ni) and lower presure rating will reduce this weight by perhaps 25%.

Table 9.1 — Experimental System Start-Up Enthalpy Estimates

	Weight, lbs	Enthalpy, BTU
Reformer Catalyst (to 1400°F)	13.2	2,995
Desulfurizer (to 440°F)	32.3	1,575
Shift reactor (to 440°F)	82.4	4,014
Structural steel (to ~ 440°F mean)	~1000	47,600
Total	1127	56,184

~ 20,000 BTU/lb diesel fuel LHV

- 1,679 BTU/lb for raising combustion products (stoichiometric) to 440°F

18,321 BTU/lb effective heat value.

∴ System heat-up requires equivalent of 3.1 lbs (.44 gal) of diesel fuel, or ~ 1 hour of full flow.

Table 9.2 -- Comparison of Fuel Cell Prototype and Diesel Electric Power Systems

System*	Size	Weight, lbs	Fuel (gph)	Efficiency, %	Price
Design 5: autothermal, with cathode water recycle, fuel cell system (PAFC)	72"Lx36"Wx60"H	1388	.55	23	82,800
Design 6: as above, with PSA/oxygen system	72"Lx36"Wx60"H	1718	.45	28	113,200
6 KW, diesel-electric electric generator, air-cooled	37"Lx22"Wx29"H (long discharge)	485 (+ 100 lbs for battery, rack, housing, and fuel tank)	.64 @ 6 KW .53 @ 4.5 KW	24 21	7,000
12 KW, diesel-electric electric generator, air-cooled	47"Lx20"Wx26"H	710 (+ 100 lbs for battery, etc.)	1.1 @ 12 KW 1 @ 9 KW	28 23	9,200
55 KW, diesel-electric generator	95"Lx35"Wx60"H	3130	2.1 @ 12 KW 2.8 @ 25 KW 3.6 @ 37 KW 4.4 @ 50 KW	14 23 26 29	20,000

*all fuel cell system values are estimated or calculated, with a maximum system efficiency of ~ 33%. Diesel system values are actual, vendor specifications.

Unfortunately, light weight, plate type heat exchangers are unsuitable for this application.

The desulfurizer presents another weight dilemma. Its design accommodates ~ 116 hours (~ 5 days) of continuous operation at the typical diesel fuel sulfur level of .3% (and 440°F), before significant breakthrough occurs. It is unlikely that this can be reduced, given the trend towards dirtier fuels (> .5% sulfur) and packing replacement requirements.

Figure 9.1 displays an analysis of shift reactor volume and exit carbon monoxide concentration (10% above equilibrium) as a function of temperature. Using 3% carbon monoxide as the maximum, allowable concentration for atmospheric, PAFC systems, then a ~ 2.6 ft^3 shift reactor is necessary, operating at 430°F. Using 10% excess water (S/C ratio = 2.2) allows operation at a higher temperature (480°F), and decreases the volume to ~ 1 ft^3. This value is used in the fuel cell system analyses. These curves assymtopically converge in the .6-1 ft^3 reactor size range at ~ 550°F, as the steam ratio is increased. Therefore, the shift reactor volume and weight can potentially be decreased by ~ 40%. However, there will be a weight increase due to the additional water recycle requirements. Valves and piping are also necessary for shift reactor heating without catalyst oxidation, and will tend to increase the shift reactor weight. The overall efect is estimated to be a shift reactor weight reduction of ~ 20%.

In the final analysis, it is unlikely that the diesel fuel cell system weight can be significantly reduced below ~ 1000 pounds, i.e., twice the comparable diesel-electric system's weight. A significant fraction of the weight is due to the shift reactor. It is not obvious that the PAFC system's performance advantages offset its size and weight penalties as compared to the diesel-electric generators. If this comparison is unfavorable, then a solid oxide fuel cell (SOFC) system should be analyzed and compared for the same applications. SOFC systems utilize carbon monoxide directly as a fuel, and, therefore, eliminate

Curve 752160-A

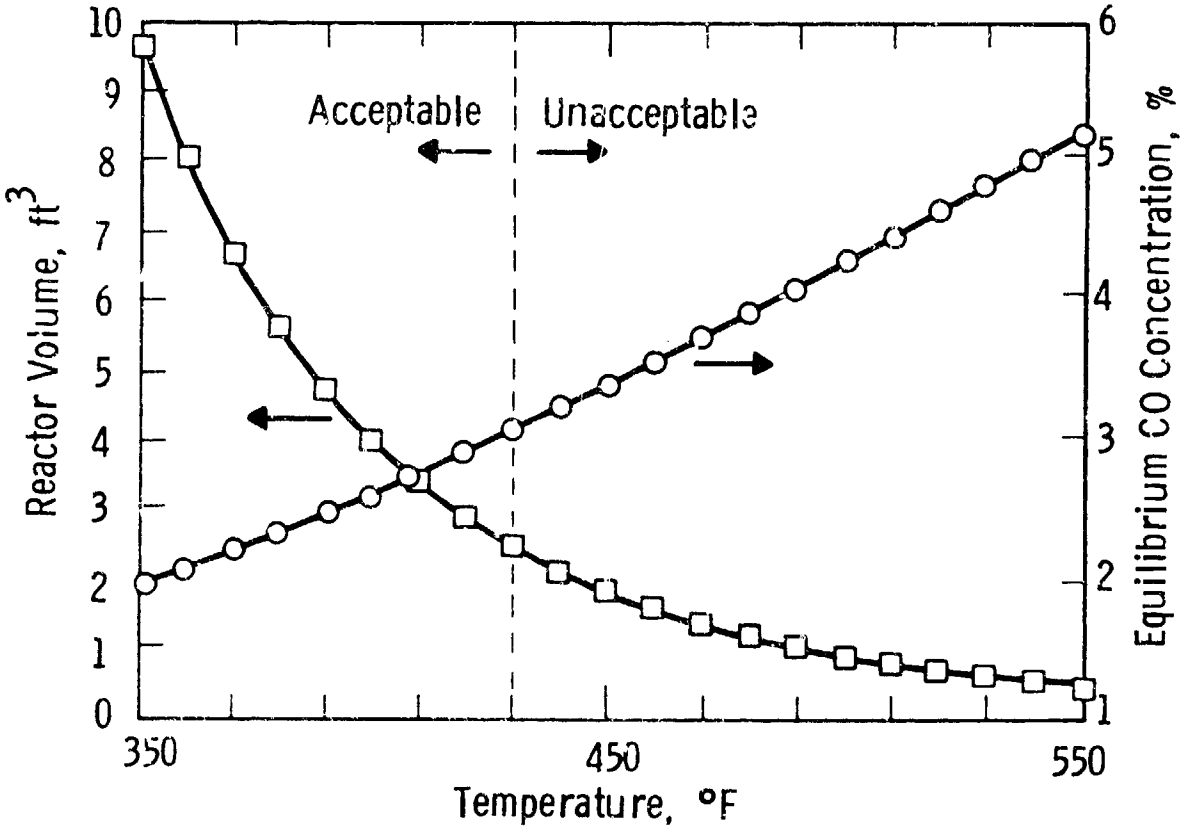

Figure 9.1 — Shift Reactor Volume Analysis

the shift reactor and its weight. They also have higher efficiencies and tolerate reformer upsets better. Thus, a diesel fuel, SOFC system offers a potentially clear advantage over diesel-electric systems and should be analyzed and investigated.

10. Acknowledgements

The author gratefully acknowledges the assistance of J. L. Emwiller and A. Carr during fabrication, assembly, and testing of the experimental system. The efforts of G. R. Marshall of the Analytical Chemistry Department for explaining and evaluating the gas chromatograph system are also appreciated. The author thanks W. G. Vaux for being the program's QA/QC monitor. The author also acknowledges the helpful suggestions of E. A. DeZubay and R. M. Chamberlin regarding burner design and nozzle operation.

11. References

1. S. Abens, R. Hayes, and W. Keil, "Three and Five KW Methanol Powerplant Program," 30th Power Sources Symposium, June 7-12, 1982, Atlantic City, New Jersey.

2. Personal communications with R. Hartye and A. L. Hausberger of United Catalysts, Louisville, Kentucky.

3. W. E. Houghtby, et al, "Sulfur-Tolerant Fuel Processors for Fuel Cell Power Plants," EPRI Report EM-2686, October 1982.

4. R. G. Minet and D. Warren, "Evaluation of Hybrid TER-ATR Fuel Processor," EPRI Report EM-2096, October 1981.

5. R. G. Minet and D. Warren, "Assessment of Fuel Processing Systems for Dispersed Fuel Cell Power Plants," EPRI Report EM-1487, August 1980.

6. K. Kikuchi, T. Tomita, T. Sakamoto and T. Ishida, "A New Catalytic Cracking Process," Chemical Engineering Progress, Volume 81, Number 6, pages 54-58 (June 1985).

7. Personal communication with T. Tomita of Toyo Engineering Company, Chiba, Japan.

8. O. L. Olesen and W. H. Johnson, "Fuel Processor Development for 11-MW Fuel Cell Power Plants," EPRI Report EM-4123, July 1985.

9. M. H. Hyman, "Simulate Methane Reformer Reactions," Hydrocarbon Processing, July 1968, pages 131-137.

10. A. P. Murray, "Steam-Fuel Oil Reformer Kinetic Computer Model," 31st Power Sources Symposium, June 1984, Cherry Hill, New Jersey.

11. Personal communication with A. Barberic of Xonbox Corporation, Tonawanda, New York.

12. "Oxygen Breathes More Life into CPI Processing," Chemical Engineering, Volume 91, Number 23, pages 30-35 (November 12, 1984).

13. G. M. Lukchis, "Adsorption Systems," Parts I, II and III, Chemical Engineering, June 11, July 9 and August 6, 1973.

14. Sales information from Airco Industrial Gases (Murray Hill, New Jersey), Nitrotec Corporation (New York City), and the C. M. Kemp Manufacturing Company (Glen Burnie, Maryland).

15. Personal communication with D. Schleiffarth of Monsanto Corporation, St. Louis, Missouri

16. J. Shirley, D. Borzik and D. Eyrnes, "Hollow Fiber Gas Separator Boosts NH_3 Output by 50 tpd," Chemical Processing, January 1982.

17. D. Q. Hoover, "Cell Module and Fuel Conditioner Development: Final Report: October 1979 - January 1982," NASA CR-165193, February 1982.

18. M. S. Peters and K. D. Timmerhaus, Plant Design and Economics for Chemical Engineers, Third Edition, McGraw-Hill Book Company, New Yorkm 1980.

19. Personal communication with E. Sonnichsen of Test Devices, Inc., Stow, Massachusetts.

20. J. J. Collins, "The LUB/Equilibrium Section Concept for Fixed-Bed Adsorption," Chemical Engineering Progress, Symposium Series Number 74.

21. C. M. Yon and P. H. Turnock, "Multicomponent Adsorption Equilibria on Molecular Sieves," AIChE Symposium Series, Number 117, Volume 67, 1971.

22. M. M. Hassan, N. S. Raghavan, D. M. Ruthven and H. A. Boniface, "Pressure Swing Adsorption, Part 71: Experimental Study of a Nonlinear Trace Component Isothermal System," AIChE Journal, Volume 31, Number 12, page 2008, (December 1985).

23. N. S. Raghavan and D. M. Ruthven, "Pressure Swing Adsorption, Part III: Numerical Simulation of a Kinetically Controlled Bulk Gas Separation," AIChE Journal, Volume 31, Number 12, page 2017, (December 1985).

24. "Hydrogen Recovery from Gas Streams," Nitrogen, March/April 1982.

25. D. L. MacLean, D. J. Stookey, and T. R. Metzger, "Fundamentals of Gas Permeation," Hydrocarbon Processing, August 1983.

26. "Unique Membrane System Spurs Gas Separations," Chemical Engineering, November 30, 1981, pages 62-66.

27. R. T. Yang and P. L. Cen, "Improved Pressure Swing Adsorption Processes for Gas Separation: By Heat Exchange Between Absorbers and by High Heat Capacity Inert Additives," I&EC, Proc. Des. & Dev., 1986, Vol. 25, pages 54-59.

28. Personal communication and literature, Caterpillar Company, June 24, 1986.

29. Personal communication and literature, A. F. Shane Company, June 24, 1986.

30. J. Holm, "Energy Recovery with Turboexpander Processes," Chemical Engineering Progress, Vol. 81, No. 7, (July 1985).

31. T. E. Cooley and W. L. Dethloff, "Field Tests Show Membrane Processing Attractive," Chemical Engineering Progress, Vol. 81, No. 10, (October 1985).

32. Chementator, in Chemical Engineering, April 14, 1986, page 17.

33. K. B. McReynolds, "A New Air Separation System," Chemical Engineering Progress, Vol. 81, No. 6 (June 1985).

Permanent Record Book Entries

#211006, pages 1-140
#211150, pages 1-23.

Alexander P. Murray 7/21/86

A. P. Murray
Chemical and Process Engineering

R. M. Chamberlin

R. M. Chamberlin, Manager
Energy Systems

Dale T Keairns

D. L. Keairns, Manager
Chemical and Process Engineering